

ผลกระทบของแรงดันตกชั่วขณะและการประสานการป้องกันต่ออุปกรณ์ที่ไวต่อแรงดันตกชั่วขณะในระบบ  
จำหน่ายไฟฟ้า

นายเทียน เวียด เล

ศูนย์วิทยพัทยากร

วิทยานิพนธ์นี้เป็นส่วนหนึ่งของการศึกษาตามหลักสูตรปริญญาวิศวกรรมศาสตรดุษฎีบัณฑิต

สาขาวิชาวิศวกรรมไฟฟ้า ภาควิชาวิศวกรรมไฟฟ้า

คณะวิศวกรรมศาสตร์ จุฬาลงกรณ์มหาวิทยาลัย

ปีการศึกษา 2552

ลิขสิทธิ์ของจุฬาลงกรณ์มหาวิทยาลัย

IMPACTS OF VOLTAGE SAGS AND PROTECTION COORDINATION  
ON SENSITIVE EQUIPMENT IN DISTRIBUTION SYSTEMS

Mr. Le Viet Tien

A Dissertation Submitted in Partial Fulfillment of the Requirements  
for the Degree of Doctor of Philosophy Program in Electrical Engineering  
Department of Electrical Engineering

Faculty of Engineering  
Chulalongkorn University

Academic Year 2009

Copyright of Chulalongkorn University

Thesis Title                    IMPACTS OF VOLTAGE SAGS AND PROTECTION COORDINATION ON SENSITIVE EQUIPMENT IN DISTRIBUTION SYSTEMS

By                                    Mr. Le Viet Tien

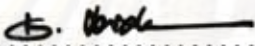
Field of Study                    Electrical Engineering

Thesis Advisor                    Assistant Professor Thavatchai Tayjasanant, Ph.D.

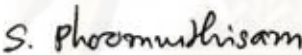
Thesis Co-Advisor                Professor Bundhit Eua-arporn, Ph.D.

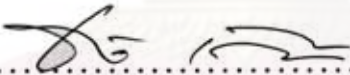
---


Accepted by the Faculty of Engineering, Chulalongkorn University in  
Partial Fulfillment of the Requirements for the Doctoral's Degree

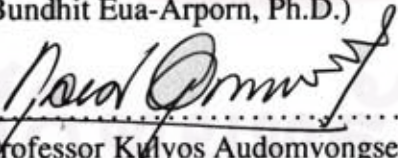
  
..... Dean of the Faculty of Engineering  
(Associate Professor Boonsom Lerthirunwong, Dr. Ing.)

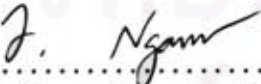
THESIS COMMITTEE

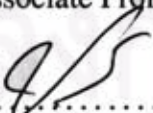
  
..... Chairman  
(Associate Professor Sukumvit Phoomthisarn, Ph.D.)

  
..... Thesis Advisor  
(Assistant Professor Thavatchai Tayjasanant, Ph.D.)

  
..... Thesis Co-Advisor  
(Professor Bundhit Eua-Arporn, Ph.D.)

  
..... Examiner  
(Assistant Professor Kalyos Audomvongseeree, Ph.D.)

  
..... External Examiner  
(Associate Professor Issarachai Ngamroo, Ph.D.)

  
..... External Examiner  
(Pradit Fuangfoo, Ph.D.)

เทียน เวียด เล : ผลกระทบของแรงดันตกชั่วขณะและการประสานการป้องกันต่ออุปกรณ์ที่ไวต่อแรงดันตกชั่วขณะในระบบจำหน่ายไฟฟ้า (IMPACTS OF VOLTAGE SAGS AND PROTECTION COORDINATION ON SENSITIVE EQUIPMENT IN DISTRIBUTION SYSTEMS) อ.ที่ปรึกษาวิทยานิพนธ์หลัก : ผศ.ดร.ธวัชชัย เศรษฐอนันต์, อ.ที่ปรึกษาวิทยานิพนธ์ร่วม : ศ.ดร. บัณฑิต เชื้ออาภรณ์, 97 หน้า.

อุปกรณ์อิเล็กทรอนิกส์ที่ไวต่อแรงดันตกชั่วขณะได้รับการนำมาใช้ในระบบไฟฟ้ากำลังเป็นจำนวนมาก ในปัจจุบัน ปัญหาแรงดันตกชั่วขณะจึงได้รับความสนใจมากขึ้นเนื่องจากส่งผลกระทบต่อสมรรถนะของอุปกรณ์เหล่านี้ แรงดันตกชั่วขณะอาจทำให้อุปกรณ์ทำงานผิดปกติหรือเกิดความผิดพลาดขึ้น ซึ่งนำไปสู่ความสูญเสียในงานหรือกระบวนการผลิต ดังนั้นจึงจำเป็นต้องมีข้อมูลเกี่ยวกับความไวของอุปกรณ์ ถ้าขนาดและระยะเวลาของแรงดันตกชั่วขณะเกินค่าขีดเริ่มความไวของอุปกรณ์ อุปกรณ์จะทำงานผิดพลาดได้ ซึ่งส่งผลกระทบต่อกระบวนการอัตโนมัติทั้งระบบ และนำไปสู่ความสูญเสียทางเศรษฐกิจ วิโครสเซอร์และฟิวส์เป็นอุปกรณ์ป้องกันกระแสเกินหลักในระบบจำหน่าย การประสานการป้องกันที่ไม่เหมาะสมจะทำให้เกิดผลกระทบเชิงลบต่ออุปกรณ์ที่ไวต่อแรงดันตกชั่วขณะ วิทยานิพนธ์นี้นำเสนอระเบียบวิธีในการวิเคราะห์ผลกระทบของแรงดันตกชั่วขณะและการประสานการป้องกันต่ออุปกรณ์ที่ไว การคำนวณแรงดันตกชั่วขณะและการตั้งค่าอุปกรณ์ป้องกันใช้วิธีหาตำแหน่งที่เกิดความผิดพลาดและสมการทางคณิตศาสตร์ที่อธิบายลักษณะสมบัติของอุปกรณ์ป้องกัน การวิเคราะห์การประสานการป้องกันกับอุปกรณ์ที่ไวใช้ค่าขีดเริ่มความทนทานแรงดันและลักษณะสมบัติของอุปกรณ์ป้องกัน จากผลการศึกษา การตั้งค่าอุปกรณ์ป้องกันใหม่สามารถปรับให้เหมาะสมกับอุปกรณ์ที่ไวต่อแรงดันตกชั่วขณะในระบบจำหน่าย การวิเคราะห์ผลกระทบของแรงดันตกชั่วขณะและการประสานการป้องกันใช้ระบบทดสอบ RBTS บัล 2

ภาควิชา ..... วิศวกรรมไฟฟ้า  
สาขาวิชา ..... วิศวกรรมไฟฟ้า  
ปีการศึกษา ..... 2552

ลายมือชื่อนิสิต .....  
ลายมือชื่ออ.ที่ปรึกษาวิทยานิพนธ์หลัก .....  
ลายมือชื่ออ.ที่ปรึกษาวิทยานิพนธ์ร่วม .....



## 4971870221: MAJOR ELECTRICAL ENGINEERING

KEYWORDS: POWER QUALITY / VOLTAGE SAG / PROTECTION COORDINATION

LE VIET TIEN: IMPACTS OF VOLTAGE SAGS AND PROTECTION COORDINATION ON SENSITIVE EQUIPMENT IN DISTRIBUTION SYSTEMS. THESIS ADVISOR: ASST. PROF. THAVATCHAI TAYJASANANT, Ph.D., AND THESIS CO-ADVISOR: PROF. BUNDHIT EUA-ARPORN, Ph.D., 97 pp.

Nowadays, a lot of sensitive electronic equipment is widely used in modern power systems such as power converters and adjustable speed drivers. Voltage sag has gained more interest due to their impacts on the performance of sensitive equipment (SE). Malfunction or failure of the equipment that leads to work or production losses can be caused by voltage sags. As a result, it is essential to have information on equipment sensitivity. If the magnitude and duration of voltage sag exceed the equipment sensitivity threshold, the equipment can malfunction, and such a consequence can affect an entire automatic process, resulting in high economical losses. Reclosers and fuses are the main overcurrent protection devices in distribution systems. Poor coordination could adversely impact on the sensitive equipment. This dissertation presents a method to analyze the impacts of voltage sags and protection coordination on sensitive equipment in distribution systems. A fault position method and mathematical equations for protective devices are used to set up the protection setting and to calculate voltage sags. Voltage tolerance thresholds and protective device characteristics are used to analyze protection and sensitive equipment coordination. Based on the results, new settings for protective devices can be adjusted to consider sensitive equipment in distribution systems. The Roy Billinton Test System (RBTS) bus 2 is used to analyze the impacts of voltage sags and protection coordination system on the sensitive equipment in distribution systems.

Department: .. Electrical Engineering  
 Field of Study: .. Electrical Engineering  
 Academic Year: ... 2009 .....

Student's Signature: .. *Le Viet Tien* ..  
 Advisor's Signature: .. *T. Tayjasanant* ..  
 Co-Advisor's Signature: .. *B. Eua-arporn* ..

## Acknowledgments

I would like to take this opportunity to express my deep gratitude to everyone who has made it possible for me to successfully complete this dissertation. First of all, I would like to thank the ASEAN University Network / Southeast Asia Engineering Education Development Network (AUN/SEED-Net) for its full financial support for my Ph.D. program in 2006.

I would like to send my gratefulness to the International School of Engineering (ISE), Chulalongkorn University, for offering me the chance of pursue my Ph.D. degree. Without their financial assistance, care, and help, my study abroad could not be possible.

I am deeply indebted to my advisor, Assistant Professor Thavatchai Tayjasanant, Ph.D., for the great deal of effort he expended upon supervising me during my study in Chulalongkorn University.

I would like also to thank my co-advisor, Professor Bundhit Eua-Arporn, Ph.D., for his kind help during my study, his interesting discussion and his constant encouragement.

I would like to express my gratitude to Professor Akihiko Yokoyama for his help and support during my short study in The University of Tokyo, Japan. Special thanks also go to friends in Yokoyama Laboratory in The University of Tokyo for their support and friendship.

I want to acknowledge my committee members, Associate Professor Sukumvit Phoomthisarn, Ph.D., Assistant Professor Kulyos Audomvongseeree, Ph.D., Associate Professor Issarachai Ngamroo, Ph.D., and Pradit Fuangfoo, Ph.D., for their contributing time, technical suggestions in the completion of this work.

My sincere appreciation to my friends for their enthusiasm and all what they have done for me during my study in Thailand. My thanks to all the people in the Power System Research Lab for helping me in different ways.

I thank my parents for their love and constant encouragement during the time of my Ph.D. studies. Without them I would not have been able to finish the dissertation.

Lastly, I want to say a big thank you to my wife, Nguyen Thi Hoa Mai, and my son, Le Tri Dung, for giving me motivation and patience while waiting for me to complete my dissertation.

จุฬาลงกรณ์มหาวิทยาลัย

# Contents

	Page
<b>Abstract (Thai)</b> .....	<b>iv</b>
<b>Abstract (English)</b> .....	<b>v</b>
<b>Acknowledgments</b> .....	<b>vi</b>
<b>Contents</b> .....	<b>vii</b>
<b>List of Tables</b> .....	<b>ix</b>
<b>List of Figures</b> .....	<b>xi</b>
<b>List of Notations</b> .....	<b>xiii</b>
<b>I INTRODUCTION</b> .....	<b>1</b>
1.1 Introduction .....	1
1.2 Problem Definition .....	1
1.3 Motivation of The Work .....	4
1.4 Outline of Dissertation .....	6
<b>II VOLTAGE SAGS IN DISTRIBUTION SYSTEMS</b> .....	<b>8</b>
2.1 Introduction .....	8
2.2 Voltage Sags Definition and Characteristic .....	8
2.3 Voltage Sags on Sensitive Equipment .....	9
2.4 Voltage Tolerance Curves .....	11
2.5 Area of Vulnerability on Sensitive Equipment .....	12
2.6 Fault Distribution Along Line .....	13
2.7 Summary .....	15
<b>III FAULT CALCULATION AND PROTECTION COORDINATION</b> .....	<b>16</b>
3.1 Introduction .....	16
3.2 Sags Calculation .....	16
3.2.1 Faults at Bus .....	17
3.2.2 Faults Along Lines .....	27
3.3 Effect of Transformers on Voltage Sags .....	33



3.4	Protection Coordination Analysis . . . . .	33
3.4.1	Protective Devices and Characteristics . . . . .	33
3.4.2	Recloser-fuse Coordination . . . . .	34
3.5	Summary . . . . .	36
<b>IV</b>	<b>VOLTAGE SAGS ESTIMATION</b> . . . . .	<b>37</b>
4.1	Introduction . . . . .	37
4.2	Voltage Sag Frequency . . . . .	37
4.3	Voltage Sag Indices . . . . .	38
4.4	Summary . . . . .	40
<b>V</b>	<b>SIMULATION AND RESULTS</b> . . . . .	<b>41</b>
5.1	Introduction . . . . .	41
5.2	Recloser-fuse Operations . . . . .	42
5.3	Simulation Results . . . . .	43
5.3.1	Simulation of Recloser–fuse Coordination with Consideration of Sensitive Equipment . . . . .	45
5.3.2	Simulation with Fault Along Line . . . . .	50
5.3.3	Sag Frequency with Different Voltage Threshold . . . . .	55
5.3.4	Sag Frequency without Protection Coordination Consideration . . . . .	58
5.3.5	Sag Frequency with Protection Coordination Consideration . . . . .	61
5.3.6	Sag Indices . . . . .	64
5.4	Discussion . . . . .	72
<b>VI</b>	<b>CONCLUSIONS AND FUTURE WORK</b> . . . . .	<b>74</b>
6.1	Conclusions . . . . .	74
6.2	Future Work . . . . .	76
	<b>REFERENCES</b> . . . . .	<b>77</b>
	<b>APPENDICES</b> . . . . .	<b>85</b>
	<b>BIOGRAPHY</b> . . . . .	<b>97</b>



## List of Tables

Table	Page
1.1 Categorization of electromagnetic phenomena [1] . . . . .	2
1.2 IEEE Standard 1159 – 1995 and EN 50160 – 2000 Categories . . . . .	3
2.1 Voltage tolerance characteristics of several equipments . . . . .	12
3.1 Summary equations of sequence and phase fault currents at bus $m$ when four types of faults occur at bus $i$ . . . . .	25
3.2 Summary equations of phase fault voltages at bus $m$ when four types of faults occur at bus $i$ . . . . .	26
3.3 Summary equations of sequence fault currents at bus $m$ when four types of faults occur along line $k - j$ at a fault position $f$ . . . . .	31
3.4 Summary equations of phase fault voltages at bus $m$ when four types of faults occur along line $k - j$ at a fault position $f$ . . . . .	32
5.1 Coefficient $a$ and $b$ for fuse setting . . . . .	44
5.2 Sag frequency with uniform fault distribution and different fault types for voltage threshold ranging from 10% to 90% of the nominal voltage . . . . .	55
5.3 Sag frequency with normal fault distribution and different fault types for voltage threshold ranging from 10% to 90% of the nominal voltage . . . . .	56
5.4 Sag frequency with exponential fault distribution and different fault types for voltage threshold ranging from 10% to 90% of the nominal voltage . . . . .	56
5.5 Sag frequency by applying Monte Carlo Simulation for voltage threshold ranging from 10% to 90% of the nominal voltage . . . . .	57
5.6 The number of line segments inside the area of vulnerability for sensitive equipment at bus 2 without protection coordination consideration . . . . .	59
5.7 The number of sag frequency for sensitive equipment at bus 2 without protection coordination consideration . . . . .	59
5.8 The number of line segments inside the area of vulnerability for sensitive equipment at bus 2 with protection coordination consideration . . . . .	62
5.9 The number of sag frequency for sensitive equipment at bus 2 with protection coordination consideration . . . . .	62
5.10 Coefficient $b$ for fuse characteristic equation . . . . .	65
5.11 $SARFI_X$ indices with the uniform fault distribution at the sensitive bus 2. . .	66

5.12	$SARFI_X$ indices with the normal fault distribution at the sensitive bus 2. . . .	66
5.13	$SARFI_X$ indices with the exponential fault distribution at the sensitive bus 2. . . .	66
5.14	$SARFI_X$ with Monte Carlo simulation taking random fault problems into considerations. . . . .	68
5.15	$SARFI_{curve}$ with ITIC and fault distribution considered . . . . .	69
5.16	$SARFI_{curve-MCS}$ with the sensitive characteristic curve and Monte Carlo Simulation consideration on analyzing fault problems. . . . .	71
5.17	$SARFI_X$ with expanding length of lines in the test system. . . . .	71
5.18	$SARFI_{curve}$ with expanding length of lines in the test system. . . . .	72
5.19	$SARFI$ with expanding length of lines in the test system and Monte Carlo simulation consideration. . . . .	72



ศูนย์วิทยทรัพยากร  
จุฬาลงกรณ์มหาวิทยาลัย

## List of Figures

Figure	Page
1.1 Sources of Power Quality Disturbances (source: Floria-Power study 1993) . .	4
1.2 Types of Power Quality Disturbances (source: EPRI 1994) . . . . .	4
2.1 Voltage sags duration and magnitude . . . . .	9
2.2 A fault in a typical distribution system . . . . .	10
2.3 Information Technology Industrial Council (ITIC) and SEMI curves . . . . .	11
2.4 A typical voltage tolerance curve . . . . .	12
2.5 Area of vulnerability and fault distribution along lines. . . . .	13
2.6 Uniform distribution with the same fault distribution value . . . . .	14
2.7 Normal distribution with the mean value $\mu = 0.5$ and the standard deviation value $\sigma = 0.1$ . . . . .	14
2.8 Exponential distribution with the mean value $\mu = 0.5$ . . . . .	15
3.1 A fault occurs at bus $i$ in a typical power system. . . . .	17
3.2 A fault occurs at point $f$ along line from bus $k$ to bus $j$ in a typical power system. . . . .	27
3.3 A typical distribution feeder. . . . .	34
3.4 Recloser–Fuse coordination range . . . . .	35
5.1 Example of voltage sags assessments based on ITIC curve . . . . .	42
5.2 Protection coordination . . . . .	43
5.3 RBTS bus 2 test system . . . . .	44
5.4 Voltage sag ride–through capacity curve from 0 to 100 $s$ . . . . .	45
5.5 100K fuse fuse coordination with the recloser to clear three–phase fault at bus 18. . . . .	46
5.6 80K fuse coordination with the recloser to clear three–phase fault at bus 18 .	46
5.7 80K fuse and 100K fuse coordination with the recloser to clear three-phase fault at bus 23 . . . . .	47
5.8 80K fuse and 100K fuse coordination with the recloser to clear three-phase fault at bus 38 . . . . .	48
5.9 80K fuse and 100K fuse coordination with the recloser to clear three-phase fault at bus 56 . . . . .	49

5.10 Protection coordination with 100K fuse when fault occurs along line from bus 5 to bus 18. . . . .	50
5.11 Protection coordination with 80K fuse when fault occurs along line from bus 5 to bus 18. . . . .	51
5.12 Protection coordination with 80K fuse and 100K fuse when fault occurs along line from bus 21 to bus 23. . . . .	52
5.13 Protection coordination with 80K fuse and 100K fuse when fault occurs along line from bus 27 to bus 38. . . . .	53
5.14 Protection coordination with 80K fuse and 100K fuse when fault occurs along line from bus 43 to bus 56. . . . .	54
5.15 Sag frequency spectrum of different fault distribution when a SLGF occurs . .	57
5.16 The areas of vulnerability for sensitive load at bus 2 without considering protection coordination due to SLGF and 3PF. . . . .	60
5.17 The areas of vulnerability for sensitive load at bus 2 without considering protection coordination due to LLF. . . . .	60
5.18 The areas of vulnerability for sensitive load at bus 2 without considering protection coordination due to DLGF. . . . .	61
5.19 The areas of vulnerability for sensitive load at bus 2 with considering protection coordination due to SLGF and 3PF. . . . .	63
5.20 The areas of vulnerability for sensitive load at bus 2 with considering protection coordination due to LLF. . . . .	63
5.21 The areas of vulnerability for sensitive load at bus 2 with considering protection coordination due to DLGF. . . . .	64
5.22 $SARFI_X$ with the voltage threshold and the uniform fault distribution along line. . . . .	67
5.23 $SARFI_X$ with the voltage threshold and the normal fault distribution along line. . . . .	67
5.24 $SARFI_X$ with the voltage threshold and the exponential fault distribution along line. . . . .	68
5.25 $SARFI_{curve}$ with fault distribution and the characteristic curves considered. .	70
5.26 $SARFI_{curve-MCS}$ with the sensitive characteristic curve and Monte Carlo Simulation consideration on analyzing fault problems. . . . .	70



## List of Notations

### Symbols

$V_{threshold}$	Voltage threshold
$T_{max}$	The maximum of time
$X\%$	Fixed voltage threshold
$\mu$	The mean value
$\sigma$	The standard deviation value
$I^z$	The zero sequence current
$I^p$	The positive sequence current
$I^n$	The negative sequence current
$V^z$	The zero sequence voltage
$V^p$	The positive sequence voltage
$V^n$	The negative sequence voltage
$a$	The transformer $a$ -operation, $a = e^{j\frac{2\pi}{3}}$
$I^a$	The current of phase $a$
$I^b$	The current of phase $b$
$I^c$	The current of phase $c$
$V^a$	The voltage of phase $a$
$V^b$	The voltage of phase $b$
$V^c$	The voltage of phase $c$
$V_{pref,i}^a$	The pre-fault voltage of phase $a$ at fault bus $i$
$Z_{ii}^z$	The diagonal element of the zero sequence impedance matrix
$Z_{ii}^p$	The diagonal element of the positive sequence impedance matrix
$Z_{ii}^n$	The diagonal element of the negative sequence impedance matrix
$V_{mi}$	The during-fault voltage at bus $m$ when a fault occurs at bus $i$
$\Delta V_{mi}$	The change in voltage at bus $m$ due to the fault at bus $i$
$Z_{mp}^z$	The zero sequence transfer impedance of bus $m$ and $p$
$Z_{mp}^p$	The positive sequence transfer impedance of bus $m$ and bus $p$
$Z_{mp}^n$	The negative sequence transfer impedance of bus $m$ and $p$
$Z_{kk}^z$	The zero sequence driving impedance at bus $k$
$t$	time
$I$	current
$I_{fault}$	Fault current
$t_{fault-SE}$	Fault duration of a sensitive equipment
$\alpha$	Fault distribution along line
$N_{fault}$	Number of fault
$n_s$	The number of events
$SARFI$	System Average Root Mean Square Variation Frequency Index
$SARFI_X$	System Average Root Mean Square Variation Frequency Index with voltage threshold
$SARFI_{curve}$	System Average Root Mean Square Variation Frequency Index with characteristic curve

## Acronyms

IEEE	The Institute of Electrical and Electronic Engineers
IEC	The International Electrotechnical Commission
BS	British Standard
HVDC	High-Voltage Direct Current
ITIC	Information Technology Industry Council
SEMI	Semiconductor
<i>pu.</i>	Per unit
RMS	Root Mean Square
AOV	Area Of Vulnerability
SE	Sensitive Equipment
SARFI	System Average Root Mean Square Variation Frequency Index
SLGF	Single Line Ground Fault
LLF	Line to Line Fault
DLGF	Double Line Ground Fault
3PF	Three Phase Fault
NSF	Number Sag Frequency
LFR	Line Failure Rate
FT	Fault Type
CB	Circuit Breaker
MM	Minimum Melting
TC	Total Clearing
TCC	Time-Current Curve
SE	Sensitive Equipment
RBTS	Roy Billinton Test System

# CHAPTER I

## INTRODUCTION

### 1.1 Introduction

Nowadays, much sensitive equipment are used in modern industrial such as adjustable speed drives, power electronics, computers or robotics. Many industrial customers using sensitive equipment suffer malfunction or failure of those equipment that can be caused by any problem in power networks, and lead to work or production shutdowns. To analyze the source of the problems, customers with sensitive equipment need to understand well about their power quality information, such as voltage and current quality. On the other hand, utilities also need power quality information for proving the quality of their power, trying to meet the demand of their customers and solving problems.

This chapter presents a general introduction to power quality with special definition of voltage sags. Many causes that may occurs and lead to problems in power system will be shown. Motivation of the research and the outline of this dissertation are presented.

### 1.2 Problem Definition

The term of power quality is the combination of voltage quality and current quality [2–4]. Voltage quality concerns the deviation of the voltage from an ideal sinusoidal voltage of constant magnitude and constant frequency. Current quality is a complementary term and concerns with the deviation of the ideal sinusoidal current of constant amplitude and frequency [5].

In a power network, the electricity moves from generation system through transmission system to distribution system. Because of the complex system, therefore, there are a lot of variations in weather, generator, transmission lines, demand and other factors that can impact the quality of supply.

The International Electrotechnical Commission (IEC) and the Institute of Electrical and Electronic Engineers (IEEE) are two the primary international organizations working on power quality issues. Table 1.1 shows the categorization of electromagnetic phenomena [3, 6]. Table 1.2 is for electric utilities control of voltage and prevention of outages [7, 8]. They are analyzed by considering the duration of phenomenon and the magnitude of remaining voltage.

Table 1.1: Categorization of electromagnetic phenomena [1]

Categories	Typical spectral content	Typical duration	Typical voltage magnitude
1.0 Transients			
1.1 Impulsive			
1.1.1 Nanosecond	5 <i>nsec</i> rise	< 50 <i>nsec</i>	
1.1.2 Microsecond	1 $\mu$ <i>sec</i> rise	50 <i>nsec</i> - 1 <i>msec</i>	
1.1.3 Millisecond	0.1 <i>msec</i> rise	> 1 <i>msec</i>	
1.2 Oscillatory			
1.2.1 Low frequency	< 5 <i>kHz</i>	0.3 – 0.5 <i>msec</i>	0 – 4 <i>pu.</i>
1.2.2 Medium frequency	5 – 500 <i>kHz</i>	20 $\mu$ <i>sec</i>	0 – 8 <i>pu.</i>
1.2.3 High frequency	0.5 – 5 <i>MHz</i>	5 $\mu$ <i>sec</i>	0 – 4 <i>pu.</i>
2.0 Short duration variations			
2.1 Instantaneous			
2.1.1 Interruption		0.5 – 30 cycles	< 0.1 <i>pu.</i>
2.1.2 Sag (Dip)		0.5 – 30 cycles	0.1 – 0.9 <i>pu.</i>
2.1.3 Swell		0.5 – 30 cycles	1.1 – 1.8 <i>pu.</i>
2.2 Momentary			
2.2.1 Interruption		30 cycles – <i>sec</i>	< 0.1 <i>pu.</i>
2.2.2 Sag (Dip)		30 cycles – <i>sec</i>	0.1 – 0.9 <i>pu.</i>
2.2.3 Swell		30 cycles – <i>sec</i>	1.1 – 1.4 <i>pu.</i>
2.3 Temporary			
2.3.1 Interruption		3 <i>sec</i> – 1 <i>min</i>	< 0.1 <i>pu.</i>
2.3.2 Sag (Dip)		3 <i>sec</i> – 1 <i>min</i>	0.1 – 0.9 <i>pu.</i>
2.3.3 Swell		3 <i>sec</i> – 1 <i>min</i>	1.1 – 1.2 <i>pu.</i>
3.0 Long duration variations			
3.1 Interruption sustained		> 1 <i>min</i>	0.0 <i>pu.</i>
3.2 Under-voltages		> 1 <i>min</i>	0.8 – 0.9 <i>pu.</i>
3.3 Overvoltage		> 1 <i>min</i>	1.1 – 1.2 <i>pu.</i>
4.0 Voltage unbalance		Steady state	0.5 – 2 %
5.0 Wave distortion			
5.1 DC offset		Steady state	0 – 0.1 %
5.2 Harmonics	0 – 100 <sup>th</sup> harmonic	Steady state	0 – 20 %
5.3 Inter-harmonics	0 – 6 <i>kHz</i>	Steady state	0 – 2 %
5.4 Notching		Steady state	
5.5 Noise	Broadband	Steady state	0.1 %
6.0 Voltage fluctuations	< 25 <i>Hz</i>	Intermittent	0.1 – 7 %
7.0 Power frequency variations		< 10 <i>sec</i>	



Table 1.2: IEEE Standard 1159 – 1995 and EN 50160 – 2000 Categories

IEEE Std. 1159 – 1995		EN 50160 – 2000
Short Duration Variation	Typical Duration	
Instantaneous Sag	0.5 – 30 cycles	<b>Supply voltage sag</b> A sudden reduction of the supply voltage to a value between of the declared voltage, 90% and 1% followed by voltage recovery after a short period of time. The duration is 10ms–1min. Momentary Sag between 30 cycles - 3 s
Momentary Sag	30 cycles – 3 sec.	
Temporary Sag	3 sec. – 1 min.	
Instantaneous	0.5 – 30 cycles	<b>Temporary power frequency over voltage</b> An over voltage, at a given location, of relatively long duration. Momentary swell between 30 cycles – 3 s
Momentary Swell	30 cycles – 3 sec.	
Temporary Swell	3 sec. – 1 min.	
Momentary Interruptions	0.5 – 30 cycles	<b>Supply interruption</b> A short interruption (up to three minutes) caused by a transient fault. Temporary interruption between 3 s - 1 min.
Temporary Interruptions	30 cycles – 3 sec.	

All of these causes occur according to Table 1.1, protection devices will be operated in power systems. The protection system will isolate the part of power network where a fault occurs, and eliminate the risk for both utilities and customers sites. However, there are some cases which protection system could not operate and isolate the fault, e.g. starting large induction motor load.

Figure 1.1 shows sources of power quality disturbances. Most of power quality disturbances are from office equipment (60%). Figure 1.2 shows types of power quality disturbances. In figure 1.2, sags is 56% among other types of power quality disturbances. There are many causes that may occur and lead to problems and faults in power systems such as

- External causes to power system, e.g. weather (storms, lightning, etc.), trees, and animals (birds, etc.).
- Human factors, e.g. human errors (auto accidents, kites etc.), scheduled interruptions.
- Internal causes, e.g. switching operations attempting to isolate an electrical problem and maintain power to customer area, fault, individual loads (motors, ASD, elevators, coolers, HVDC etc.), office equipment and computers, wiring, changing loads, and etc.

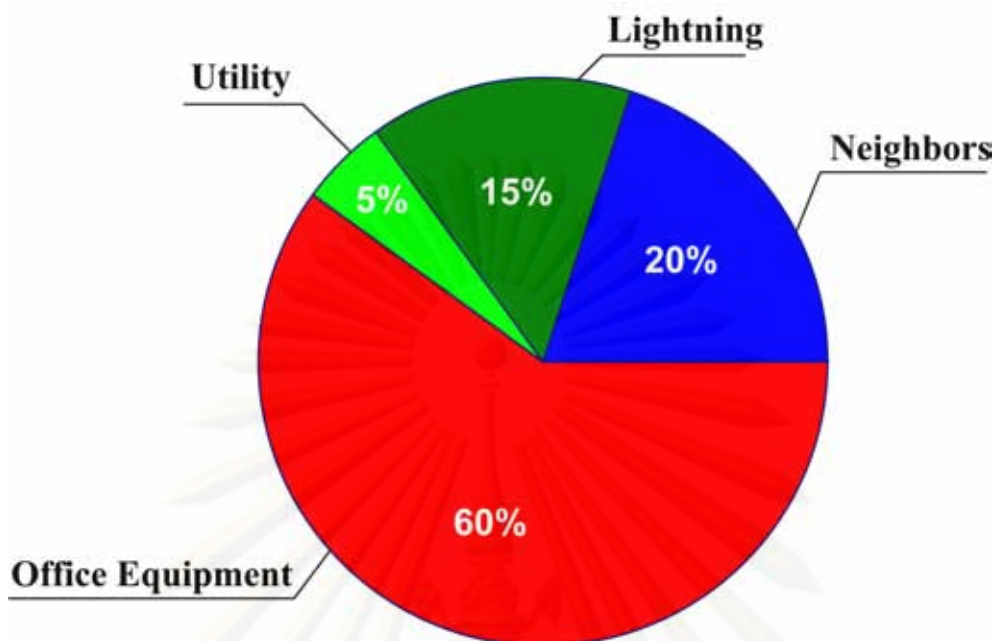


Figure 1.1: Sources of Power Quality Disturbances (source: Floria-Power study 1993)

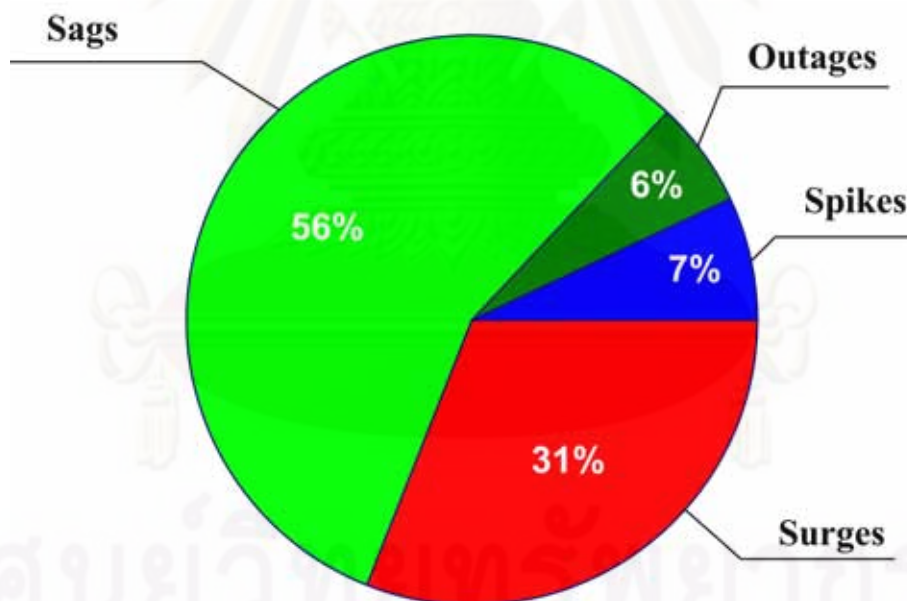


Figure 1.2: Types of Power Quality Disturbances (source: EPRI 1994)

### 1.3 Motivation of The Work

Voltage sag is a short-duration reduction in rms voltage between 0.1 and 0.9 *pu.* with duration from 0.5 cycles to 1 *min* [1,3,9,10]. Voltage sags that affect sensitive load are usually caused by faults somewhere on transmission and distribution systems [11].

Voltage magnitude and duration are essential characteristics of voltage sag. The magnitude of voltage sags mainly depends on the fault location, fault type and some other factors such as the pre-fault voltage, transformer connection, and fault impedance [3, 6, 12]. The voltage sag magnitude, which is expressed in percent or per unit, is calculated by short-circuit analysis. The voltage sag duration is defined as the flow duration of the fault current in a network. Therefore, the duration is determined by the characteristics of the system protection devices such as overcurrent relays, circuit breakers and fuses. Generally, the duration is calculated by adding the intentional time delay considering protection coordination to the fault clearing time of each device.

Much sensitive equipment is used in modern industrial such as computers, programmable logic controllers, adjustable speed drives, and robotics. Many industrial customers using sensitive equipment suffer from voltage sags. Malfunctioning or failure of this equipment can be caused by voltage sags that lead to work or production shutdowns [13–17]. To analyze these cases, it is essential to have information of equipment sensitivity. If the magnitude and duration of voltage sag exceed the threshold of equipment, the equipment is damaged, and such damage can effect an entire process at the customer site with an associate cost. Therefore, characteristics of the equipment sensitivity must be provided by the manufacturer or obtained by tests. System performance, which can be expressed by the expected sag frequency in the site, can be estimated through the monitoring of the supply or stochastic prediction methods [18].

In a distribution system, protection devices are circuit breakers, reclosers and fuses. The coordination of protection devices is presented as fault clearing process. Poor coordination adversely impacts the overall power quality especially from the momentary voltage interruption and voltage sags [19, 20]. For example, improper coordination between a midline recloser and downstream fuses in a fuse-saving scheme can cause unnecessary momentary interruptions and voltage sags downstream from the recloser. In practice, the recloser in fast mode should operate for a temporary fault and give the fault a chance to clear and operate faster than the fuse. For a permanent fault, a lateral fuse should be opened to clear the fault. However, the duration of recloser and fuse setting may be longer than an allowed duration of sensitive equipment. Therefore, recloser-fuse system could not protect the sensitive equipment.

To mitigate the impacts of voltage sags, the sensitivity of the equipment at a point of interest and the coordination of protection devices need to be determined [21–23]. Normally, monitoring power quality is a common way to evaluate the voltage sags. However, the limitation of this method is the high cost and time for recording events. Two stochastic prediction methods that are the method of critical distance and the method of fault position have been proposed. The method of critical distance is a simple technique of voltage sags

prediction based on the voltage divider model [2, 24–29]. It is suitable for radial system, but not to meshed systems. For the method of fault position, several points of a network are chosen and the voltage sags is determined by fault calculation at the chosen point. The limitation of the method of fault position is not efficient for large power system because many fault positions have to be simulated in order to obtain more accurate sags prediction. However, the method of fault position can be used to obtain the voltage sags and analyze fault events in a distribution system.

Regarding the above mentioned issues, the objective of this research can be summarized as follows:

- **To develop a method of fault position for voltage sags calculation**

Various parameters in a method of fault position have been developed and simulated to analyze the voltage sags events in a distribution system. This method uses the influence of fault distribution along line that enables the characterization of voltage sags at any point of interest.

- **To develop a stochastic method for voltage sags prediction**

A stochastic method has been developed for voltage sags prediction. This method applies a coordination of protection devices and a sensitive characteristic of the equipment sensitivity to predict the characterization of voltage sags at any point of interest, e.g. using the protection device characteristics, the characteristics of the sensitive equipment.

- **To investigate and analyze an area of vulnerability at any sensitive point of interest**

An area of vulnerability to investigate for voltage sags prediction. This area is analyzed by considering a sags threshold, a characteristic of protection device.

- **To determine sags frequency and sags index for voltage sags prediction**

Sags frequency and index is determined and analyzed with consideration of the influence of fault distribution along line, and uncertainty of fault.

As a result of this thesis, impacts of voltage sags and protection coordination on sensitive equipment can be evaluated. Accurate estimates of voltage sags and protection coordination can serve sensitive customers and power distribution companies for assuring their own status among the several demand customers as well as the electricity authorities.

## **1.4 Outline of Dissertation**

This section presents the summary of all chapters in this dissertation.



## **Chapter 2**

In this chapter several definitions of voltage sags in distribution systems are presented. Impacts of voltage sags on a sensitive equipment are also discussed in this chapter. For the characteristic of sensitive equipment, voltage tolerance curves are shown for understanding the limited of voltage sags on the sensitive equipment. Area of vulnerability for the sensitive equipment also presents in this chapter. Moreover, the influence of the fault distribution along distribution line (uniform, normal, and exponential) are also presented.

## **Chapter 3**

Chapter 3 presents the calculation of fault current and also fault voltage at all buses when a fault occurs. This presents fault equations of symmetrical and asymmetrical fault occurring at bus or along line by using the method of fault position. Coordination of protection devices are also shown and discussed in this chapter to show the coordination range of protection. The formulation of protection devices is provided in order to determine the protection coordination range.

## **Chapter 4**

In this chapter, voltage sags frequency and voltage sags index are presented. They are able to analyze sags on the sensitive equipment in the distribution system. The formulation of sags index consists of two equations that are  $SARFI_X$  and  $SARFI_{curve}$ . They are based on the voltage sags threshold and the sensitive equipment characteristic curve.

## **Chapter 5**

Results of the assessment of voltage sags are presented in this chapter. This presents the approach to analyze type of protection device that can be chosen by considering the coordination of protection with the sensitive equipment. Area of vulnerability where the fault will lead to voltage sags on the sensitive equipment at a given observation bus is also described with consideration of protection coordination. Moreover, results of sag indices are also presented with considering Monte Carlo Simulation for stochastic fault events.

## **Chapter 6**

This chapter presents conclusions and suggests for further work.

## CHAPTER II

### VOLTAGE SAGS IN DISTRIBUTION SYSTEMS

#### 2.1 Introduction

This chapter presents definitions and characteristics of voltage sags which is also known as voltage dips. The main causes of voltage sags are faults occurring in a power systems. The characteristic of a sensitive equipment is also presented as voltage tolerance curves in this chapter. The area of vulnerability of equipment is defined to help customers to understand the sensitivity of their equipment about voltage sags. Moreover, fault distribution is presented for analyzing fault occurrence along line.

#### 2.2 Voltage Sags Definition and Characteristic

The main characteristics of voltage sags are the sags duration, the sags magnitude and the sags frequency. The International Electrotechnical Commission (IEC) has defined a voltage sag in IEC 61000-4-30 "Power Quality Measurement Standard" as "*Voltage sag or voltage dip is temporary reduction of the voltage at a point in the electrical system below a threshold*" [10].

According to the IEEE Standard 1159 – 1995 "IEEE recommended practice for monitoring electric power quality", a voltage sag defines as "*Voltage sag or voltage dip is a decrease to between 0.1 and 0.9 pu. in rms voltage at the power frequency for duration of 0.5 cycle to 1 min*" [1].

BS EN 501560 : 2000 "Voltage characteristics of electricity supplied by public distribution systems" defines a voltage sag as "*A sudden reduction of the supply voltage to a value between 90 % and 1% of the declared voltage, followed by a voltage recovery after a short period of time. Conventionally the duration of a voltage dip is between 10 ms and 1 minute. The depth of a voltage sags is defined as the difference between the minimum rms voltage during the voltage dip and the declared voltage. Voltage changes which do not reduce the supply voltage to less than 90 % of the declared voltage are not considered to be dips*" [8].

From the previous definition, it is shown that the meaning of voltage sags and voltage dip are the same. The values of voltage sags in this dissertation are referred as the remaining voltage or the during-fault voltage.

According to [3] voltage magnitude and duration are essential characteristics of voltage

sags. The magnitude of voltage sags is the remaining magnitude expressed in percent or per unit. Voltage sags magnitude mainly depends on the fault location, fault type and some other factors such as the pre-fault voltage, transformer connection, and fault impedance [6, 30].

The voltage sag duration is defined as the flow duration of the fault current in a network when the voltage magnitude is below the sag threshold. For three phase system, sag duration is the amount of time during at least one of the rms voltages is below the voltage threshold. The duration of voltage sags can be determined from the start of voltage sags and ends of voltage sags. The voltage sags starts when at least one of rms voltages reduce below the voltage threshold. The ends of voltage sags is determined when all three rms voltages have above the voltage threshold. Figure 2.1 shows rms voltage with sag magnitude and duration in a three-phase system [31].

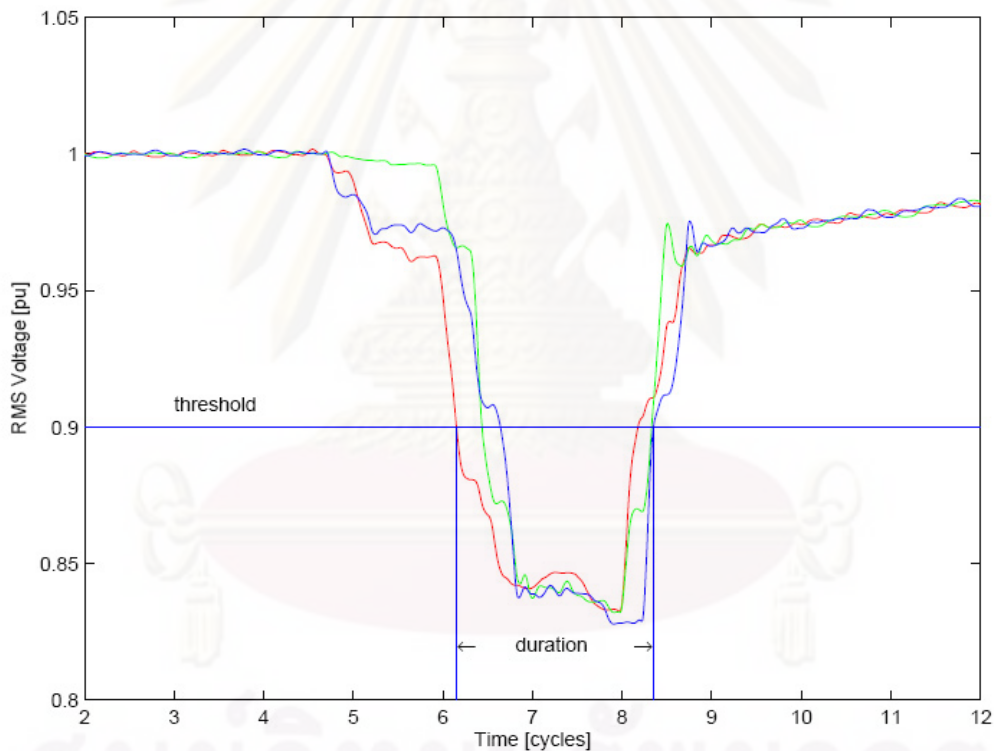


Figure 2.1: Voltage sags duration and magnitude

### 2.3 Voltage Sags on Sensitive Equipment

In the past, there were not many complaints about power quality conditions from customers because their equipments were analog clocks or standard induction motors. Nowadays, a lot of sensitive electronic equipment is widely used in modern power systems such as digital

clocks, VCRs, electronic equipment, power converters and adjustable speed drivers or digital equipments [32]. All sensitive equipment rely on continuous power to operate correctly.

Therefore, voltage sags are the most important power quality for customers and have gained more interest due to their consequences on the performance of the sensitive equipment. Malfunction or failure of the equipment that leads to work or production losses can be caused by voltage sags [33–35]. The impact to the customers depends on the voltage sag magnitude, the sag duration, and the sensitivity of the customer equipment [1].

In this dissertation, the main causes of voltage sags are faults occurring in power systems. A typical distribution system which consists of customers, and protection devices; is shown in figure 2.2. In this figure, a fault occurs on feeder 3 and is a fault downstream of customer C then customer C will be experienced voltage sags that is a reduction in voltage. If the remaining voltage of customer C is under the voltage threshold, the protection device of the main feeder will operate and isolate the fault. Therefore, customer C will experience an interruption due to the fault. In other feeders, customers A and B also have an experienced voltage sags because of the fault occurs on the feeder 3. However, those customers will not be interrupted if the remaining voltages are higher than the voltage threshold of customers A and B.

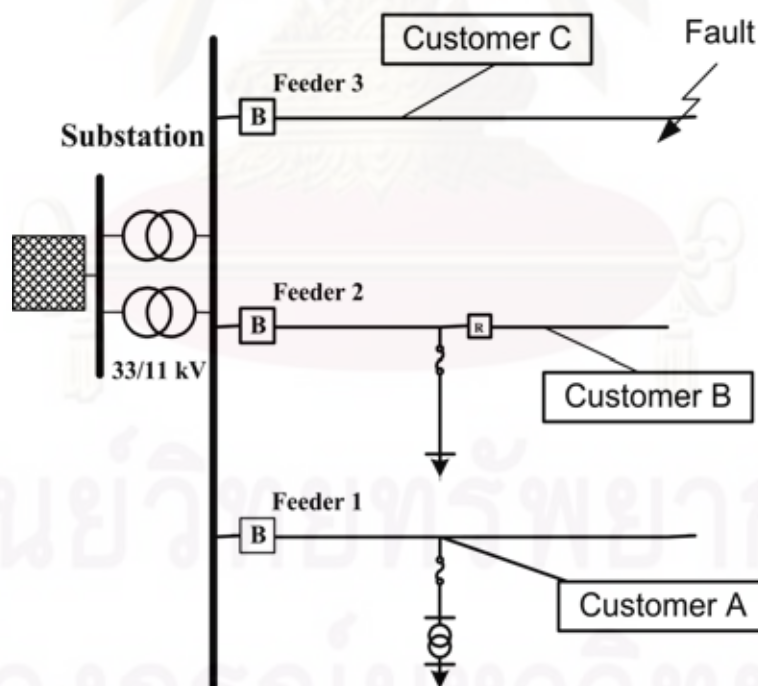


Figure 2.2: A fault in a typical distribution system



## 2.4 Voltage Tolerance Curves

Information Technology Industry Council curve (ITIC) provides guidelines and defines the withstand capability of sensitive equipment loads and devices for protection from power quality variations [36]. It is useful for understanding the limited of voltage sag on sensitive equipment [1,36–38]. Each type of sensitive equipment has different curve [39]. An example of ITIC curve represents magnitude and duration of the event as shown in Fig. 2.3.

SEMI F47 [40] "Specification for semiconductor processing equipment voltage sag immunity" is a standard that defines the voltage threshold that semiconductor processing must be controlled through without interruption during conditions identified in the area above the standard line (Fig. 2.3). Points above the threshold are presumed to cause damage to the equipment. The lower region will use to determine the acceptable sag magnitude and duration level.

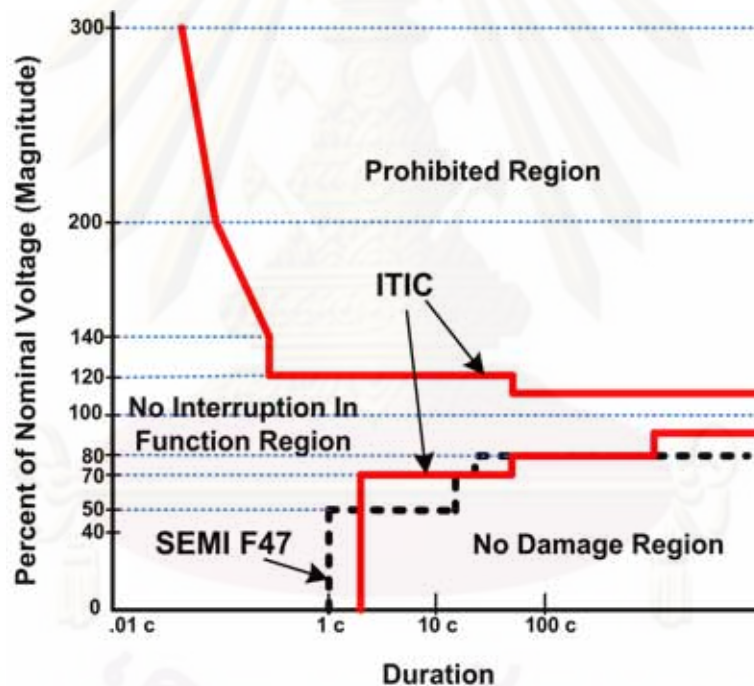


Figure 2.3: Information Technology Industrial Council (ITIC) and SEMI curves

A typical voltage tolerance curve is shown in figure 2.4 where the voltage threshold  $V_{threshold}$  is a minimum voltage that the equipment can operate correctly. The maximum of time  $T_{max}$  is defined as the time during which the equipment can operate and control when its voltage is below the threshold of voltage  $V_{threshold}$ .

According to [3] table 2.1 shows the voltage tolerance characteristic of sensitive equipments (PLC, AC control relay, motor starter, personal computer, etc.) [41]. In table 2.1, the

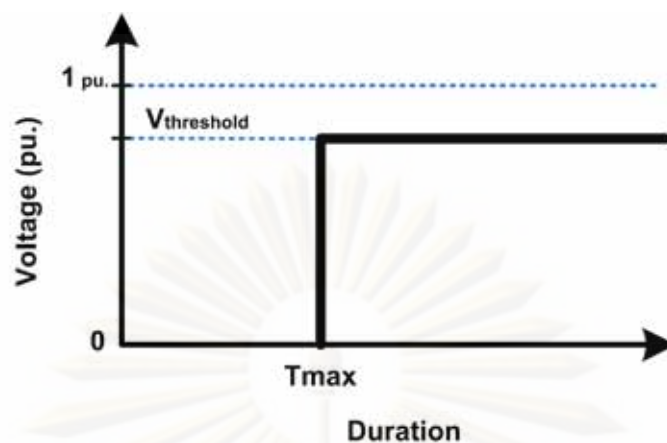


Figure 2.4: A typical voltage tolerance curve

voltage threshold  $V_{threshold}$  and the maximum of time  $T_{max}$  of PLC are  $0.60 pu.$  and  $260 ms$ , respectively. It means that any sags event with the fault duration longer than  $260 ms$  and the voltage sags lower than  $0.60 pu.$ ; will lead to interrupt or malfunction of the equipment.

In several research, the typical voltage tolerance curve is used to analysis the sags event as a fixed voltage threshold  $X\%$  in the conventional method [42, 43]. Voltage threshold can be determined by a given sag duration. However, the conventional method cannot give an accurate result because it does not consider the change in characteristic of sag [42, 44–46], e.g. the magnitude of voltage and the duration of fault event. In this thesis, ITIC curve is defined as the voltage tolerance curve of the sensitive equipment.

Table 2.1: Voltage tolerance characteristics of several equipments

Equipment	$V_{threshold}$	$T_{max}$
PLC	$0.60 pu.$	$260 ms$
PLC Input Card	$0.55 pu.$	$40 ms$
5hp AC Drive	$0.75 pu.$	$50 ms$
AC Control Relay	$0.65 pu.$	$20 ms$
Motor Starter	$0.50 pu.$	$50 ms$
Personal Computer	$0.60 pu.$	$50 ms$

## 2.5 Area of Vulnerability on Sensitive Equipment

A region of the network that includes a part of line or whole line where the occurrence of the faults will lead to the reduction in voltage at a sensitive load to drop below the voltage

ride-through capability of the sensitive equipment is called the area of vulnerability (AOV). The area of vulnerability responding to the sensitive load is essential to estimate the expected number of voltage sags from the utility systems as shown in Fig. 2.5. It is important for customers to understand the sensitivity of their equipments to voltage sags [13,47,48]. The area of vulnerability for fault problems in the power network can be determined when the sensitive equipment is known [44, 49, 50]. Moreover, it can also help in evaluating problems due to utility system faults. The area of vulnerability also can be applied to analyze impacts of problems from other voltage level system to the sensitive equipment, i.e. from transmission system.

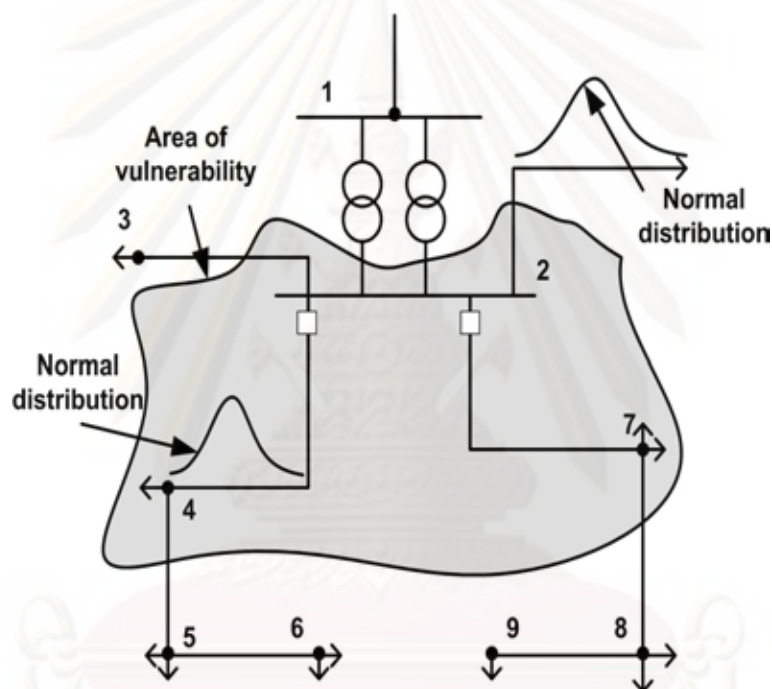


Figure 2.5: Area of vulnerability and fault distribution along lines.

## 2.6 Fault Distribution Along Line

The main causes of voltage sags on the sensitive equipment or load points are faults occurring on lines of a power system. Faults in the power system consists of symmetrical faults (three-phase fault) and asymmetrical faults (single line-to-ground fault, line-to-line fault, and double line-to-ground fault) [45]. The symmetrical fault makes more impacts on the customers or load points in the power system because it leads to deep sags on the system (large load points in the system experience voltage sags). However, the symmetrical fault is rare in the power system. Major faults in the power system are asymmetrical faults. Single

line-to-ground fault occurs most often among asymmetrical faults in the system (about 75 – 80%). Asymmetrical faults are common problems in the power system.

Typical causes of faults in the power system are the adverse weather (lightning, storm), equipment errors, etc. All of those causes are random nature of fault, therefore, they might not be distributed uniformly occurrence along line. Actually, some lines or parts of line have higher fault occurrence than other lines or parts of line because of the random causes and the nature of fault, therefore, the rate of fault occurrence maybe higher than other [51]. It is necessary to concern the fault rate to predict voltage sags in the power system. Normally, the fault rate is used and analyzed by the uniform distribution. However, the fault rate may consists of uniform, normal, and exponential distribution of fault [45, 46, 52–54]. Those of fault distribution are shown in figures 2.6 to 2.8 and will be analyzed.

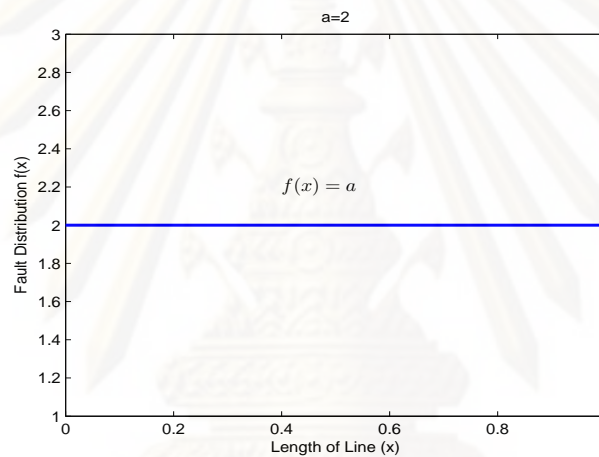


Figure 2.6: Uniform distribution with the same fault distribution value

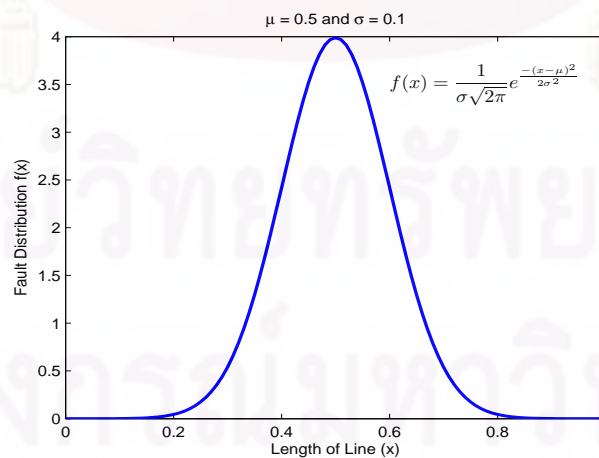


Figure 2.7: Normal distribution with the mean value  $\mu = 0.5$  and the standard deviation value  $\sigma = 0.1$



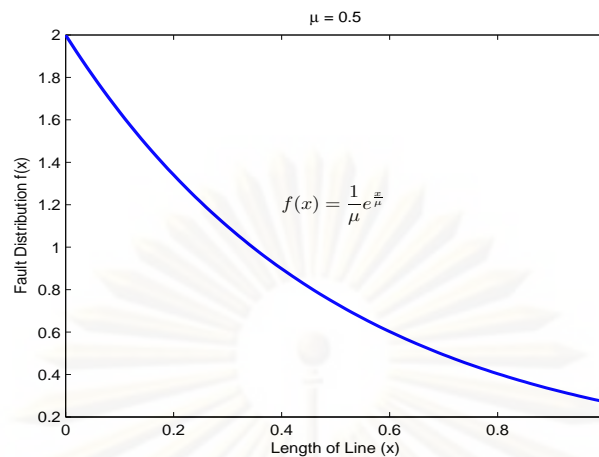


Figure 2.8: Exponential distribution with the mean value  $\mu = 0.5$

## 2.7 Summary

The analysis presented in this chapter offers the means for voltage sags, i.e. definitions of voltage sags (sag magnitude and duration), voltage sag tolerance curves (ITIC and SEMI curves), and the fault distribution.

Impacts of voltage sags on the power system are very important issues in power quality problems for customers and utilities. Voltage sags have more concerns in the modern power system in the present. Fault events could be the most important of power quality problems (voltage sags, interruption). Magnitude and duration of voltage sags are presented in this chapter. Furthermore, the information of impacts of voltage sags is also necessary for both customers and utilities for their improved power network.

In this chapter, the sags tolerance curves is also presented for sensitive equipment in customer site. ITIC and SEMI curves will show how to analysis voltage sags on sensitive equipment, and voltage threshold for determining equipment conditions (damage, interruption, or safe conditions). From that, area of vulnerability for customers can be analyzed to know which line or parts of line lie inside the vulnerability area. It is very useful for customers and utilities in their power quality analysis.

Moreover, the fault distribution is also presented in the analysis, e.g. uniform, normal and exponential fault distributions. Based on that, a random condition by fault distribution in the power system is considered and analyzed for voltage sags.

# CHAPTER III

## FAULT CALCULATION AND PROTECTION COORDINATION

### 3.1 Introduction

Main causes of voltage sags in sensitive equipment are faults in power systems, i.e. symmetrical and asymmetrical faults. Moreover, faults can occur anywhere in the power system, e.g. occurring at buses or along a line. Therefore, a short-circuit method should be chosen for calculating voltage sags not only faults occurring at bus but also along the line.

A fault position method is shown as a short-circuit calculation for formulating during-fault voltage and current when a fault occurs along a line [46, 55]. This chapter presents equations of a during-fault voltage and current when a fault occurs at bus or along a line for symmetrical and asymmetrical faults in the power system based on the fault position method.

In a distribution system, overcurrent relays, reclosers, and fuses are main protective devices for protecting faults. This chapter presents protective devices and characteristics for evaluating voltage sags. Equations of circuit breakers, reclosers, and fuses are shown in order to take into account the effect of protection coordination with sensitive equipment. From that, a coordination of protective devices shows to have a correct operation for isolating faults and protecting sensitive equipment.

### 3.2 Sags Calculation

Voltage sags can be determined by computational network analysis as measurements. Therefore, the modeling of the network and the calculation of voltage sags are very important to archive the best results for the system behavior in the sags analysis [56–58].

In this dissertation, voltage sag is caused by a fault occurring in a power system. The category of faults consists of temporary, permanent, and self-clearing. The fault position method has been applied for voltage sag calculation when the fault occurs at bus or along the line.

### 3.2.1 Faults at Bus

Figure 3.1 shows a fault occurring in a typical power system. In this figure, a sensitive equipment is connected at bus  $m$  as an observing bus or a sensitive bus [59]. The fault occurs at bus  $i$  leads to voltage sags on the sensitive bus  $m$ .

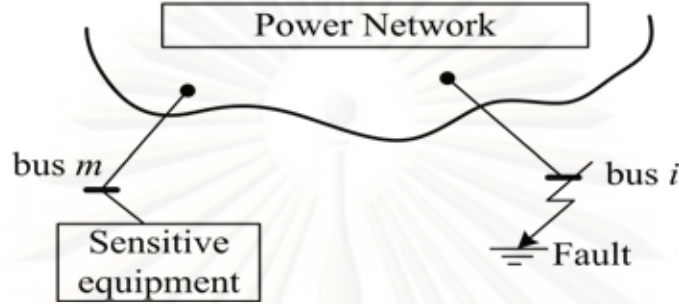


Figure 3.1: A fault occurs at bus  $i$  in a typical power system.

Positive, negative and zero sequences are used for describing and representing the behavior of the power system. Equations (3.1) and (3.2) show the basic transformation for currents and voltages sequence components, respectively. The sequences of  $I^z$ ,  $I^p$ , and  $I^n$  are identified by the zero, positive and negative sequence currents. In equation (3.2),  $V^z$ ,  $V^p$ , and  $V^n$  are the zero, positive, and negative sequence of voltages.

$$\begin{bmatrix} I^z \\ I^p \\ I^n \end{bmatrix} = \frac{1}{3} \begin{bmatrix} 1 & 1 & 1 \\ 1 & a^2 & a \\ 1 & a & a^2 \end{bmatrix} \begin{bmatrix} I^a \\ I^b \\ I^c \end{bmatrix} \quad (3.1)$$

$$\begin{bmatrix} V^z \\ V^p \\ V^n \end{bmatrix} = \frac{1}{3} \begin{bmatrix} 1 & 1 & 1 \\ 1 & a & a^2 \\ 1 & a^2 & a \end{bmatrix} \begin{bmatrix} V^a \\ V^b \\ V^c \end{bmatrix} \quad (3.2)$$

where

$I^a$ ,  $I^b$ , and  $I^c$  : the currents of phase  $a$ ,  $b$ , and  $c$ , respectively,

$V^a$ ,  $V^b$ , and  $V^c$  : the voltages of phase  $a$ ,  $b$ , and  $c$ , respectively.

The  $a$ -operator equals to  $e^{j\frac{2\pi}{3}}$ .

In this section, the fault position method will be defined to determine during-fault voltages and currents when the fault occurs at bus in the power system. From figure 3.1, when fault occurs at bus  $i$  of the power system, the during-fault voltage and current at bus  $m$  can be expressed and calculated based on the Z-bus matrix.

#### 3.2.1.1 During-fault Current

Four short-circuit types in the power system will be calculated and defined for determining during-fault current.

### a. Three-phase Fault

The negative and zero sequence currents are zero when the three-phase fault occurs. Therefore, fault currents are determined as shown in equation (3.3).

$$I = I^p = \frac{V_{pref,i}}{Z_{ii}^p} \quad \text{and} \quad I^n = I^z = 0 \quad (3.3)$$

where

- $I^p, I^n,$  and  $I^z$  : the positive, negative, and zero sequence currents,
- $V_{pref,i}$  : the pre-fault voltage at fault bus  $i$ ,
- $Z_{ii}^p$  : the diagonal element  $Z_{ii}$  of the positive sequence impedance matrix.

### b. Single line-to-ground Fault (phase $a$ )

Equations (3.4) and (3.5) show the during-fault currents and voltages of a single line (phase  $a$ )–to–ground fault at fault bus  $i$ .

$$I^b = I^c = 0 \quad (3.4)$$

$$V^a = 0 \quad (3.5)$$

Based on the sequence transformation (in equation (3.1)) and equations of current (3.4) and voltage (3.5), the sequence currents and fault currents can be shown as follows.

$$I^z = I^p = I^n = \frac{V_{pref}}{Z_{ii}^z + Z_{ii}^p + Z_{ii}^n} \quad (3.6)$$

$$I^a = \frac{3V_{pref}}{Z_{ii}^z + Z_{ii}^p + Z_{ii}^n} \quad (3.7)$$

### c. Line-to-line Fault (phases $b$ and $c$ )

Equations (3.8) and (3.9) show the sequence currents and fault voltages when the line-to-line fault occurs.

$$I^a = 0 \quad \text{and} \quad I^b = -I^c \quad (3.8)$$

$$V^b = V^c \quad (3.9)$$

Applying the sequence transformation (3.1), the sequence and fault currents are shown in equations (3.10) and (3.11).



$$I^z = 0 \quad \text{and} \quad I^p = I^n = \frac{V_{pref}}{Z_{ii}^p + Z_{ii}^n} \quad (3.10)$$

$$I^b = -I^c = -j\sqrt{3} \frac{V_{pref}}{Z_{ii}^p + Z_{ii}^n} \quad (3.11)$$

#### d. Double line-to-ground Fault (phases *b* and *c*)

Fault currents and voltages when a double-line-to-ground fault occurs, are shown in equations (3.12) and (3.13).

$$I^a = 0 \quad (3.12)$$

$$V^b = V^c = 0 \quad (3.13)$$

The sequence and fault currents are shown from equations (3.14) to (3.18) by applying the sequence transformation.

$$I^p = \frac{V_{pref}}{Z_{ii}^p + \frac{Z_{ii}^z Z_{ii}^n}{Z_{ii}^z + Z_{ii}^n}} \quad (3.14)$$

$$I^z = -I^p \frac{Z_{ii}^n}{Z_{ii}^n + Z_{ii}^z} \quad (3.15)$$

$$I^n = -I^p \frac{Z_{ii}^z}{Z_{ii}^n + Z_{ii}^z} \quad (3.16)$$

$$I^b = \frac{V_{pref}}{Z_{ii}^p + \frac{Z_{ii}^z Z_{ii}^n}{Z_{ii}^z + Z_{ii}^n}} \left( \frac{-Z_{ii}^n}{Z_{ii}^z + Z_{ii}^n} + a^2 + \frac{-a Z_{ii}^z}{Z_{ii}^z + Z_{ii}^n} \right) \quad (3.17)$$

$$I^c = \frac{V_{pref}}{Z_{ii}^p + \frac{Z_{ii}^z Z_{ii}^n}{Z_{ii}^z + Z_{ii}^n}} \left( \frac{-Z_{ii}^n}{Z_{ii}^z + Z_{ii}^n} + a + \frac{-a^n Z_{ii}^z}{Z_{ii}^z + Z_{ii}^n} \right) \quad (3.18)$$

#### 3.2.1.2 During-fault Voltages

Based on the sequence currents and Z-bus matrix, the during-fault voltage can be formulated for different types of faults in the power system. The during-fault phase voltage can be calculated based on its sequence voltages, e.g. positive, negative and zero sequence voltages. The change in voltage when a fault occurs can be expressed as

$$\begin{bmatrix} \Delta V^z \\ \Delta V^p \\ \Delta V^n \end{bmatrix} = \begin{bmatrix} 1 & 1 & 1 \\ 1 & a^2 & a \\ 1 & a & a^2 \end{bmatrix} \begin{bmatrix} \Delta V^a \\ \Delta V^b \\ \Delta V^c \end{bmatrix} \quad (3.19)$$

When a symmetrical fault occurs at fault bus  $i$ , the during-fault voltage at bus  $m$  is expressed as

$$V_{mi} = V_{pref,m} + \Delta V_{mi} \quad (3.20)$$

where

- $V_{mi}$  : the during-fault voltage at bus  $m$  when a fault occurs at bus  $i$ ,
- $V_{pref,m}$  : the pre-fault voltage at bus  $m$ ,
- $\Delta V_{mi}$  : the change in voltage at bus  $m$  due to the fault at bus  $i$ .

For an asymmetrical fault, the during-fault voltages can be calculated based on the sequence components, e.g. positive, negative, and zero sequences. Similarly equation (3.20), the during-fault voltage for each sequence component can be formulated as follows.

$$V^z = 0 + \Delta V^z \quad (3.21)$$

$$V^p = V_{pref}^p + \Delta V^p \quad (3.22)$$

$$V^n = 0 + \Delta V^n \quad (3.23)$$

where

- $V^z, V^p, \text{ and } V^n$  : the zero, positive, and negative sequence during-fault voltages,
- $V_{pref}^p$  : the positive sequence pre-fault voltage,
- $\Delta V^z, \Delta V^p, \text{ and } \Delta V^n$  : the change in sequence voltages.

Applying the symmetrical components transformation, the phase during-fault voltages can be expressed as follows.

$$V^a = V^z + V^p + V^n \quad (3.24)$$

$$V^b = V^z + a^2 V^p + a V^n \quad (3.25)$$

$$V^c = V^z + a V^p + a^2 V^n \quad (3.26)$$

where

$V^a, V^b,$  and  $V^c$  : the phase voltage,  
 $a$  : the  $a$ -operator.

Substitute equations (3.21), (3.22) and (3.23) into equations (3.24), (3.25), and (3.26), the phase during-fault voltages can be given.

$$V^a = V_{pref}^p + \Delta V^z + \Delta V^p + \Delta V^n \quad (3.27)$$

$$V^b = a^2 V_{pref}^p + \Delta V^z + a^2 \Delta V^p + a \Delta V^n \quad (3.28)$$

$$V^c = a V_{pref}^p + \Delta V^z + a \Delta V^p + a^2 \Delta V^n \quad (3.29)$$

In this section, during-fault voltages for a symmetrical or asymmetrical fault occurs at fault bus  $i$  (in figure 3.1) are calculated as following.

#### a. Three-phase (or balanced) Fault

When a three-phase fault occurs at bus  $i$ , the current injected into fault bus  $i$  due to a three-phase fault can be calculated as

$$I_i = \frac{-V_{pref,i}}{Z_{ii}} \quad (3.30)$$

where

$V_{pref,i}$  : the pre-fault voltage of fault bus  $i$ ,  
 $Z_{ii}$  : the diagonal elements of the  $Z$ -bus matrix.

Therefore, the change in voltage due to the fault current in equation (3.30) can be shown as follows.

$$\Delta V_{mi} = -Z_{mi} \frac{V_{pref,i}}{Z_{ii}} \quad (3.31)$$

Applying equation (3.31) to equation (3.20), the during-fault voltage when the three-phase fault occurs at bus  $i$  can be shown in equation (3.32).

$$V_{mi} = V_{pref,m} - Z_{mi} \frac{V_{pref,i}}{Z_{ii}} \quad (3.32)$$

#### b. Single line-to-ground Fault (phase a)

When a single line-to-ground fault occurs in the power system, the positive, negative, and zero sequence currents are the same. The sequence currents can be shown in following equation (3.33).

$$I_i^p = \frac{-V_{pref,i}}{Z_{ii}^p + Z_{ii}^n + Z_{ii}^z} \quad \text{and} \quad I_i^z = I_i^p = I_i^n \quad (3.33)$$

The change in sequence voltages at bus  $m$  when a single line-to-ground fault occurs at bus  $i$  are shown in equations from (3.34) to (3.36).

$$\Delta V_{mi}^p = -Z_{mi}^p \frac{V_{pref,i}}{Z_{ii}^p + Z_{ii}^n + Z_{ii}^z} \quad (3.34)$$

$$\Delta V_{mi}^n = -Z_{mi}^n \frac{V_{pref,i}}{Z_{ii}^p + Z_{ii}^n + Z_{ii}^z} \quad (3.35)$$

$$\Delta V_{mi}^z = -Z_{mi}^z \frac{V_{pref,i}}{Z_{ii}^p + Z_{ii}^n + Z_{ii}^z} \quad (3.36)$$

Therefore, the during-fault sequence voltages can be calculated as following.

$$V_{mi}^p = V_{pref,m} - Z_{mi}^p \frac{V_{pref,i}}{Z_{ii}^p + Z_{ii}^n + Z_{ii}^z} \quad (3.37)$$

$$V_{mi}^n = -Z_{mi}^n \frac{V_{pref,i}}{Z_{ii}^p + Z_{ii}^n + Z_{ii}^z} \quad (3.38)$$

$$V_{mi}^z = -Z_{mi}^z \frac{V_{pref,i}}{Z_{ii}^p + Z_{ii}^n + Z_{ii}^z} \quad (3.39)$$

From the during-fault sequence voltages, we can write the phase voltages as in equations from (3.40) to (3.42).

$$V_{mi}^a = V_{pref,m} - (Z_{mi}^p + Z_{mi}^n + Z_{mi}^z) \frac{V_{pref,i}}{Z_{ii}^p + Z_{ii}^n + Z_{ii}^z} \quad (3.40)$$

$$V_{mi}^b = a^2 V_{pref,m} - (a^2 Z_{mi}^p + a Z_{mi}^n + Z_{mi}^z) \frac{V_{pref,i}}{Z_{ii}^p + Z_{ii}^n + Z_{ii}^z} \quad (3.41)$$

$$V_{mi}^c = a V_{pref,m} - (a Z_{mi}^p + a^2 Z_{mi}^n + Z_{mi}^z) \frac{V_{pref,i}}{Z_{ii}^p + Z_{ii}^n + Z_{ii}^z} \quad (3.42)$$

### c. Line-to-line Fault (phases $b$ and $c$ )

The injected sequence current due to a line-to-line fault is shown in equation (3.43).

$$I_i^p = \frac{-V_{pref,i}}{Z_{ii}^p} \quad \text{and} \quad I_i^n = -I_i^p \quad (3.43)$$

When a line-to-line fault occurs, the zero sequence change in the voltage is zero. The changes in sequence voltages are shown as follows.

$$\Delta V_{mi}^p = -Z_{mi}^p \frac{V_{pref,i}}{Z_{ii}^p + Z_{ii}^n} \quad (3.44)$$



$$\Delta V_{mi}^n = Z_{mi}^n \frac{V_{pref,i}}{Z_{ii}^p + Z_{ii}^n} \quad (3.45)$$

From equations (3.44) and (3.45), we can formulated the phase voltages as follows.

$$V_{mi}^a = V_{pref,m} + (Z_{mi}^n - Z_{mi}^p) \frac{V_{pref,i}}{Z_{ii}^p + Z_{ii}^n} \quad (3.46)$$

$$V_{mi}^b = a^2 V_{pref,m} + (a Z_{mi}^n - a Z_{mi}^p) \frac{V_{pref,i}}{Z_{ii}^p + Z_{ii}^n} \quad (3.47)$$

$$V_{mi}^c = a V_{pref,m} + (a^2 Z_{mi}^n - a Z_{mi}^p) \frac{V_{pref,i}}{Z_{ii}^p + Z_{ii}^n} \quad (3.48)$$

#### d. Double line-to-ground Fault (phases $b$ and $c$ )

The sequence currents due to a double line-to-ground fault at fault bus  $i$  can be formulated.

$$I_i^p = \frac{-V_{pref,i}}{Z_{ii}^p + \frac{Z_{ii}^z Z_{ii}^n}{Z_{ii}^z + Z_{ii}^n}} = \frac{-V_{pref,i}(Z_{ii}^z + Z_{ii}^n)}{Z_{ii}^p Z_{ii}^z + Z_{ii}^n Z_{ii}^p + Z_{ii}^z Z_{ii}^n} \quad (3.49)$$

$$I_i^n = \frac{Z_{ii}^z}{Z_{ii}^p Z_{ii}^z + Z_{ii}^n Z_{ii}^p + Z_{ii}^z Z_{ii}^n} V_{pref,i} \quad (3.50)$$

$$I_i^z = \frac{Z_{ii}^n}{Z_{ii}^p Z_{ii}^z + Z_{ii}^n Z_{ii}^p + Z_{ii}^z Z_{ii}^n} V_{pref,i} \quad (3.51)$$

Equations from (3.52) to (3.54) show the change in sequence voltages due to the fault as follows.

$$\Delta V_{mi}^z = Z_{mi}^z \frac{Z_{ii}^z}{Z_{ii}^p Z_{ii}^z + Z_{ii}^n Z_{ii}^p + Z_{ii}^z Z_{ii}^n} V_{pref,p} \quad (3.52)$$

$$\Delta V_{mi}^p = V_{pref,p} + Z_{mi}^p \frac{-(Z_{ii}^z + Z_{ii}^n)}{Z_{ii}^p Z_{ii}^z + Z_{ii}^n Z_{ii}^p + Z_{ii}^z Z_{ii}^n} V_{pref,p} \quad (3.53)$$

$$\Delta V_{mi}^n = Z_{mi}^n \frac{Z_{ii}^n}{Z_{ii}^p Z_{ii}^z + Z_{ii}^n Z_{ii}^p + Z_{ii}^z Z_{ii}^n} V_{pref,p} \quad (3.54)$$

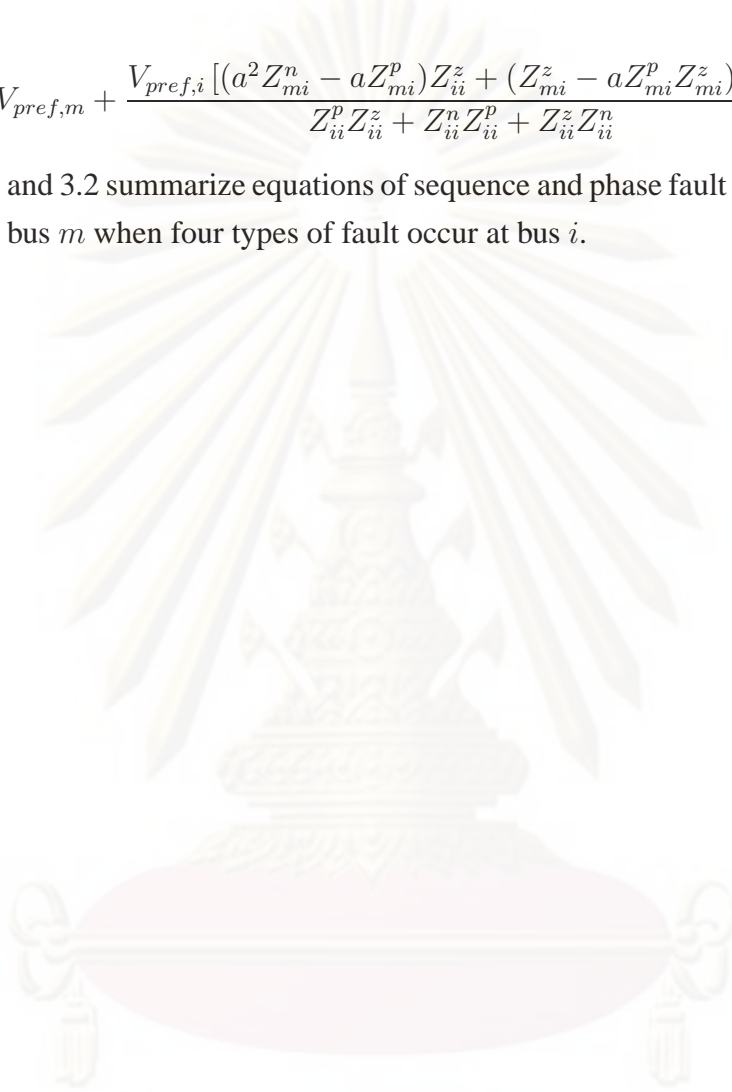
From above equations, the sequence phase voltage at bus  $m$  due to the fault at bus  $i$  can be expressed in equations (3.55), (3.56), and (3.57).

$$V_{mi}^a = V_{pref,m} + \frac{V_{pref,i} [(Z_{mi}^n - Z_{mi}^p) Z_{ii}^z + (Z_{mi}^z - Z_{mi}^p Z_{mi}^z) Z_{ii}^n]}{Z_{ii}^p Z_{ii}^z + Z_{ii}^n Z_{ii}^p + Z_{ii}^z Z_{ii}^n} \quad (3.55)$$

$$V_{mi}^b = a^2 V_{pref,m} + \frac{V_{pref,i} [(aZ_{mi}^n - a^2 Z_{mi}^p) Z_{ii}^z + (Z_{mi}^z - a^2 Z_{mi}^p Z_{mi}^z) Z_{mi}^z]}{Z_{ii}^p Z_{ii}^z + Z_{ii}^n Z_{ii}^p + Z_{ii}^z Z_{ii}^n} \quad (3.56)$$

$$V_{mi}^c = a V_{pref,m} + \frac{V_{pref,i} [(a^2 Z_{mi}^n - a Z_{mi}^p) Z_{ii}^z + (Z_{mi}^z - a Z_{mi}^p Z_{mi}^z) Z_{mi}^z]}{Z_{ii}^p Z_{ii}^z + Z_{ii}^n Z_{ii}^p + Z_{ii}^z Z_{ii}^n} \quad (3.57)$$

Tables 3.1 and 3.2 summarize equations of sequence and phase fault currents and phase fault voltages at bus  $m$  when four types of fault occur at bus  $i$ .



ศูนย์วิทยทรัพยากร  
จุฬาลงกรณ์มหาวิทยาลัย

Table 3.1: Summary equations of sequence and phase fault currents at bus  $m$  when four types of faults occur at bus  $i$ .

Fault types	The sequence fault current	The phase fault current
3PF	$I^p = \frac{V_{pref,i}}{Z_{ii}^p}$ and $I^z = I^n = 0$	$I = \frac{V_{pref,i}}{Z_{ii}^p}$
SLGF	$I^z = I^p = I^n = \frac{V_{pref}}{Z_{ii}^z + Z_{ii}^p + Z_{ii}^n}$	$I^b = I^c = 0$ and $I^a = \frac{3V_{pref}}{Z_{ii}^z + Z_{ii}^p + Z_{ii}^n}$
LLF	$I^z = 0$ and $I^p = I^n = \frac{V_{pref}}{Z_{ii}^p + Z_{ii}^n}$	$I^a = 0$ and $I^b = -I^c = -j\sqrt{3} \frac{V_{pref}}{Z_{ii}^p + Z_{ii}^n}$
DLGF	$I^p = \frac{V_{pref}}{Z_{ii}^p + \frac{Z_{ii}^z Z_{ii}^n}{Z_{ii}^z + Z_{ii}^n}}$ $I^z = -I^p \frac{Z_{ii}^n}{Z_{ii}^n + Z_{ii}^z}$ $I^n = -I^p \frac{Z_{ii}^z}{Z_{ii}^n + Z_{ii}^z}$	$I^a = 0$ $I^b = \frac{V_{pref}}{Z_{ii}^p + \frac{Z_{ii}^z Z_{ii}^n}{Z_{ii}^z + Z_{ii}^n}} \left( \frac{-Z_{ii}^n}{Z_{ii}^z + Z_{ii}^n} + a^2 + \frac{-a Z_{ii}^z}{Z_{ii}^z + Z_{ii}^n} \right)$ $I^c = \frac{V_{pref}}{Z_{ii}^p + \frac{Z_{ii}^z Z_{ii}^n}{Z_{ii}^z + Z_{ii}^n}} \left( \frac{-Z_{ii}^n}{Z_{ii}^z + Z_{ii}^n} + a + \frac{-a^2 Z_{ii}^z}{Z_{ii}^z + Z_{ii}^n} \right)$

Table 3.2: Summary equations of phase fault voltages at bus  $m$  when four types of faults occur at bus  $i$ .

Fault types	The phase fault voltage
3PF	$V_{mi} = V_{pref,m} - Z_{mi} \frac{V_{pref,i}}{Z_{ii}}$
SLGF	$V_{mi}^a = V_{pref,m} - (Z_{mi}^p + Z_{mi}^n + Z_{mi}^z) \frac{V_{pref,i}}{Z_{ii}^p + Z_{ii}^n + Z_{ii}^z}$ $V_{mi}^b = a^2 V_{pref,m} - (a^2 Z_{mi}^p + a Z_{mi}^n + Z_{mi}^z) \frac{V_{pref,i}}{Z_{ii}^p + Z_{ii}^n + Z_{ii}^z}$ $V_{mi}^c = a V_{pref,m} - (a Z_{mi}^p + a^2 Z_{mi}^n + Z_{mi}^z) \frac{V_{pref,i}}{Z_{ii}^p + Z_{ii}^n + Z_{ii}^z}$
LLF	$V_{mi}^a = V_{pref,m} + (Z_{mi}^n - Z_{mi}^p) \frac{V_{pref,i}}{Z_{ii}^p + Z_{ii}^n}$ $V_{mi}^b = a^2 V_{pref,m} + (a Z_{mi}^n - a Z_{mi}^p) \frac{V_{pref,i}}{Z_{ii}^p + Z_{ii}^n}$ $V_{mi}^c = a V_{pref,m} + (a^2 Z_{mi}^n - a Z_{mi}^p) \frac{V_{pref,i}}{Z_{ii}^p + Z_{ii}^n}$
DLGF	$V_{mi}^a = V_{pref,m} + \frac{V_{pref,i} [(Z_{mi}^n - Z_{mi}^p) Z_{ii}^z + (Z_{mi}^z - Z_{mi}^p Z_{mi}^z) Z_{mi}^z]}{Z_{ii}^p Z_{ii}^z + Z_{ii}^n Z_{ii}^p + Z_{ii}^z Z_{ii}^n}$ $V_{mi}^b = a^2 V_{pref,m} + \frac{V_{pref,i} [(a Z_{mi}^n - a^2 Z_{mi}^p) Z_{ii}^z + (Z_{mi}^z - a^2 Z_{mi}^p Z_{mi}^z) Z_{mi}^z]}{Z_{ii}^p Z_{ii}^z + Z_{ii}^n Z_{ii}^p + Z_{ii}^z Z_{ii}^n}$ $V_{mi}^c = a V_{pref,m} + \frac{V_{pref,i} [(a^2 Z_{mi}^n - a Z_{mi}^p) Z_{ii}^z + (Z_{mi}^z - a Z_{mi}^p Z_{mi}^z) Z_{mi}^z]}{Z_{ii}^p Z_{ii}^z + Z_{ii}^n Z_{ii}^p + Z_{ii}^z Z_{ii}^n}$



### 3.2.2 Faults Along Lines

In this section, the voltage sag at bus  $m$  will be calculated when a fault occurs along line  $k - j$  at a fault position  $f$  which is defined as the ratio of length between bus  $k$  and fault location  $f$  ( $L_{kf}$ ) to the length of the line  $k - j$  ( $L_{kj}$ ) or  $p = L_{kf}/L_{kj}$  as shown in figure 3.2.

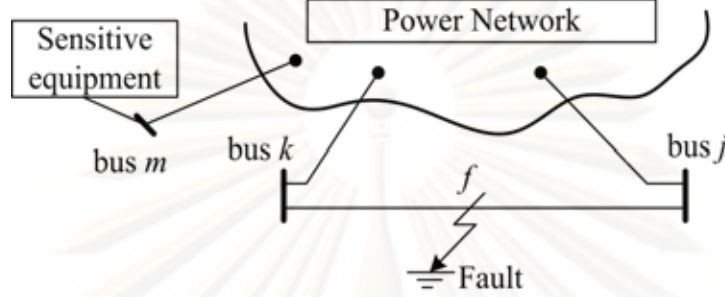


Figure 3.2: A fault occurs at point  $f$  along line from bus  $k$  to bus  $j$  in a typical power system.

The sequence transfer impedances between bus  $m$  to the fault position  $f$  can be determined as follows [46, 60].

$$Z_{mf}^z = Z_{mk}^z + (Z_{mj}^z - Z_{mk}^z)p \quad (3.58)$$

$$Z_{mf}^p = Z_{mk}^p + (Z_{mj}^p - Z_{mk}^p)p \quad (3.59)$$

$$Z_{mf}^n = Z_{mk}^n + (Z_{mj}^n - Z_{mk}^n)p \quad (3.60)$$

where

$Z_{mf}^z$ ,  $Z_{mf}^p$ , and  $Z_{mf}^n$  : the sequence transfer impedances of the sensitive load bus  $m$  and fault position  $f$ ,

$Z_{mk}^z$ ,  $Z_{mk}^p$ , and  $Z_{mk}^n$  : the sequence transfer impedances of buses  $m$  and  $k$ ,

$Z_{mj}^z$ ,  $Z_{mj}^p$ , and  $Z_{mj}^n$  : the sequence transfer impedances of buses  $m$  and  $j$ .

Moreover, the sequence driving impedance at the fault position  $f$  can be shown as follows.

$$Z_{ff}^z = (1-p)^2 Z_{kk}^z + p^2 Z_{jj}^z + 2p(1-p)Z_{kj}^z + p(1-p)z_{kj}^z \quad (3.61)$$

$$Z_{ff}^p = (1-p)^2 Z_{kk}^p + p^2 Z_{jj}^p + 2p(1-p)Z_{kj}^p + p(1-p)z_{kj}^p \quad (3.62)$$

$$Z_{ff}^n = (1-p)^2 Z_{kk}^n + p^2 Z_{jj}^n + 2p(1-p)Z_{kj}^n + p(1-p)z_{kj}^n \quad (3.63)$$

where

$$\begin{aligned} Z_{kk}^z, Z_{kk}^p, \text{ and } Z_{kk}^n &: \text{ the sequence driving impedances at bus } k, \\ Z_{jj}^z, Z_{jj}^p, \text{ and } Z_{jj}^n &: \text{ the sequence driving impedances at bus } j, \\ z_{kj}^z, z_{kj}^p, \text{ and } z_{kj}^n &: \text{ the sequence line impedances between buses } k \text{ and } j. \end{aligned}$$

The sequence voltages at bus  $m$ , when a fault occurs at fault position  $f$  between buses  $k$  and  $j$ , can be calculated from

$$V_{mf}^z = V_{pref,m}^z - Z_{mf}^z I_f^z \quad (3.64)$$

$$V_{mf}^p = V_{pref,m}^p - Z_{mf}^p I_f^p \quad (3.65)$$

$$V_{mf}^n = V_{pref,m}^n - Z_{mf}^n I_f^n \quad (3.66)$$

In equations from (3.64) to (3.66),  $Z_{mf}^z$ ,  $Z_{mf}^p$ , and  $Z_{mf}^n$  are the transfer bus impedances between bus  $m$  and the fault position  $f$  on the line  $k-j$  and can be calculated from equations (3.58), (3.59), and (3.60), respectively. The pre-fault voltage at the fault position  $f$  is

$$V_{pref,f} = V_{pref,k} + (V_{pref,j} - V_{pref,k})p \quad (3.67)$$

where  $V_{pref,k}$  and  $V_{pref,j}$  are the pre-fault voltages at buses  $k$  and  $j$ , respectively.

When a short-circuit fault occurs along line  $k-j$ , the fault currents and fault voltages at the sensitive load bus can be calculated and shown as follows.

### 3.2.2.1 Three-phase Fault (3PF)

For a balanced fault, sequence fault currents are

$$I_f^1 = \frac{V_{pref,f}^1}{Z_{ff}^1} \quad (3.68)$$

and  $I_f^z = I_f^n = 0$ .

The phase fault voltage for bus  $m$  due to a three-phase fault at the fault location  $f$  can be expressed as

$$V_{mf} = V_{pref,m} - \frac{Z_{mf}^p}{Z_{ff}^p} V_{pref,f} \quad (3.69)$$

### 3.2.2.2 Single line–ground Fault (SLGF)

Sequence fault currents for a phase  $a$  line–to–ground fault are

$$I_f^z = I_f^p = I_f^n = \frac{V_{pref,f}^p}{Z_{ff}^z + Z_{ff}^p + Z_{ff}^n} \quad (3.70)$$

From equation (3.70), phase voltages for three phase at the sensitive load bus  $m$  are

$$V_{mf}^a = V_{pref,m} - (Z_{mf}^z + Z_{mf}^p + Z_{mf}^n) \frac{V_{pref,f}^p}{Z_{ff}^z + Z_{ff}^p + Z_{ff}^n} \quad (3.71)$$

$$V_{mf}^b = a^2 V_{pref,m} - (Z_{mf}^z + a^2 Z_{mf}^p + a Z_{mf}^n) \frac{V_{pref,f}^p}{Z_{ff}^z + Z_{ff}^p + Z_{ff}^n} \quad (3.72)$$

$$V_{mf}^c = a V_{pref,m} - (Z_{mf}^z + a Z_{mf}^p + a^2 Z_{mf}^n) \frac{V_{pref,f}^p}{Z_{ff}^z + Z_{ff}^p + Z_{ff}^n} \quad (3.73)$$

where  $V_{pref,m}$  is the pre–fault phase voltage at bus  $m$ .

### 3.2.2.3 Line–to–line Fault (LLF)

For this type of fault, the sequence fault currents when a fault occurs between phases  $b$  and  $c$  are

$$I_f^p = I_f^n = \frac{V_{pref,f}^p}{Z_{ff}^p + Z_{ff}^n} \quad (3.74)$$

and  $I_f^z = 0$ .

Therefore, phase voltages at bus  $m$  due to a line–to–line fault occurs at fault position  $f$  along line  $k - j$  can be given as follows.

$$V_{mf}^a = V_{pref,m} - (Z_{mf}^p - Z_{mf}^n) \frac{V_{pref,f}^p}{Z_{ff}^p + Z_{ff}^n} \quad (3.75)$$

$$V_{mf}^b = a^2 V_{pref,m} - (a^2 Z_{mf}^p - a Z_{mf}^n) \frac{V_{pref,f}^p}{Z_{ff}^p + Z_{ff}^n} \quad (3.76)$$

$$V_{mf}^c = a V_{pref,m} - (a Z_{mf}^p - a^2 Z_{mf}^n) \frac{V_{pref,f}^p}{Z_{ff}^p + Z_{ff}^n} \quad (3.77)$$

### 3.2.2.4 Double line–to–ground Fault (DLGF)

Sequence fault currents for a double line–to–ground (phases  $b$  and  $c$ ) fault are

$$I_f^p = \frac{V_{pref,f}^p}{Z_{ff}^p + \frac{Z_{ff}^n Z_{ff}^z}{Z_{ff}^z + Z_{ff}^n}} \quad (3.78)$$

$$I_f^n = -I_f^p \frac{Z_{ff}^z}{Z_{ff}^z + Z_{ff}^n} \quad (3.79)$$

$$I_f^z = -I_f^p \frac{Z_{ff}^n}{Z_{ff}^z + Z_{ff}^n} \quad (3.80)$$

Equations from (3.81) to (3.83) show phase voltages at bus  $m$  due to a double line-to-ground fault occurring at the fault position  $f$ .

$$V_{mf}^a = V_{pref,m} - \frac{(Z_{mf}^p - Z_{mf}^z)Z_{ff}^n + (Z_{mf}^p - Z_{mf}^n)Z_{ff}^z}{Z_{ff}^z Z_{ff}^p + Z_{ff}^p Z_{ff}^n + Z_{ff}^n Z_{ff}^z} V_{pref,f} \quad (3.81)$$

$$V_{mf}^b = a^2 V_{pref,m} - \frac{(a^2 Z_{mf}^p - Z_{mf}^z)Z_{ff}^n + (a^2 Z_{mf}^p - a Z_{mf}^n)Z_{ff}^z}{Z_{ff}^z Z_{ff}^p + Z_{ff}^p Z_{ff}^n + Z_{ff}^n Z_{ff}^z} V_{pref,f} \quad (3.82)$$

$$V_{mf}^c = a V_{pref,m} - \frac{(a Z_{mf}^p - Z_{mf}^z)Z_{ff}^n + (a Z_{mf}^p - a^2 Z_{mf}^n)Z_{ff}^z}{Z_{ff}^z Z_{ff}^p + Z_{ff}^p Z_{ff}^n + Z_{ff}^n Z_{ff}^z} V_{pref,f} \quad (3.83)$$

Tables 3.3 and 3.4 summarize equations of sequence fault currents and phase fault voltages at bus  $m$  when four types of faults occur along line  $k - j$ .



Table 3.3: Summary equations of sequence fault currents at bus  $m$  when four types of faults occur along line  $k - j$  at a fault position  $f$ .

Fault Types	The sequence fault current
3PF	$I_f^p = \frac{V_{pref,f}^p}{Z_{ff}^p} \text{ and } I_f^z = I_f^n = 0$
SLGF	$I_f^z = I_f^p = I_f^n = \frac{V_{pref,f}^p}{Z_{ff}^z + Z_{ff}^p + Z_{ff}^n}$
LLF	$I_f^p = I_f^n = \frac{V_{pref,f}^p}{Z_{ff}^1 + Z_{ff}^n}$ $I_f^z = 0$
DLGF	$I_f^p = \frac{V_{pref,f}^p}{Z_{ff}^p + \frac{Z_{ff}^n Z_{ff}^z}{Z_{ff}^z + Z_{ff}^n}}, I_f^z = -I_f^p \frac{Z_{ff}^n}{Z_{ff}^z + Z_{ff}^n}, \text{ and } I_f^n = -I_f^p \frac{Z_{ff}^z + 3z_f}{Z_{ff}^z + Z_{ff}^n}$

Table 3.4: Summary equations of phase fault voltages at bus  $m$  when four types of faults occur along line  $k - j$  at a fault position  $f$ .

Fault Types	The phase fault voltage
3PF	$V_m = V_{pref,m} - \frac{Z_{mf}^p}{Z_{ff}^p} V_{pref,f}$
SLGF	$V_{mf}^a = V_{pref,m} - (Z_{mf}^z + Z_{mf}^p + Z_{mf}^n) \frac{V_{pref,f}}{Z_{ff}^z + Z_{ff}^p + Z_{ff}^n}$ $V_{mf}^b = a^2 V_{pref,m} - (Z_{mf}^z + a^2 Z_{mf}^p + a Z_{mf}^n) \frac{V_{pref,f}}{Z_{ff}^z + Z_{ff}^p + Z_{ff}^n}$ $V_{mf}^c = a V_{pref,m} - (Z_{mf}^z + a Z_{mf}^p + a^2 Z_{mf}^n) \frac{V_{pref,f}}{Z_{ff}^z + Z_{ff}^p + Z_{ff}^n}$
LLF	$V_{mf}^a = V_{pref,m} - (Z_{mf}^p - Z_{mf}^n) \frac{V_{pref,f}}{Z_{ff}^p + Z_{ff}^n}$ $V_{mf}^b = a^2 V_{pref,m} - (a^2 Z_{mf}^p - a Z_{mf}^n) \frac{V_{pref,f}}{Z_{ff}^p + Z_{ff}^n}$ $V_{mf}^c = a V_{pref,m} - (a Z_{mf}^p - a^2 Z_{mf}^n) \frac{V_{pref,f}}{Z_{ff}^p + Z_{ff}^n}$
DLGF	$V_{mf}^a = V_{pref,m} - \frac{(Z_{mf}^p - Z_{mf}^z) Z_{ff}^n + (Z_{mf}^p - Z_{mf}^n) Z_{ff}^z}{Z_{ff}^z Z_{ff}^p + Z_{ff}^p Z_{ff}^n + Z_{ff}^n Z_{ff}^z} V_{pref,p}$ $V_{mf}^b = a^2 V_{pref,m} - \frac{(a^2 Z_{mf}^p - Z_{mf}^z) Z_{ff}^n + (a^2 Z_{mf}^p - a Z_{mf}^n) Z_{ff}^z}{Z_{ff}^z Z_{ff}^p + Z_{ff}^p Z_{ff}^n + Z_{ff}^n Z_{ff}^z} V_{pref,f}$ $V_{mf}^c = a V_{pref,m} - \frac{(a Z_{mf}^p - Z_{mf}^z) Z_{ff}^n + (a Z_{mf}^p - a^2 Z_{mf}^n) Z_{ff}^z}{Z_{ff}^z Z_{ff}^p + Z_{ff}^p Z_{ff}^n + Z_{ff}^n Z_{ff}^z} V_{pref,f}$

### 3.3 Effect of Transformers on Voltage Sags

This section shows the effect of transformer connection on the phase voltage. In previous sections, fault equations for different fault types, i.e. three-phase, single line-to-ground, line to-line, and double line-to-ground faults, were considered and formulated. However, those equations are not considered the effect of transformer connections. There are two effects of the transformer connection which are: changing the symmetrical component and phase shift due to winding connection.

Depending winding connection of transformer, the during-fault voltage due to asymmetrical fault at primary side may be changed and modified at the secondary side of transformer.

We know that a delta or unground wye winding connection removes the zero sequence component when going through the transformer. This means that the zero sequence component of voltage and current in the secondary side of the transformer must sum up to zero.

In the case of delta-wye transformers, the positive sequence phase voltage on high voltage side leads the corresponding phase voltage on the low voltage side by  $30^\circ$ . For the negative sequence phase voltage, the corresponding phase shift is  $-30^\circ$ .

Therefore, fault calculations should consider the effect of phase shift in transformers. The accuracy fault calculation could be improved; and more reliable information could be supplied for relay protection setting and analyzed voltage sags.

### 3.4 Protection Coordination Analysis

#### 3.4.1 Protective Devices and Characteristics

The devices frequently used in a distribution protection system are overcurrent relays, reclosers, and fuses [61–63]. Fuse is one of the most common forms of protection used to deal with excessive currents. A fuse has two characteristics, i.e. the minimum melting (MM) and the total clearing (TC). The minimum melting is the relationship between the magnitude of the current and the time large enough to cause fuse to melt. The total clearing time is the total time required from the beginning of the fuse element to melt to the final circuit interruption; i.e. TC time is the minimum melting time plus the subsequent arcing time. For a recloser, S and F are two characteristics of the recloser which are slow and fast operation modes, respectively [20, 64].

Fuses contain inverse-time overcurrent characteristics. The straight line  $I^2t$  log-log plot is usually expressed for the minimum melting and total clearing time for fuses [65]. From the fuse characteristic on the log-log curve, it is better to approximate by the second order polynomial function. The general equation describing the fuse characteristic curve can

be expressed as the following equation [66].

$$\log(t) = a \times \log(I) + b \quad (3.84)$$

where

- $t$  and  $I$  : the associated time and current,
- $a$  and  $b$  : can be calculated from the curve fitting.

Circuit breakers (CB) and reclosers usually locate at the beginning and middle of main feeders [67]. The general characteristics of these devices can be shown as the following equation.

$$t(I) = \frac{A}{M^p - 1} + B \quad (3.85)$$

where

- $t$  : the operating time of inverse-time overcurrent device,
- $I$  : fault current seen by the device,
- $M$  : the ratio of  $I/I_{pickup}$  ( $I_{pickup}$  is relay current set point),
- $A, B, p$  : constants for selected curve characteristics.

For the protection settings, this dissertation uses mathematical equations for over-current relays and the straight line  $I^2t$  log–log curve to formulate protection coordination [68, 69]. The protection settings are done in the initial or existing condition. CBs and reclosers characteristics are assumed to be equipped with the extremely inverse characteristic of overcurrent relays. A typical radial distribution system is shown with protection devices

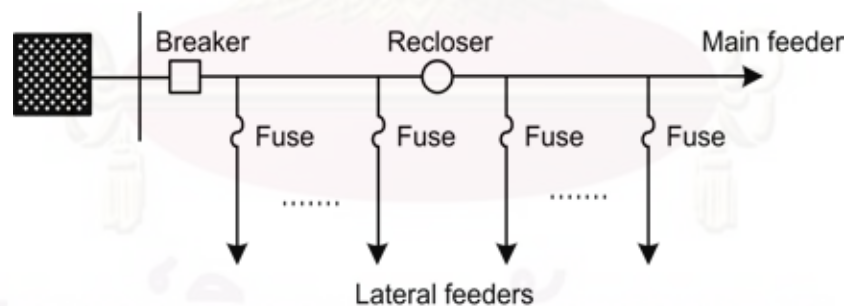


Figure 3.3: A typical distribution feeder.

in figure 3.3. In the typical distribution system, all demand loads are supplied from the main feeder.

### 3.4.2 Recloser-fuse Coordination

Figure 3.4 shows traditional recloser–fuse coordination in distribution systems [20, 70–74]. A recloser has two characteristic curves which are fast and slow (buck up) operation. In



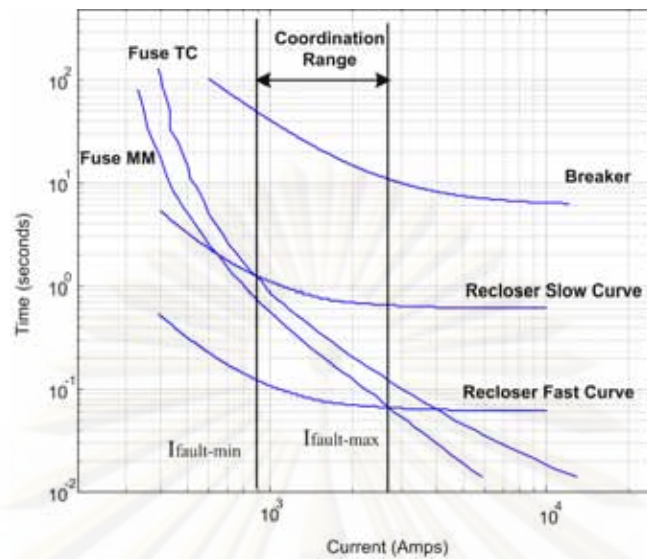


Figure 3.4: Recloser–Fuse coordination range

recloser function, there is an interval between each operation when the recloser remains open. If a fault is temporary, a recloser will clear before a fuse. If the fault persists after the recloser closes then the fault has to be a permanent one and hence fuse must operate.

The general coordination is that the fuse should only operate for a permanent fault on the load feeder. However, if the fault is a temporary fault or a fault occurs behind the recloser (downstream fault), the recloser should disconnect the circuit with fast operation and give the fault a chance to clear. Recloser also provides back up function when a fuse fails to blow up. In order to have a correct operation, a fuse must be coordinated with a recloser on the main feeder. On the other hand, if a fault occurs before a recloser (upstream fault), the fuse should isolate and coordinate with a sensitive equipment.

In figure 3.4, the TC curve of the fuse is below the slow curve of recloser in coordination range. Therefore, for a permanent fault, fuse will open before recloser will back it up by operating in slow mode and finally locking out. The coordination curves of recloser and fuse have to be modified. The area between  $I_{fault-max}$  and  $I_{fault-min}$  shows as the recloser-fuse coordination range. Therefore, as long as the fault current values for faults on lateral feeder are within coordination range, the recloser-fuse coordination is accepted. We can see that the fast characteristic of the recloser lies below the MM characteristic of fuse between  $I_{fault-max}$  and  $I_{fault-min}$ . So, in coordination range the recloser operates in less time than the time sufficient to damage the fuse.

### 3.5 Summary

A fault location method for voltage sags calculation has been presented in this chapter. Phase voltages due to the fault occurs at bus or along line in the power system are formulated in section 3.2. Based on the fault position method [46], voltage sags at any bus in the power system can be calculated when a fault occurs. Moreover, voltage sags calculation also has been presented with different types of fault (single line-to-ground, line-to-line, double line-to-ground, and three-phase faults).

Summary equations of fault currents and fault voltages when a fault occurs at bus  $m$  are shown in tables 3.1 and 3.2. Similarly, tables 3.3 and 3.4 show equations of fault currents and voltages when a fault occurs along line.

Protection coordination also has been described in this chapter. It illustrates the definition of protection coordination and protective device characteristic equations. Based on protection characteristics, the coordination of protective devices and impacts of fault can be considered and analyzed.

# CHAPTER IV

## VOLTAGE SAGS ESTIMATION

### 4.1 Introduction

Voltage sag frequency and voltage sag index are presented in this chapter. Fault distribution is taken into account in the analysis expected sags frequency. In this chapter, voltage sag index is also presented based on sag threshold and characteristic of equipment.

### 4.2 Voltage Sag Frequency

Frequently, adverse environmental and weather conditions can lead sections of lines exposed to higher fault rates than others. This effect can have a considerable impact on the expected number of sags at the bus of interest [25]. Fault rates along the line can be distributed uniformly (same fault probability along the whole line) or, on the opposite, some locations can experience higher fault rates than others. Therefore, the random nature of different fault probability distribution should be considered. Fault distribution on lines are likely to be normal or exponential distribution in practice [45, 75].

The line failure rate (LFR) is normally expressed as the number of faults per year per unit length. However, because of the short length of line in a distribution system, the line failure rate ( $LFR$ ) is calculated for the whole line  $i$  as follows

$$LFR_i = \alpha \times N_{fault} \times \frac{l_i}{\sum_{k=1}^n l_k} \quad (4.1)$$

where

- $\alpha$  : uniform, normal or exponential distributions of the fault on the line  $i$ ,
- $N_{fault}$  : number of fault in the test system,
- $l_i$  : length of the line  $i$ ,
- $n$  : total number of line in the test system.

After taking into account the line failure rate, the expected sag frequency due to faults at the sensitive bus can be calculated from

$$NSF = \sum_{i=1}^m \sum_{j=1}^{LS} L_{ij} \times LFR_i \quad (4.2)$$

where

- $NSF$  : the number of sag frequency,  
 $L_{ij}$  : length of line segment  $j$  of line  $i$  inside the area of vulnerability,  
 $LS$  : the number of line segment of line  $i$ ,  
 $m$  : the total number of line inside the area of vulnerability.

Assuming that all phases have equal probability of fault statistics, the expected number of sag frequency for one phase can be calculated as following

$$NSF_{SP} = \frac{1}{3} \sum_{FT=1}^4 \sum_{P=1}^3 NSF_{FT,P} \quad (4.3)$$

where

- $FT$  : type of fault (i.e. single line-to-ground; line-to-line, and double line-to-ground and three-phase faults),  
 $P$  : the number of phases.

### 4.3 Voltage Sag Indices

System Average Root Mean Square Variation Frequency Index (SARFI) is one of frequently used indices for voltage sag analysis. SARFI gives the average number of voltage sags over the assessment period, usually one year, per customer served [76, 77]. Based on voltage threshold,  $SARFI_X$  can be calculated by including all of customers that the magnitude of voltage sag is below a specified threshold, e.g.  $SARFI_{80}$  shows the number of customers experiencing an sag event where the remaining magnitude of voltage is less than 80%. The  $SARFI_X$  index calculation can be shown as equation 4.4

$$SARFI_X = \frac{\sum_{i=1}^{n_s} N_i}{N_T} \quad (4.4)$$

where

- $X$  : voltage threshold in percentage %,  
 $n_s$  : the number of event,  
 $N_i$  : the number of customers experiencing an event,  
 $N_T$  : the number of customers served from the section to be assessed.

SARFI index has gained more interest from many industry customers due to the reliability and quality of the process. However, sensitive equipment of industrial customers need an appropriated SARFI index, therefore, the SARFI index will depend on the sensitivity of customer's equipment and voltage tolerance [78, 79].

Despite being widely used, the  $SARFI_X$  index only considers the magnitude of voltage sag. This may gives an actual number of equipment tripping much higher than expected



value because short–duration sags will also be counted. Therefore, the SARFI index should consider and include the acceptability curves of the sensitive equipment in order not only analyzing sags magnitude but also taking into account sag duration [77,80].  $SARFI_{curve}$  index is developed from  $SARFI_X$  corresponds to voltage sags below an equipment compatibility curve, e.g. ITIC and SEMI curves. Equation 4.3 shows  $SARFI_{curve}$  as following

$$SARFI_{curve} = \frac{\sum_{j=1}^{n_s} N_j}{N_T} \quad (4.5)$$

where

- $N_j$  : the number of customers experiencing an event which below an equipment compatibility curve,  
 $N_T$  : the number of customers served from the section to be assessed.

Moreover, voltage sags based on system performance and random causes (e.g. adverse weather, animal etc.), are usually predicted by using probabilistic techniques.  $SARFI_X$  is insufficient for voltage sag analysis. This thesis gives a proposed method to simulate fault factors (e.g. fault types, fault locations, fault lines etc.) by using Monte Carlo Simulation (MCS) [81–83].

The advantage of MCS is its capability to simulate complex characteristics of systems that cannot be modeled by the probabilistic techniques [84–88]. It presents several aspects associated with the behavior of the system. In this thesis, MCS is used to simulate the components of fault, e.g. fault types, fault locations etc.  $SARFI_X$  and  $SARFI_{curve}$  equations based on the stochastic technique are calculated as following

$$SARFI_{X-MCS} = \frac{\sum_{i=1}^{NS} SARFI_X(i)}{NS} \quad (4.6)$$

$$SARFI_{curve-MCS} = \frac{\sum_{i=1}^{NS} SARFI_{curve}(i)}{NS} \quad (4.7)$$

where

- $SARFI_X(i)$  : values of the  $SARFI_X$  indices for the simulation  $i$ ,  
 $SARFI_{curve}(i)$  : values of the  $SARFI_{curve}$  indices for the simulation  $i$ ,  
 $NS$  : the total number of simulation events.

#### 4.4 Summary

This chapter discusses about equations to calculate voltage sag frequency and sag indices. Faults are the random nature of probability distributions. Therefore, the line failure rate should be determined by using fault distribution as equation 4.1. From that, voltage sag frequency is formulated in equation 4.2 for sag analysis.

Moreover,  $SARFI_X$  and  $SARFI_{curve}$  indices described in this chapter.  $SARFI_{curve}$  index is developed from  $SARFI_X$  with consideration of characteristic curve. Monte Carlo Simulation is used to simulate fault factors and applied for determined  $SARFI$  indices.



ศูนย์วิทยทรัพยากร  
จุฬาลงกรณ์มหาวิทยาลัย

# CHAPTER V

## SIMULATION AND RESULTS

### 5.1 Introduction

Normally, voltage tolerance of sensitive equipment is analyzed by using voltage threshold [20]. The voltage threshold is determined by this fixed duration of fault current. Based on this voltage threshold, sag assessments are determined and shown in many studies.

However, protective devices also impact on voltage sag assessments because of the tripping time of protection when a fault occurs in the power system [89, 90]. For example, if the duration of fault current is greater than this fixed duration, it will impact on sensitive equipment because the during-fault voltage after the fixed duration is lower than the voltage threshold.

Figure 5.1 shows an example of voltage sag assessments based on ITIC curve [36]. In this figure, the fixed duration, the voltage threshold, and the during-fault voltage are 20 ms, 0.7 pu. and 0.5 pu., respectively. If the fault duration (or the tripping-time of protective devices) is shorter than the fixed duration, the sensitive equipment does not damage. However, if the fault duration is greater than the fixed duration, e.g. point B in figure 5.1, the equipment is in the equipment problems area.

From the above analysis, this dissertation will present an approach to determine vulnerability time  $t_{fault-SE}$  based on remaining voltage at sensitive equipment bus and protection protective devices. Sensitive equipment will be impacted by voltage sags  $V_{fault}$  when a fault occurs in the system. Then  $t_{fault-SE}$  will be determined by using sensitive equipment characteristics. If a fault duration is less than  $t_{fault-SE}$ , sensitive equipment can withstand and ride-through. On the other hand, if the fault duration is greater than  $t_{fault-SE}$ , the sensitive equipment will be in the damage area. Therefore, the fault time  $t_{fault-SE}$  should be input to protection coordination for considering impacts of voltage sags on sensitive equipment.

The problem addressed in this dissertation can be stated as follows: Knowing a fault location and the fault current and voltage in the system, it is to determine which protective device interrupts the fault. Moreover, this dissertation concentrates on fuse and recloser operations based on sensitive equipment characteristics [91]. Two parameters are estimated and input to the algorithm as follows: 1) the magnitude of the fault current  $I_{fault}$ , 2) the fault duration of sensitive equipment  $t_{fault-SE}$ . These two parameters will be compared to fuse and recloser characteristic curves. The point  $(I_{fault}, t_{fault-SE})$  is defined as the protec-

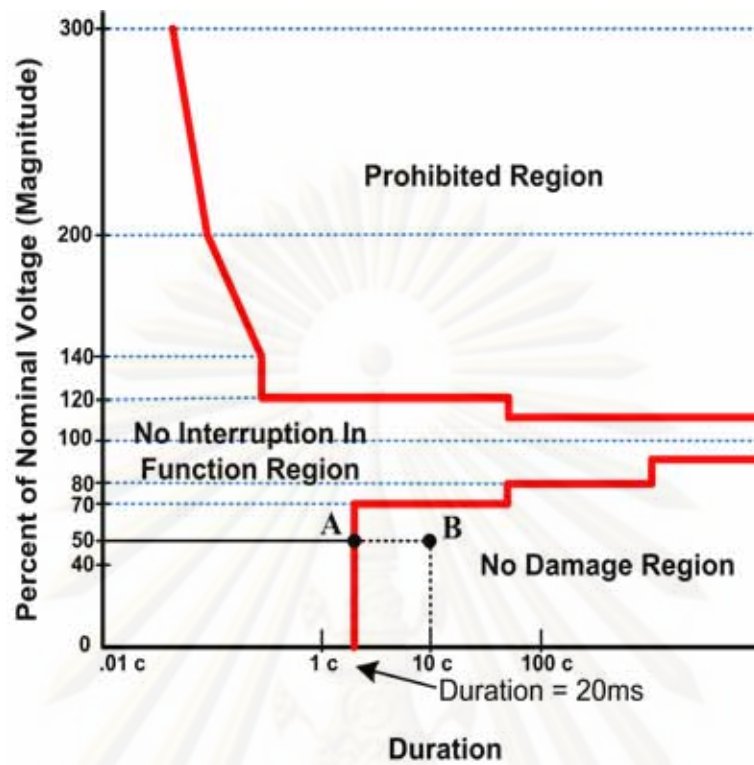


Figure 5.1: Example of voltage sags assessments based on ITIC curve

tive coordination point which must be in the coordination range and above fuses minimum melting time in the case of a fuse operation, or the recloser fast or slow curve in the case of recloser operation (see Fig. 5.2).

## 5.2 Recloser-fuse Operations

When a permanent or temporary fault occurs, a recloser or fuse should blow to isolate the short-circuit. Times corresponding to  $I_{fault}$  on the fuse time-current curves (TCC) and the recloser TCC are determined as  $t_{fault-fuse-MM}$  and  $t_{fault-fuse-TC}$ ,  $t_{fault-rec-fast}$  and  $t_{fault-rec-slow}$  respectively as shown in Fig. 5.2.

For considering sensitive equipment, the time  $t_{fault-SE}$  when the fault occurs must be greater than  $t_{fault-fuse-MM}$  or  $t_{fault-fuse-TC}$ . Therefore,

$$t_{fault-fuse-MM} \leq t_{fault-SE} \text{ or } t_{fault-fuse-TC} \leq t_{fault-SE} \quad (5.1)$$

Any fuses whose corresponding  $t_{fault-fuse-MM}$  and  $t_{fault-fuse-TC}$  satisfy the above requirement indicate an operation of the fuse.



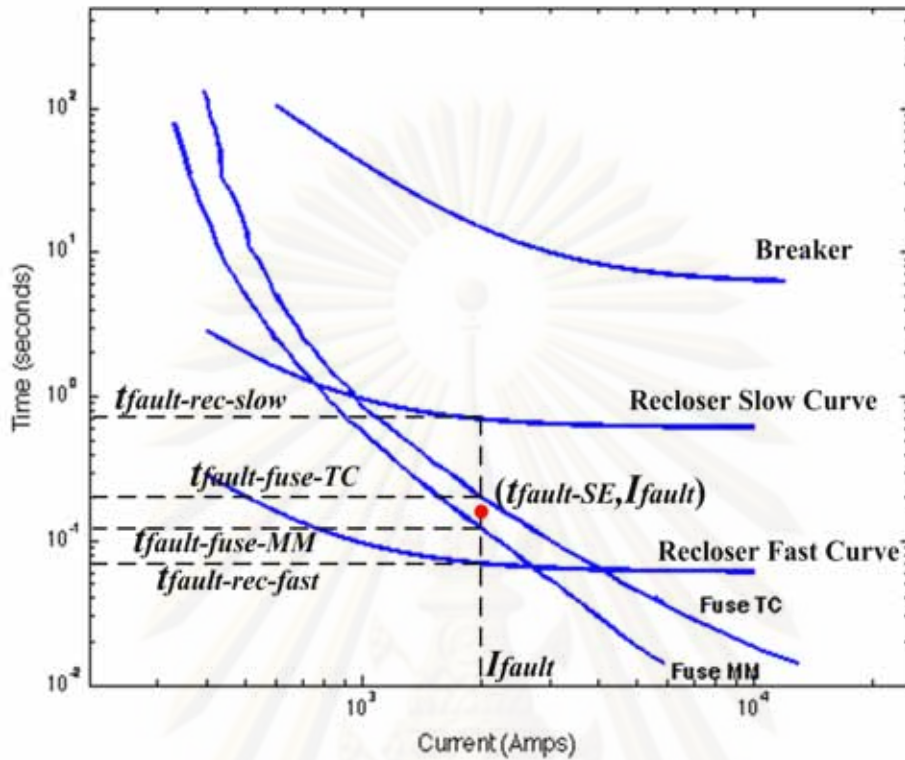


Figure 5.2: Protection coordination

Moreover, coordination of fuse and recloser is based on the recloser TCC. The fuse TCC must be located between the recloser fast and slow curves.

$$t_{fault-rec-fast} \leq t_{fault-fuse-MM} \leq t_{fault-rec-slow} \quad (5.2)$$

$$t_{fault-rec-fast} \leq t_{fault-fuse-TC} \leq t_{fault-rec-slow} \quad (5.3)$$

### 5.3 Simulation Results

The proposed method is applied to the RBTS bus 2 (see figure 5.3) [92–94]. The fault position method [45, 49, 95] is used to calculate the fault current and voltage. Bus 2 is assumed to be a sensitive bus. In the simulation, the operation range of the recloser and fuses are set to be 200 to 6000 A. The recloser has fast and slow pickup currents of 184 A and 452 A, respectively.

For recloser and breaker, the standard extremely inverse trip characteristic is used with the parameters  $A$ ,  $B$  and  $p$  of TCC to be 28.2, 0.127 and 2, respectively. However, two types

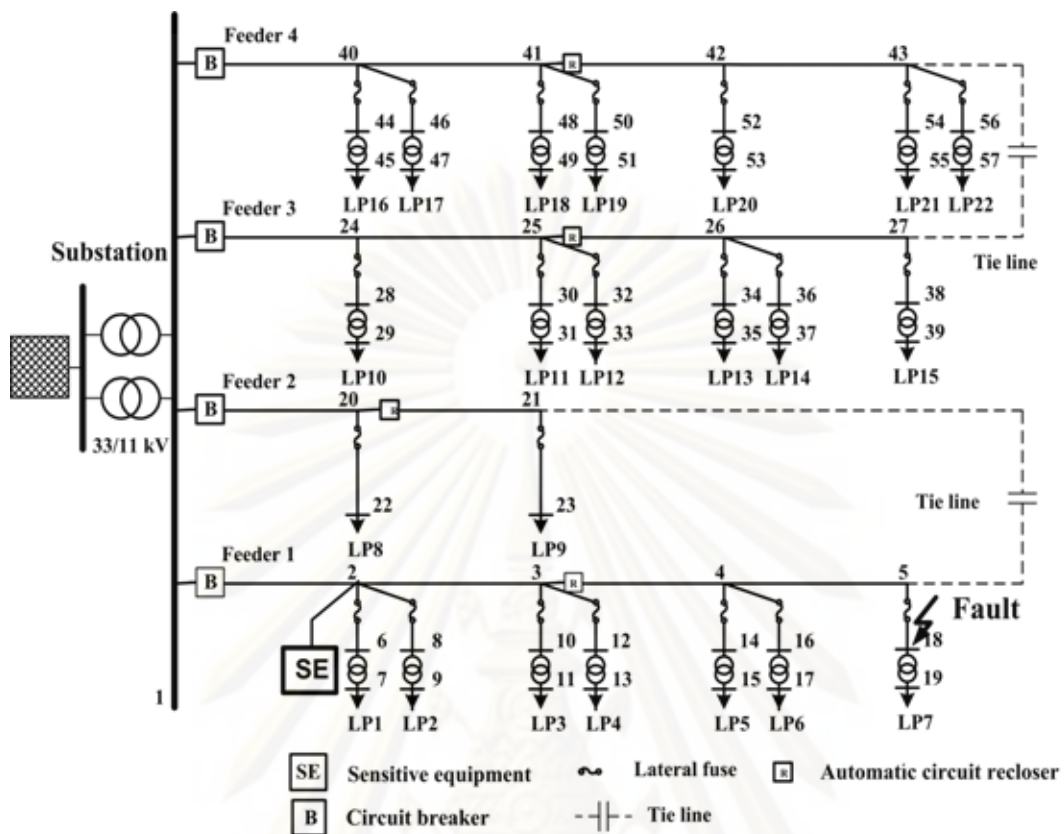


Figure 5.3: RBTS bus 2 test system

of fuse link (80K and 100K) are used as examples in this thesis. Parameters  $a$  and  $b$  of the straight line  $I^2t$  of protection equation (3.84) are shown in table 5.1.

Let us make the following assumptions: 1) time–current characteristic curves of fuses and reclosers used in the feeder and 2) sensitive equipment characteristics are available [49] (see figure 5.4). Each line is divided into five equal line segments. 500 faults occurring in the test system are assumed in a year. Monte Carlo Simulation applies with 5000 simulated years. Besides that, the details of system fault statistics are also assumed as follows [96]

- Single-Line-Ground fault (SLGF): 85%

Table 5.1: Coefficient  $a$  and  $b$  for fuse setting

Type of fuse	Minimum melting time		Total clearing time	
	$a_{MM}$	$b_{MM}$	$a_{TC}$	$b_{TC}$
100K	-2.9199	9.4467	-2.5132	8.4378
80K	-2.8378	8.9102	-2.6175	8.5325

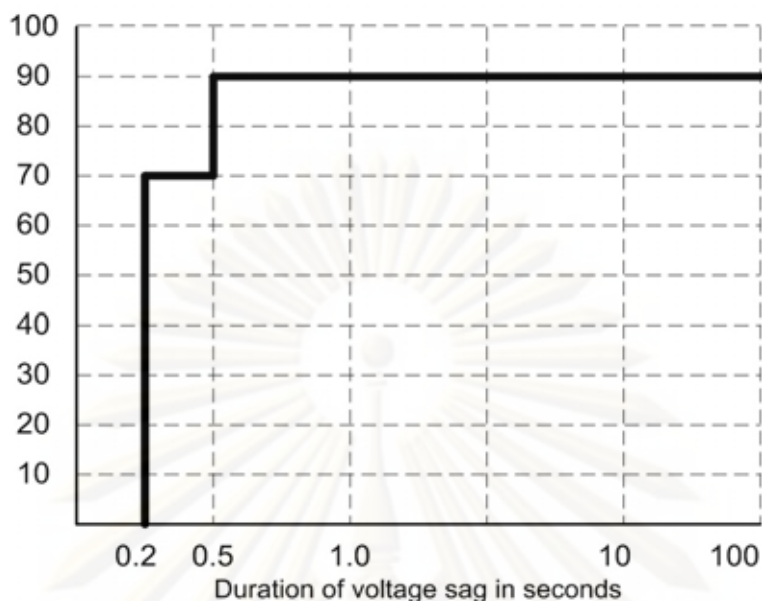


Figure 5.4: Voltage sag ride-through capacity curve from 0 to 100 s

- Line-to-Line fault (LLF): 8%
- Double-Line-Ground fault (DLGF): 5%
- Three-Phase fault: 2%

Based on the list of percentages of different fault types, number of SLGF, LLF, DLGF and 3PF are 425, 40, 25 and 10 faults, respectively.

### 5.3.1 Simulation of Recloser–fuse Coordination with Consideration of Sensitive Equipment

Assume that the distribution network is protected by a 100K fuse link and a recloser on the main feeder upstream from the fuse. Three-phase fault occurs at bus 18 in the test system. Voltage sag measured at the sensitive equipment is analyzed by using the fault position method. In this case, the duration and magnitude of the fault current are estimated to be  $t_{fault-SE} = 0.5s$  and  $I_{fault} = 2.45$  kA based on the approach described before.

Figure 5.5 shows that the operation point ( $t_{fault-SE}, I_{fault}$ ) is in the coordination area. It means that the protection coordination of protective devices can protect and determine what kind of fault (e.g. permanence fault or temporary fault) to isolate and protect the sensitive equipment. From figure 5.5, we can see that the recloser will be controlled to isolate the fault at the fault bus 18 before the fuse melting. It is very good to improve the old distribution systems for applying a new sensitive equipment by considering the type of protective devices.

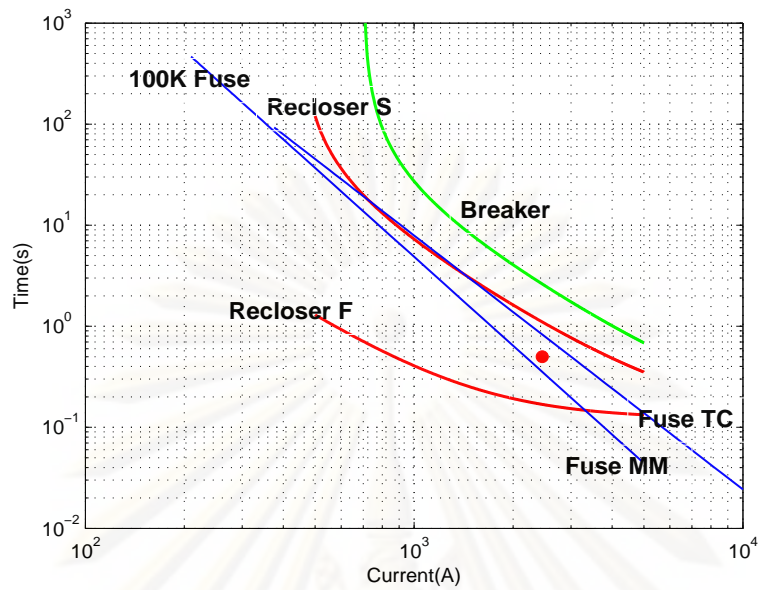


Figure 5.5: 100K fuse coordination with the recloser to clear three-phase fault at bus 18

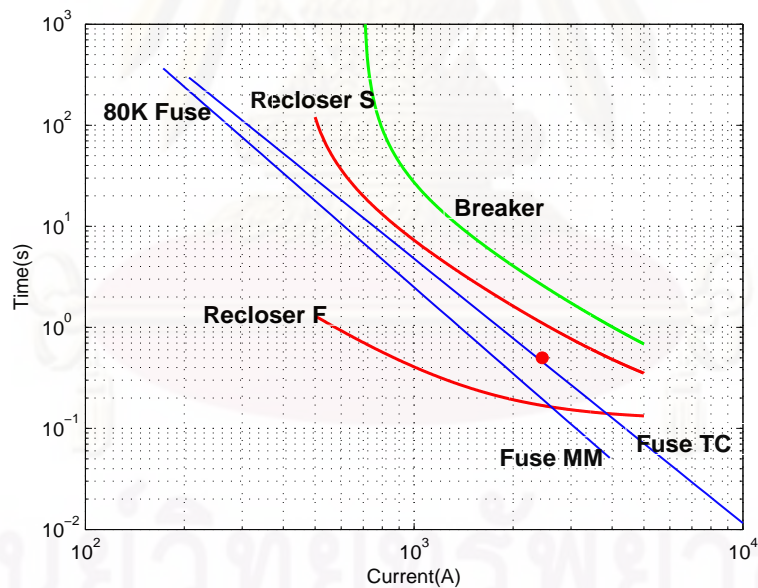


Figure 5.6: 80K fuse coordination with the recloser to clear three-phase fault at bus 18

Besides that, in figure 5.6, 80K fuses are also analyzed with the test system. We can also see that the operation point lies inside the coordination range of protective devices. It also means that the 80K fuse can coordinate to protect the sensitive equipment and satisfy the sensitive characteristic curve of the equipment.

The results indicate that the 100K and 80K fuses coordinate well with the recloser



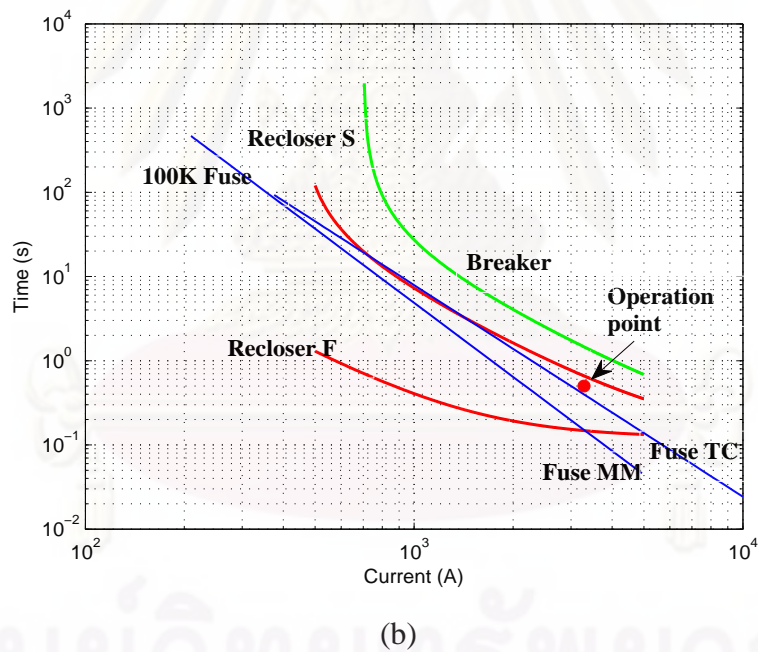
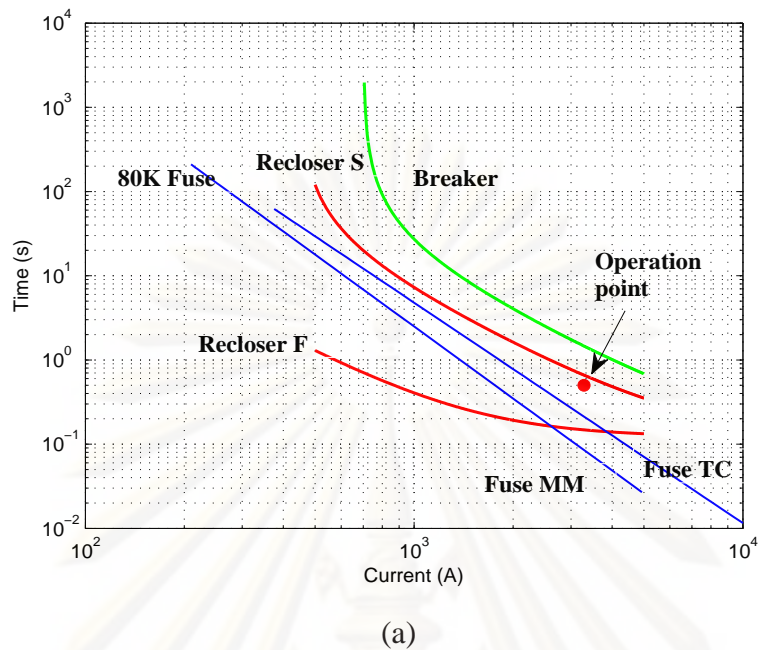
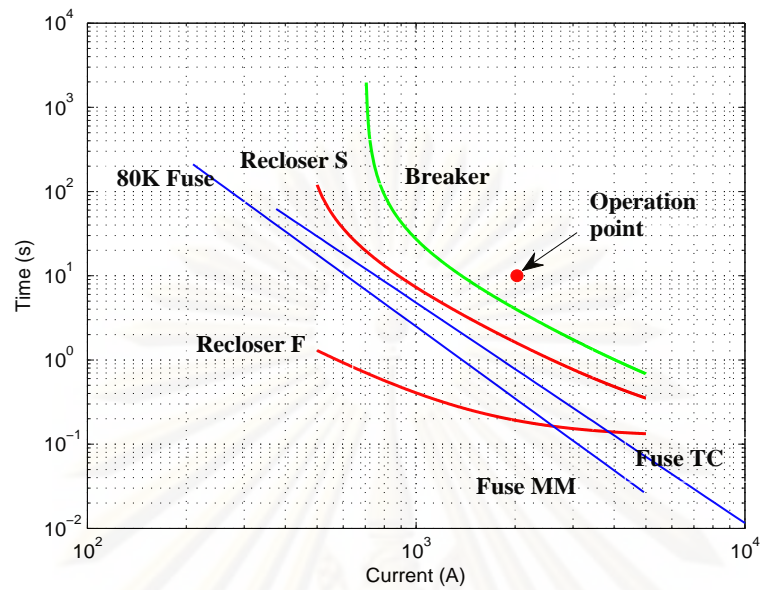
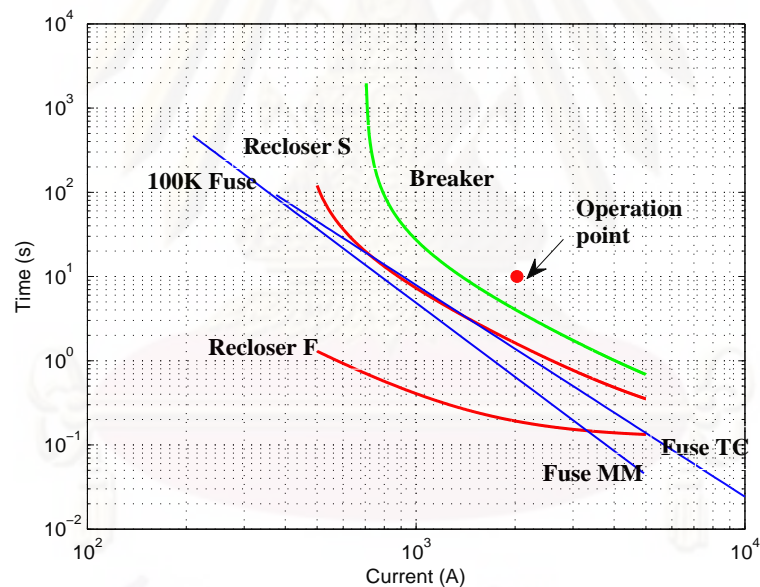


Figure 5.7: 80K fuse and 100K fuse coordination with the recloser to clear three-phase fault at bus 23

considering sensitive equipment. Both figures 5.5 and 5.6 show the protection coordination points are inside the recloser-fuse coordination range. Figures 5.7, 5.8, and 5.9 show the operation points of coordination analysis when a three-phase fault occurs at the fault buses 23, 38, and 56 in the feeders 2, 3, and 4 of the RBTS bus 2 test system, respectively. Such figures show impacts of fuse type on the protection of the sensitive equipment. Therefore,



(a)



(b)

Figure 5.8: 80K fuse and 100K fuse coordination with the recloser to clear three-phase fault at bus 38

the protection coordination in other feeders should also be considered in order to analyze the voltage sag impacts on the sensitive equipment.

For example, if the fault occurs in the other feeders, e.g. feeder 2, 3, or 4, the voltage sags will impact on the sensitive equipment in the feeder 1. In figures 5.8 and 5.9, 80K fuse and 100K fuse can coordinate with the sensitive equipment, therefore, they can be used in

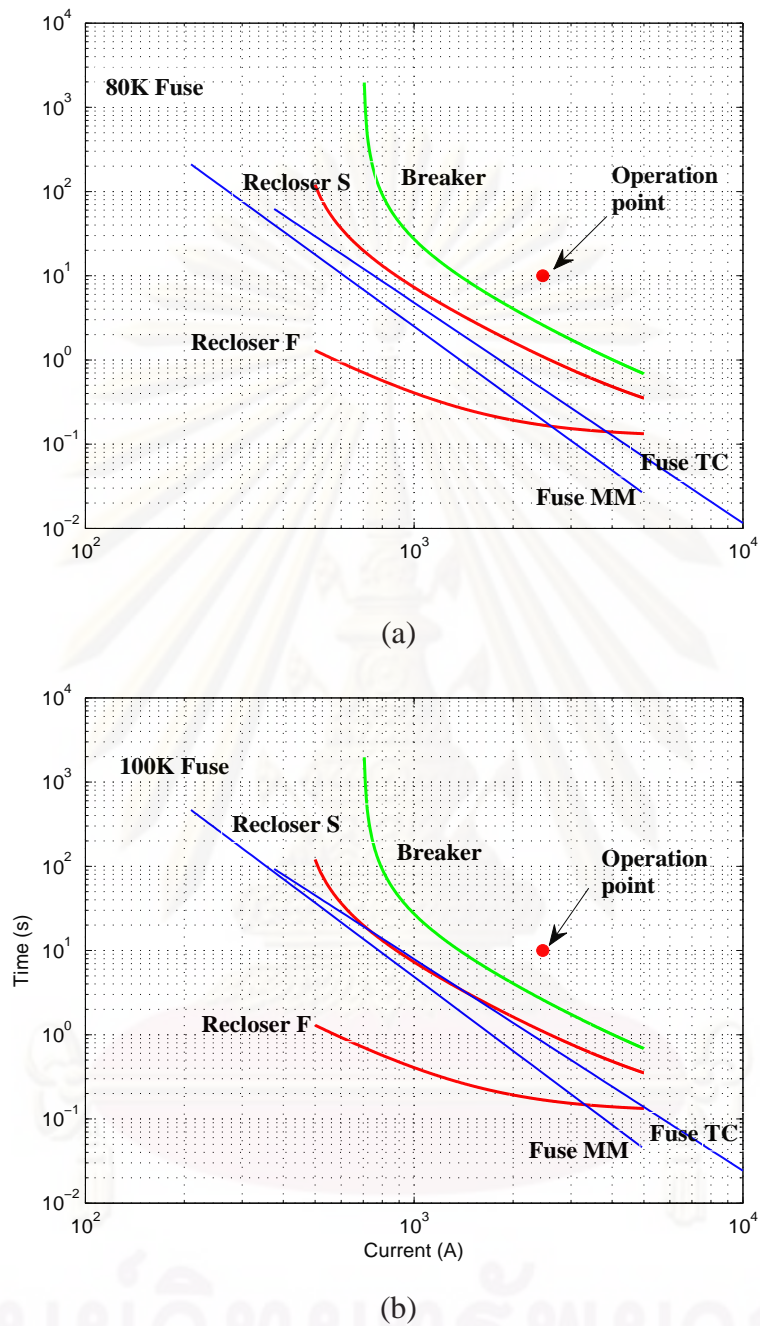


Figure 5.9: 80K fuse and 100K fuse coordination with the recloser to clear three-phase fault at bus 56

the test system. However, figure 5.7 (a) shows that 80K fuse does not coordinate with the sensitive equipment and can not protect the equipment in the feeder 1 if the fault occurs in the bus 23. In this case, 100K fuse can be used as a coordinated protective device for the sensitive equipment in feeder 1.

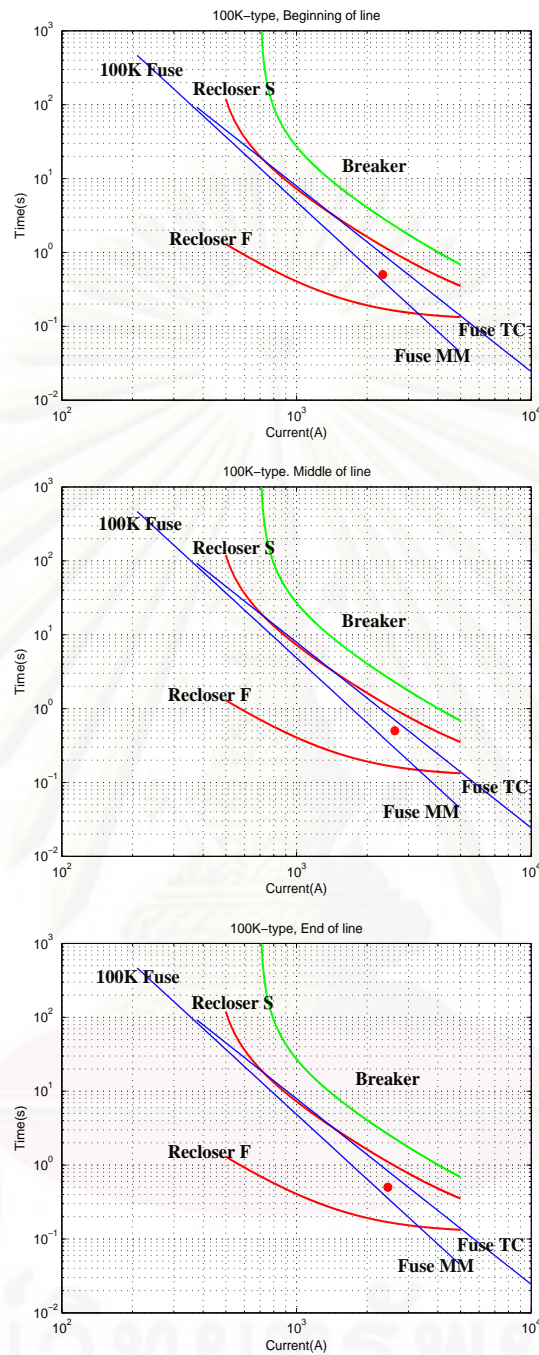


Figure 5.10: Protection coordination with 100K fuse when fault occurs along line from bus 5 to bus 18.

### 5.3.2 Simulation with Fault Along Line

In this case, the fault location method will show how to analyze what kind of the protection device type should be used to protect the sensitive equipment when a fault occurs along line.

Based on the fault position method, a three-phase fault occurs along line from bus



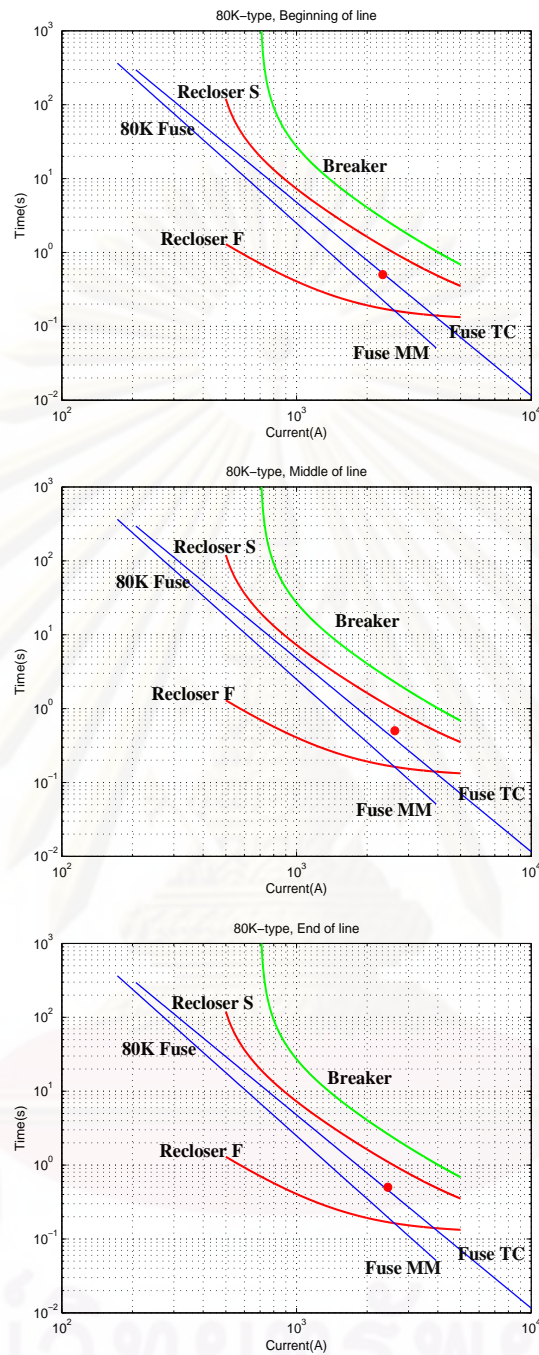


Figure 5.11: Protection coordination with 80K fuse when fault occurs along line from bus 5 to bus 18.

5 to bus 18 on the feeder 1 as shown in figures 5.10 and 5.11. The estimated fault current flowing in the fuse were 2.33 kA, 2.62 kA and 2.45 kA corresponding with a fault at the beginning, midline and end of the line, respectively. The sag duration is 0.5s based on the sensitive equipment characteristic.

Figure 5.10 shows that the 100K fuse can protect the sensitive equipment when a fault

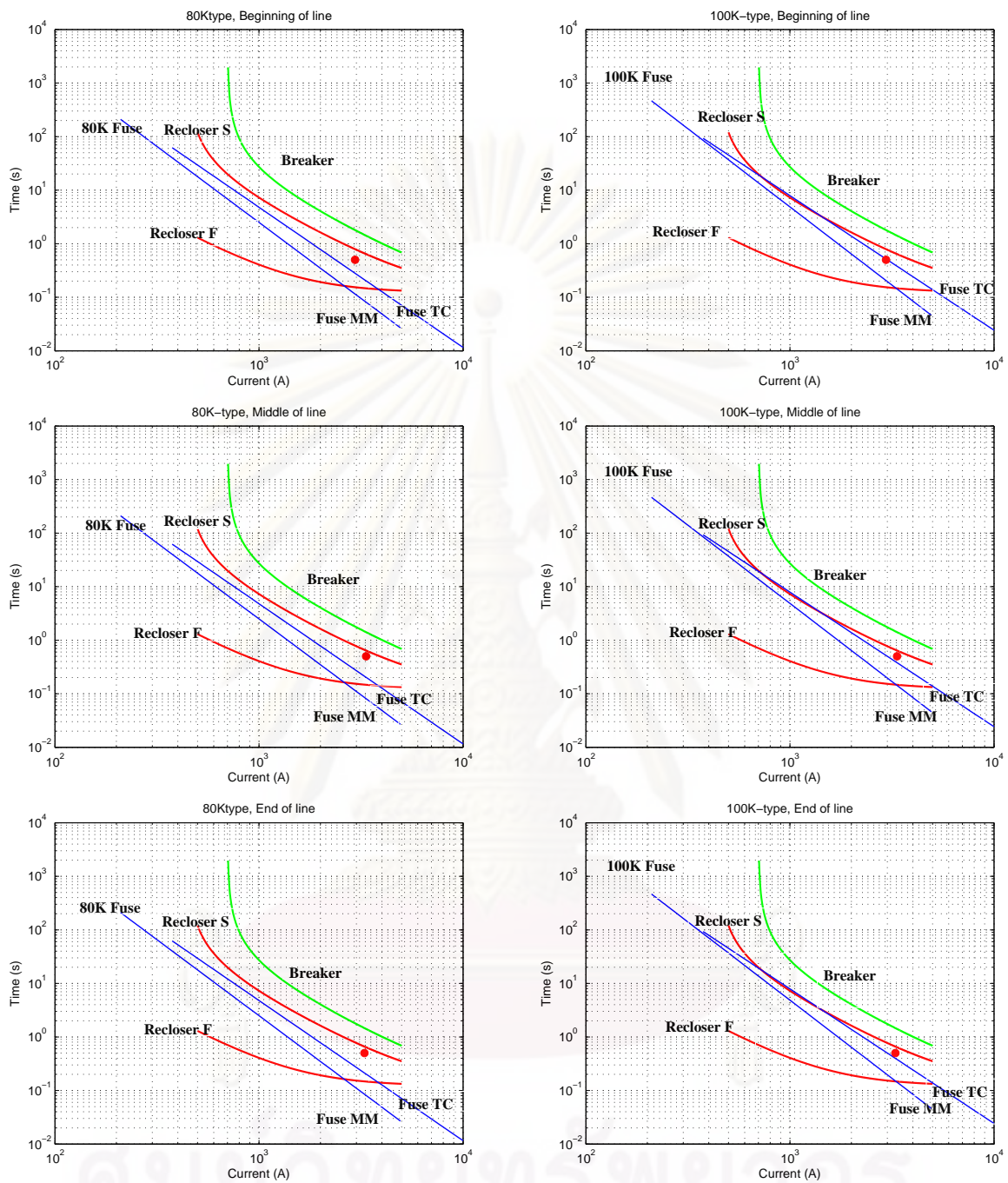


Figure 5.12: Protection coordination with 80K fuse and 100K fuse when fault occurs along line from bus 21 to bus 23.

occurs along line from bus 5 to bus 18 with the protection coordination. However, figure 5.11 shows that if a fault occurs at midline, 80K fuse cannot protect the sensitive equipment. It is very useful to analyze what type of protective device should be used to isolate the fault in the power system and protect industrial customers with the protection coordination and

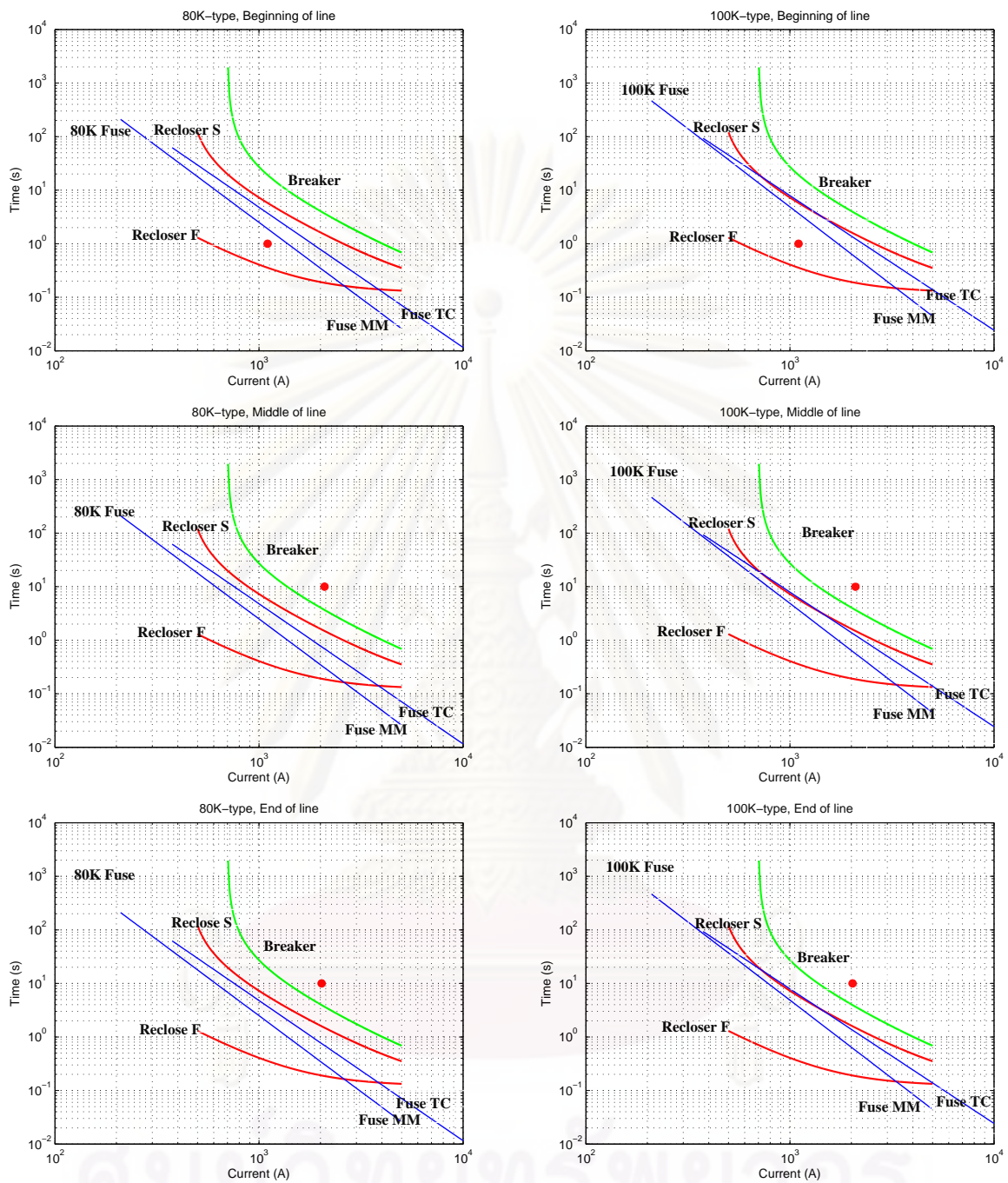


Figure 5.13: Protection coordination with 80K fuse and 100K fuse when fault occurs along line from bus 27 to bus 38.

the sensitive characteristic of equipment.

Moreover, figures 5.12, 5.13, and 5.14 also show the protection coordination with the sensitive equipment in the feeder 1 when a fault occurs along line in feeders 2, 3, and 4, respectively. In figure 5.12, we can see that 80K fuse of the line from bus 21 to bus 23 can

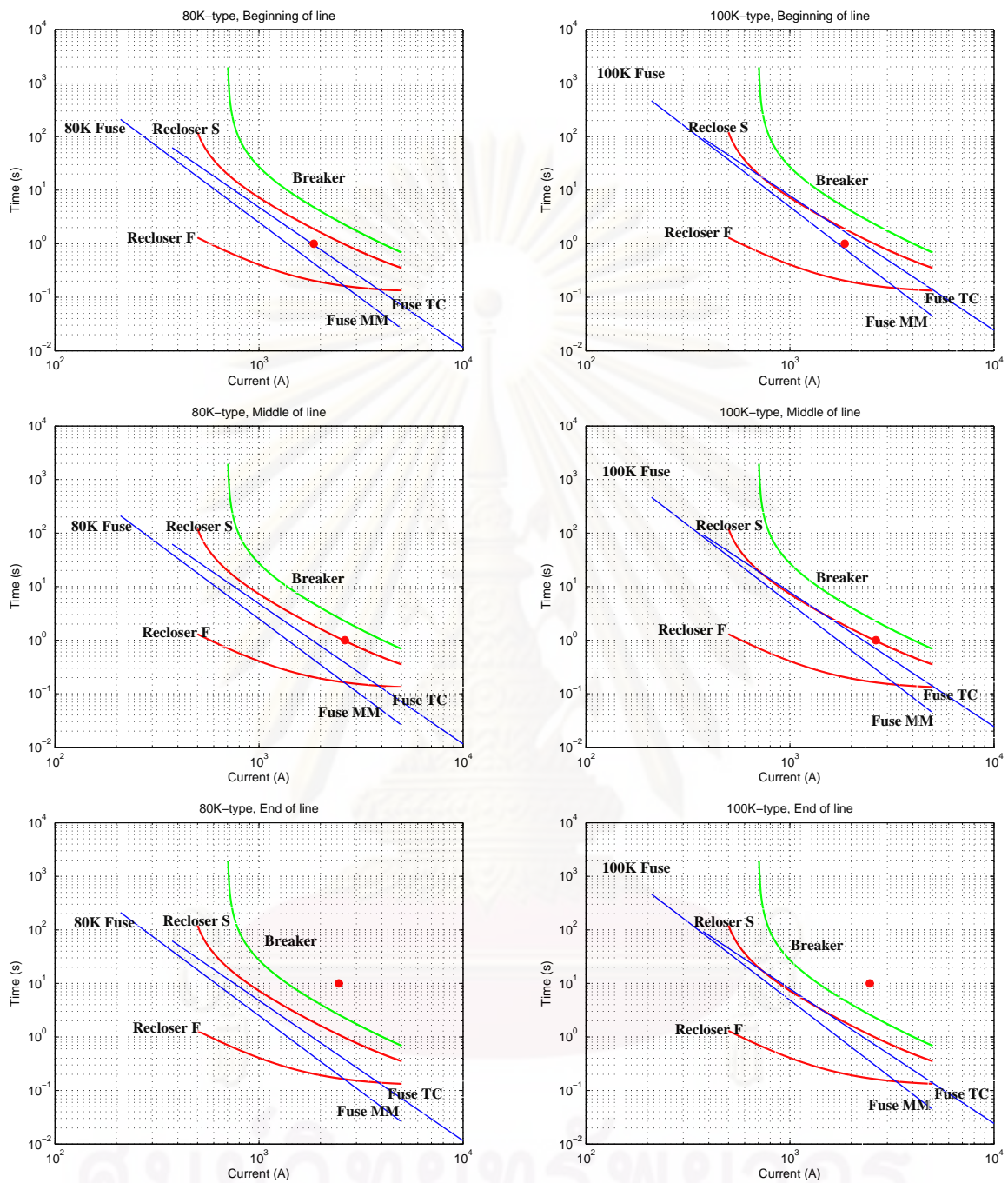


Figure 5.14: Protection coordination with 80K fuse and 100K fuse when fault occurs along line from bus 43 to bus 56.

not coordinate with the sensitive equipment in the feeder 1 if the fault occurs along line from bus 21 to bus 23. However, 100K fuse can coordinate well with the equipment.

Figures 5.13 and 5.14 show that we can use both 80K and 100K fuses for coordination with the sensitive equipment in the feeder 1. It means that the fault occurs along line, e.g.



Table 5.2: Sag frequency with uniform fault distribution and different fault types for voltage threshold ranging from 10% to 90% of the nominal voltage

Voltage Threshold (%)	SLGF (phase <i>a</i> )	LLF		DLGF		3PF
		(phase <i>b</i> )	(phase <i>c</i> )	(phase <i>b</i> )	(phase <i>c</i> )	
0-10	16.64	0	0	1.13	1.13	0.45
10-20	16.97	0	0	0.96	0.96	0.44
20-30	18.76	0	0	1.10	1.83	0.62
30-40	28.88	0	1.38	1.29	1.96	0.67
40-50	35.24	0	11.30	2.07	3.71	1.22
50-60	74.39	3.35	10.53	3.83	5.22	1.87
60-70	101.64	4.27	9.04	4.77	5.078	2.00
70-80	83.37	8.14	7.32	5.019	5.10	2.27
80-90	49.11	15.71	0.41	4.82	0	0.46

from bus 27 to bus 38 in the feeder 3, or from bus 43 to bus 56 in the feeder 4, can be isolated with recloser before the fuse operates.

### 5.3.3 Sag Frequency with Different Voltage Threshold

This case shows the number of sag frequency with different voltage threshold and fault distributions. Table 5.2 shows the number of sag frequency for voltage threshold ranging from 10% to 90% of the nominal voltage with different fault types and with uniform fault distribution. Similarly, tables 5.3 and 5.4 also show the number of sag frequency with normal and exponential fault distributions, respectively.

From table 5.2, most of sag frequency are from 50% to 80% when a SLGF occurs. Figure 5.15 shows voltage sag frequency spectrums for voltage threshold ranging from 10% to 90% of the nominal voltage when the SLGF occurs with different fault distributions. Figure 5.15 shows that most of sag frequency are from 50 – 70% of the nominal voltage, the highest sag frequency is obtained by applying uniform distribution for the fault occurs along line.

Moreover, table 5.5 shows the number of sag frequency when Monte Carlo Simulation is applied to simulate fault type, fault location, and fault line as a random value with voltage threshold ranging from 10% to 90% of the nominal voltage. In table 5.5, the maximum value of sag frequency for phase *a* is 27.01 with ranging from 70% to 80% of the nominal voltage by considering MCS. For phase *b*, the maximum sag frequency is 27.49 with the nominal voltage ranging from 60% to 70%, while, the maximum sag frequency of phase *c* is 27.46 from 60 – 70% of the nominal voltage.

Table 5.3: Sag frequency with normal fault distribution and different fault types for voltage threshold ranging from 10% to 90% of the nominal voltage

Voltage Threshold (%)	SLGF (phase <i>a</i> )	LLF		DLGF		3PF
		(phase <i>b</i> )	(phase <i>c</i> )	(phase <i>b</i> )	(phase <i>c</i> )	
0-10	13.44	0	0	0.83	0.83	0.33
10-20	11.28	0	0	0.85	0.85	0.46
20-30	28.46	0	0	1.47	2.57	0.79
30-40	27.76	0	2.23	1.25	1.53	0.68
40-50	34.97	0	10.31	2.47	3.28	0.74
50-60	85.12	2.69	10.73	3.37	5.31	2.46
60-70	92.48	4.70	9.37	4.52	5.57	1.92
70-80	77.98	7.62	7.25	5.38	5.05	2.21
80-90	53.50	17.05	0.11	4.84	0	0.39

Table 5.4: Sag frequency with exponential fault distribution and different fault types for voltage threshold ranging from 10% to 90% of the nominal voltage

Voltage Threshold (%)	SLGF (phase <i>a</i> )	LLF		DLGF		3PF
		(phase <i>b</i> )	(phase <i>c</i> )	(phase <i>b</i> )	(phase <i>c</i> )	
0-10	20.63	0	0	1.51	1.51	0.60
10-20	27.94	0	0	1.45	1.45	0.63
20-30	17.92	0	0	0.99	1.51	0.51
30-40	26.67	0	1.47	1.36	1.89	0.74
40-50	35.11	0	13.63	1.52	4.71	1.43
50-60	85.39	4.73	9.51	5.06	4.44	1.63
60-70	94.93	4.42	8.25	3.75	4.84	2.01
70-80	79.39	8.34	6.97	4.84	4.65	2.22
80-90	37.01	15.41	0.16	4.51	0	0.23

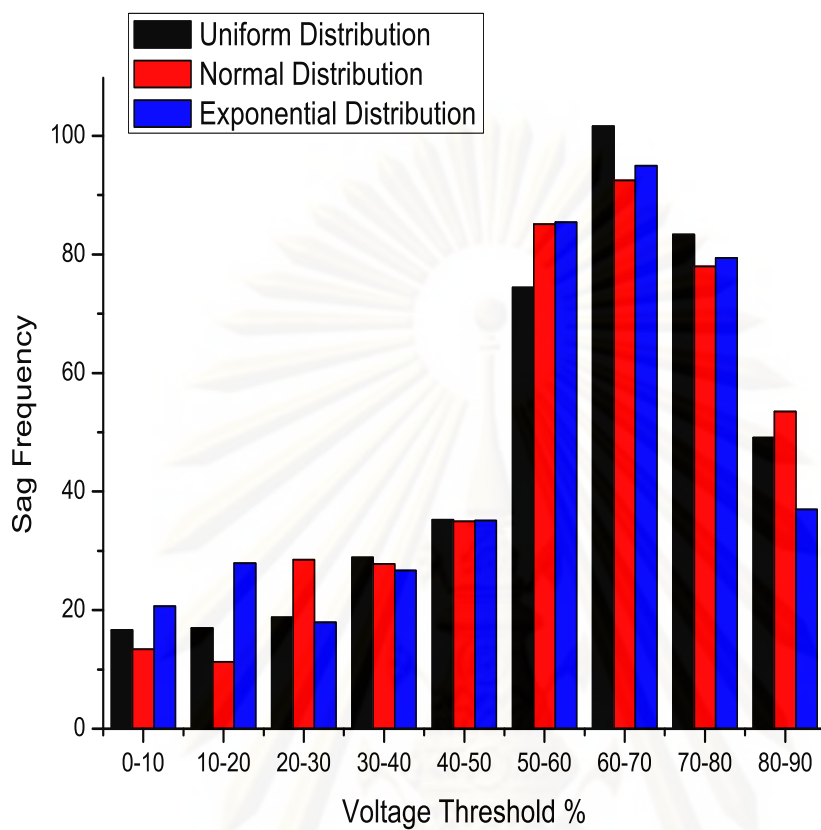


Figure 5.15: Sag frequency spectrum of different fault distribution when a SLGF occurs

Table 5.5: Sag frequency by applying Monte Carlo Simulation for voltage threshold ranging from 10% to 90% of the nominal voltage

Voltage Threshold (%)	Phase <i>a</i>	Phase <i>b</i>	Phase <i>c</i>
0-10	7.40	7.53	7.42
10-20	4.36	4.31	4.28
20-30	5.25	5.33	5.23
30-40	7.04	7.08	7.07
40-50	14.40	14.61	14.26
50-60	22.73	22.99	22.66
60-70	26.88	27.49	27.46
70-80	27.01	26.36	26.59
80-90	24.04	23.60	23.85

### 5.3.4 Sag Frequency without Protection Coordination Consideration

In this case, sag frequency is considered with an assumption of 0.7 *pu.* of voltage threshold of sensitive equipment. Voltage threshold is used to determine the area of vulnerability of the sensitive equipment based on the fault position method. After that sags frequency will be calculated for the equipment based on the area of vulnerability. Coordination of protective devices and sensitive equipment characteristics curve are not considered in this case. The sensitive equipment in this test case is located at bus 2 and analyzed for sag frequency assessments.

Table 5.6 shows the number of line segments inside the area of vulnerability without protection coordination consideration for all types of fault, e.g. single line-to-ground fault, line-to-line fault, double line-to-ground fault and three-phase fault. In table 5.6, numbers of line segment inside the area of vulnerability when line-to-line and double line-to-ground fault occur between phases *b* and *c* are not the same because of resistance of line and transformers in the test system (more details on proof can be found in the appendix G). Figures 5.16 to 5.18 show the areas of vulnerability for the fault in the power system. Figure 5.16 shows that the area of vulnerability of the sensitive equipment when three-phase faults occur in the power system is greater than the ones when single line-to-ground faults occur. Figures 5.17 and 5.18 are the areas of vulnerability of the sensitive equipment at bus 2 when line-to-line fault and double line-to-ground fault occur respectively.

As shown in figures 5.16, 5.17, and 5.18, the areas of vulnerability for sensitive load at bus 2 are illustrated. The influence of two kinds of fault distributions along line are considered in order to calculate expected sags frequency [45]. Uniform and normal fault distributions along line are considered. The resulting sag frequency for three phases for sensitive equipment in this case is obtained by using the numbers of line segment inside the area of vulnerability in table 5.7.

From table 5.7, the expected sag frequency for one phase with uniform fault distribution along line is calculated by using equation (4.3).

$$NSF_{SP} = \frac{1}{3} [292.52 + (7.62 + 32.26) + (15.16 + 20.72) + 3 \times 7.27] = 130.03$$

Similarly, the expected sag frequency for one phase with normal fault distributions along lines is

$$NSF_{SP} = \frac{1}{3} [293.42 + (7.29 + 32.75) + (14.68 + 20.46) + 3 \times 7.42] = 130.29$$



Table 5.6: The number of line segments inside the area of vulnerability for sensitive equipment at bus 2 without protection coordination consideration

Type of Fault	Number of line segments inside AOV		
	Phase A	Phase B	Phase C
SLGF (A)	124	0	0
LLF (B,C)	0	34	145
DLGF (B,C)	0	109	143
3PF	131	131	131

Table 5.7: The number of sag frequency for sensitive equipment at bus 2 without protection coordination consideration

Type of fault	Number of sag frequency for sensitive equipment at bus 2					
	Uniform distribution			Normal distribution		
	Phase A	Phase B	Phase C	Phase A	Phase B	Phase C
SLGF	292.52	0	0	293.42	0	0
LLF	0	7.62	32.26	0	7.29	32.75
DLGF	0	15.16	20.72	0	14.68	20.46
3PF	7.27	7.27	7.27	7.42	7.42	7.42

ศูนย์วิทยทรัพยากร

จุฬาลงกรณ์มหาวิทยาลัย

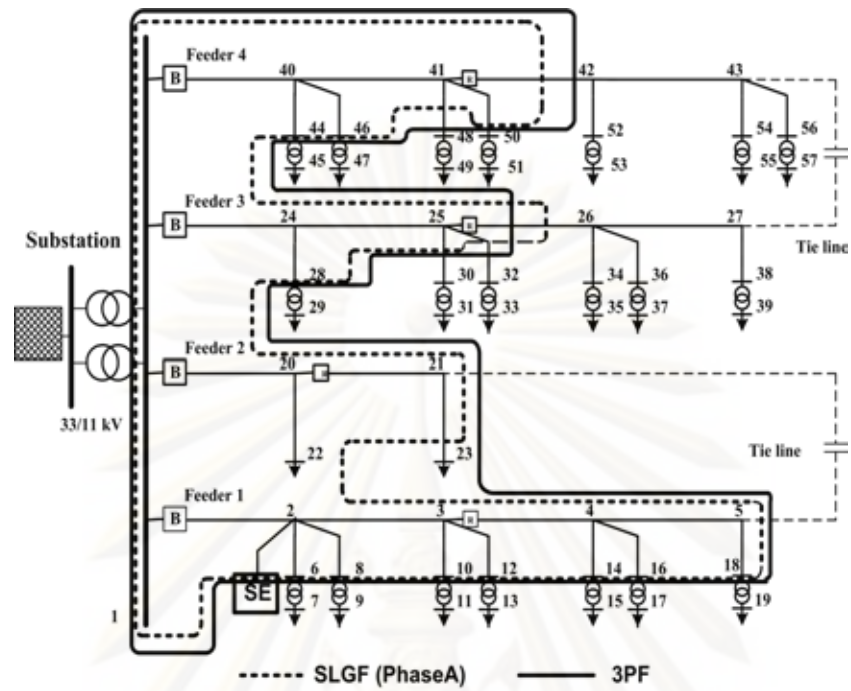


Figure 5.16: The areas of vulnerability for sensitive load at bus 2 without considering protection coordination due to SLGF and 3PF.

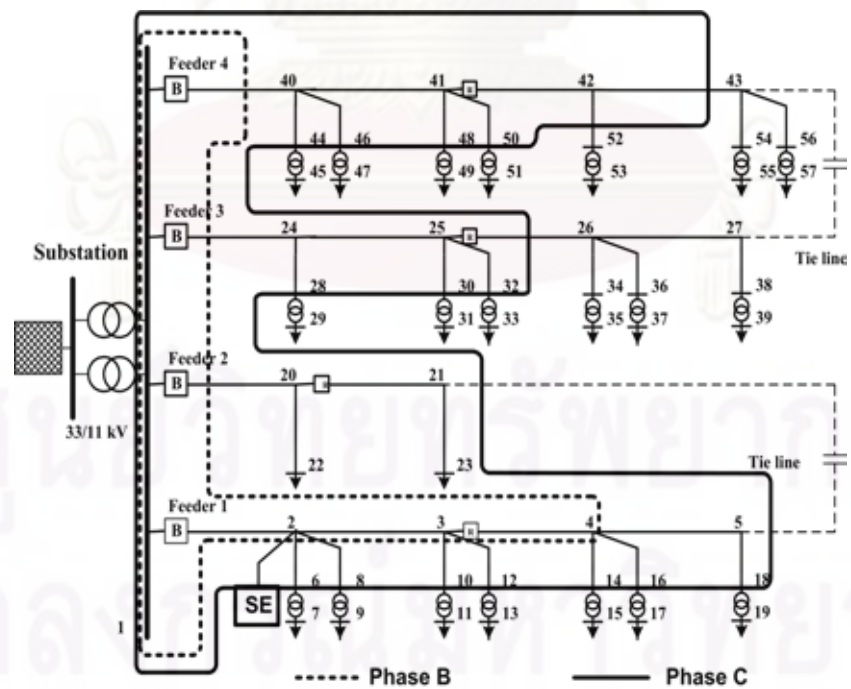


Figure 5.17: The areas of vulnerability for sensitive load at bus 2 without considering protection coordination due to LLF.

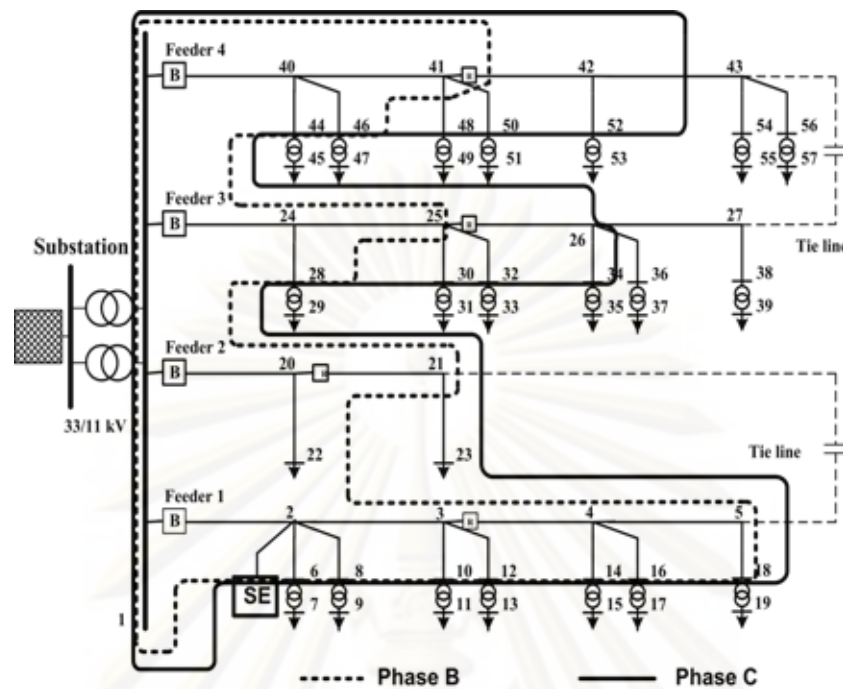


Figure 5.18: The areas of vulnerability for sensitive load at bus 2 without considering protection coordination due to DLGF.

### 5.3.5 Sag Frequency with Protection Coordination Consideration

Protection coordination is considered in order to show impacts on sensitive equipment in this case. Sensitive equipment characteristic curves (ITIC or SEMI F47) are used to analyze fault duration with protection coordination. It means that the proposed method considers not only the magnitude of voltage, but also its duration. Two kinds of fault distributions along line (uniform and normal distributions) are used to analyze the expected sag frequency.

Based on the sensitive equipment characteristics and protection coordination, the number of line segments inside the area of vulnerability are shown in table 5.8. The areas of vulnerability for sensitive load at bus 2 are shown in figures 5.19, 5.20, and 5.21.

Table 5.9 shows the expected sag frequencies for three phases for all type of faults in the test system based on the area of vulnerability. The tables clearly show that the number of sag frequency decreases with protection coordination consideration.

In this case, the number of sag frequency for one phase with uniform fault distribution along lines is calculated from table 5.9 and equation (4.3).

$$NSF_{SP} = \frac{1}{3} [274.90 + (4.60 + 13.86) + (13.74 + 19.89) + 3 \times 6.84] = 115.84$$

The number of sag frequency for one phase with normal fault distribution along lines is

$$NSF_{SP} = \frac{1}{3} [279.87 + (4.60 + 14.19) + (13.56 + 19.95) + 3 \times 7.01] = 117.73$$

Table 5.8: The number of line segments inside the area of vulnerability for sensitive equipment at bus 2 with protection coordination consideration

Type of fault	Number of line segments inside AOV		
	Phase A	Phase B	Phase C
SLGF (A)	117	0	0
LLF (B,C)	0	20	62
DLGF (B,C)	0	99	143
3PF	123	123	123

Table 5.9: The number of sag frequency for sensitive equipment at bus 2 with protection coordination consideration

Type of fault	Number of sag frequency for sensitive equipment at bus 2					
	Uniform distribution			Normal distribution		
	Phase A	Phase B	Phase C	Phase A	Phase B	Phase C
SLGF	274.90	0	0	279.87	0	0
LLF	0	4.60	13.86	0	4.60	14.19
DLGF	0	13.74	19.89	0	13.56	19.95
3PF	6.84	6.84	6.84	7.01	7.01	7.01

ศูนย์วิทยทรัพยากร

จุฬาลงกรณ์มหาวิทยาลัย



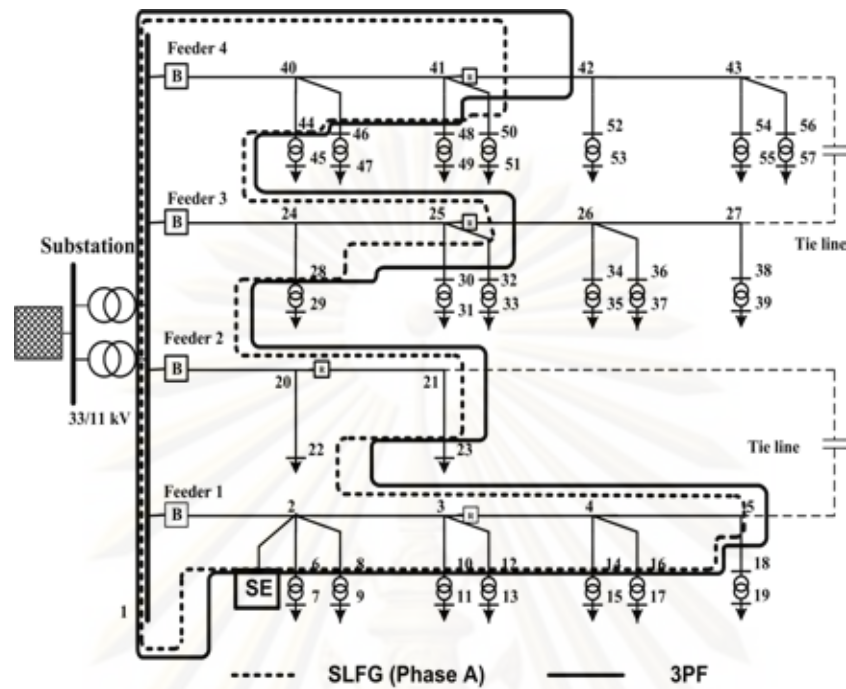


Figure 5.19: The areas of vulnerability for sensitive load at bus 2 with considering protection coordination due to SLGF and 3PF.

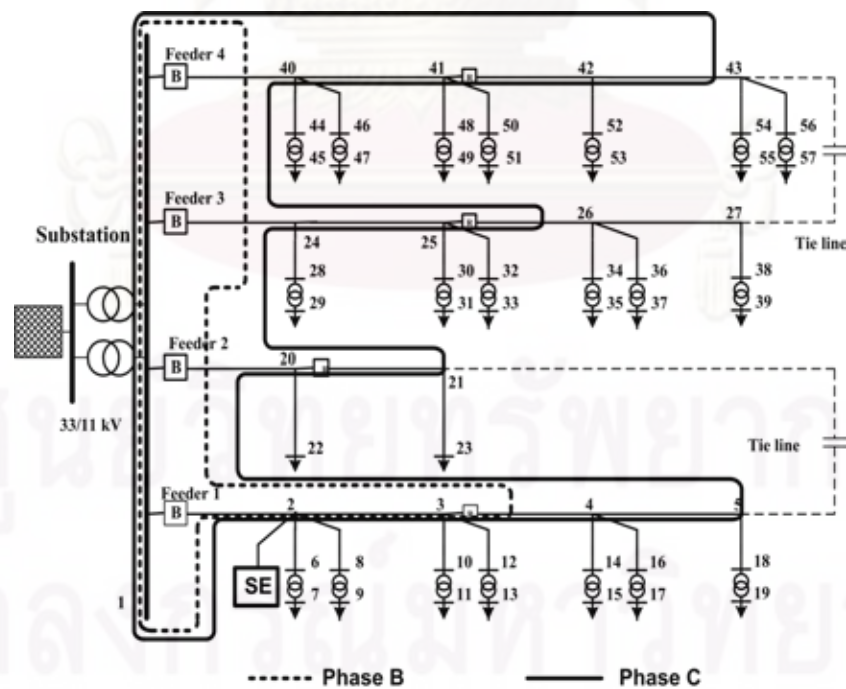


Figure 5.20: The areas of vulnerability for sensitive load at bus 2 with considering protection coordination due to LLF.

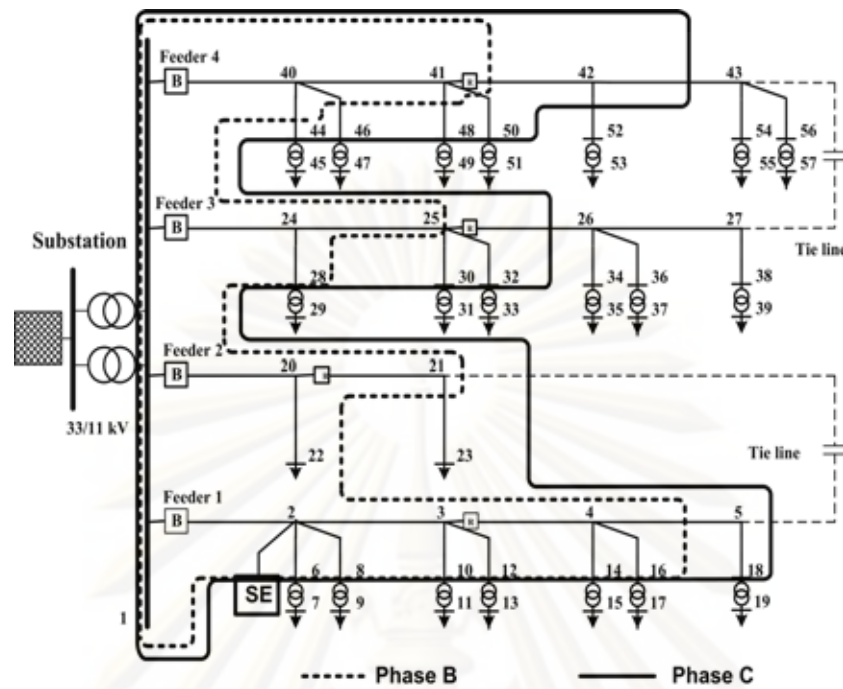


Figure 5.21: The areas of vulnerability for sensitive load at bus 2 with considering protection coordination due to DLGF.

### 5.3.6 Sag Indices

In this section, sag indices will be discussed and calculated by considering the sensitive characteristic curve and applying the stochastic method.  $SARFI_X$  and  $SARFI_{curve}$  indices are indices to analyze the number of customer that cannot be served or impacted by voltage sags.

The equation of the fuse protective devices will be applied for all fuses in the RBTS bus 2 test system. The parameters of the equation for fuse can be calculated by chosen the parameter  $a$  and the initial setting operation point for protective devices. In this test case, the parameter  $a$  of the fuse equation is chosen to be  $-2$ . This value is just for calculation and easier to simulate characteristic of fuse. Therefore, with parameter  $a$  and the operation point, the parameter  $b$  in the fuse equation can be calculated as shown in table 5.10.

#### 5.3.6.1 $SARFI_X$

$SARFI$  index will be determined based on the voltage threshold. Analytical method and Monte Carlo simulation (MCS) method [87] will be applied to estimate the number of sags.

In this section,  $SARFI_X$  will be analyzed with different fault distributions, e.g. uniform distribution, normal distribution, and exponential distribution; and different types of fault, e.g. single line-to-ground fault (SLGF), line-to-line fault (LLF), double line-

Table 5.10: Coefficient  $b$  for fuse characteristic equation

Fuse number	Coefficient $b$			
	Feeder 1	Feeder 2	Feeder 3	Feeder 4
1	5.4973	5.3997	5.3619	5.4964
2	5.4386	5.2329	5.1921	5.4378
3	5.2660	—	5.2092	5.2652
4	5.3140	—	4.8412	5.3137
5	5.1136	—	4.9181	5.1126
6	5.1258	—	4.8553	5.0141
7	5.0043	—	—	5.0079

to-ground fault (DLGF), and three-phase fault (3PF). Moreover, MCS presents the behavior of fault problems in the distribution system, e.g. fault type, fault location, fault line.

Tables 5.11 to 5.13 show the number of  $SARFI_X$  with the uniform, normal, and exponential fault distributions for different types of faults.

Figure 5.22 shows  $SARFI_X$  indices for the sensitive equipment at bus 2 with different fault type and the uniform fault distribution system. Similarly, figures 5.23 and 5.24 demonstrate the numbers of  $SARFI_X$  of the sensitive equipment at bus 2 with the normal and exponential fault distributions.

Table 5.14 shows  $SARFI_X$  based on Monte Carlo simulation take random fault problems into consideration in the test system.

Table 5.11:  $SARFI_X$  indices with the uniform fault distribution at the sensitive bus 2.

Voltage threshold (%)	10	20	30	40	50	60	70	80	90
SLGF	0.12	0.18	0.24	3.41	13.78	29.01	44.36	82.91	136.69
LLF	0	0	0	0.01	0.03	3.80	8.68	15.57	21.27
DLGF	0.01	0.02	0.03	1.20	2.36	4.19	7.31	11.48	16.00
3PF	0	0.01	0.21	0.89	1.85	2.89	5.24	7.70	10.00

Table 5.12:  $SARFI_X$  indices with the normal fault distribution at the sensitive bus 2.

Voltage threshold (%)	10	20	30	40	50	60	70	80	90
SLGF	0.13	0.18	0.25	3.40	16.28	27.87	46.95	84.19	136.00
LLF	0	0	0	0	0.04	3.66	8.62	15.20	21.60
DLGF	0.01	0.02	0.03	1.29	2.54	4.16	7.20	11.38	16.00
3PF	0	0.01	0.21	0.95	1.84	2.90	5.14	7.66	10.00

Table 5.13:  $SARFI_X$  indices with the exponential fault distribution at the sensitive bus 2.

Voltage threshold (%)	10	20	30	40	50	60	70	80	90
SLGF	0.12	0.18	0.24	3.37	13.38	30.06	44.07	82.32	137.00
LLF	0	0	0	0.01	0.03	3.86	8.77	15.72	21.20
DLGF	0.01	0.02	0.03	1.18	2.29	4.24	7.38	11.50	16.00
3PF	0	0.01	0.21	0.86	1.84	2.91	5.46	7.74	10.00



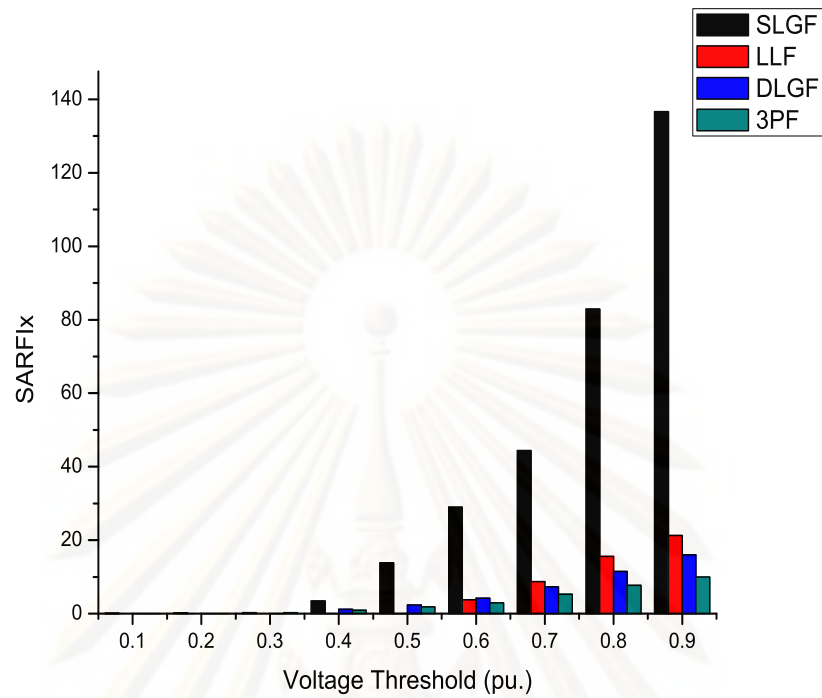


Figure 5.22:  $SARFI_X$  with the voltage threshold and the uniform fault distribution along line.

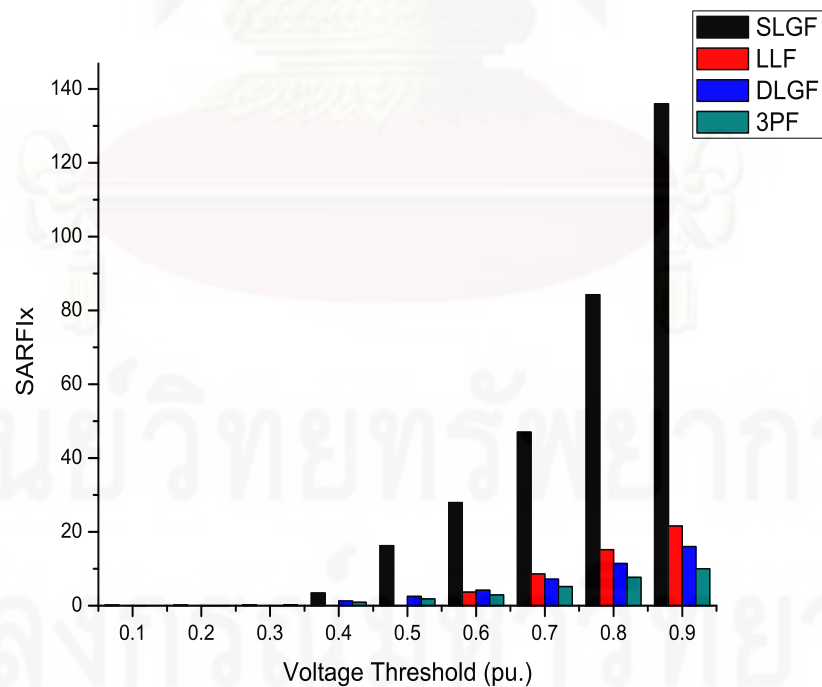


Figure 5.23:  $SARFI_X$  with the voltage threshold and the normal fault distribution along line.

Table 5.14:  $SARFI_X$  with Monte Carlo simulation taking random fault problems into considerations.

Voltage Threshold (pu.)	Phase a	Phase b	Phase c
0.1	0.56	0.55	0.56
0.2	1.18	1.20	1.18
0.3	2.07	2.09	2.07
0.4	6.64	6.61	6.63
0.5	18.32	18.40	18.30
0.6	31.09	31.16	31.21
0.7	51.59	51.60	51.72
0.8	84.60	84.35	84.83
0.9	130.89	129.85	129.75

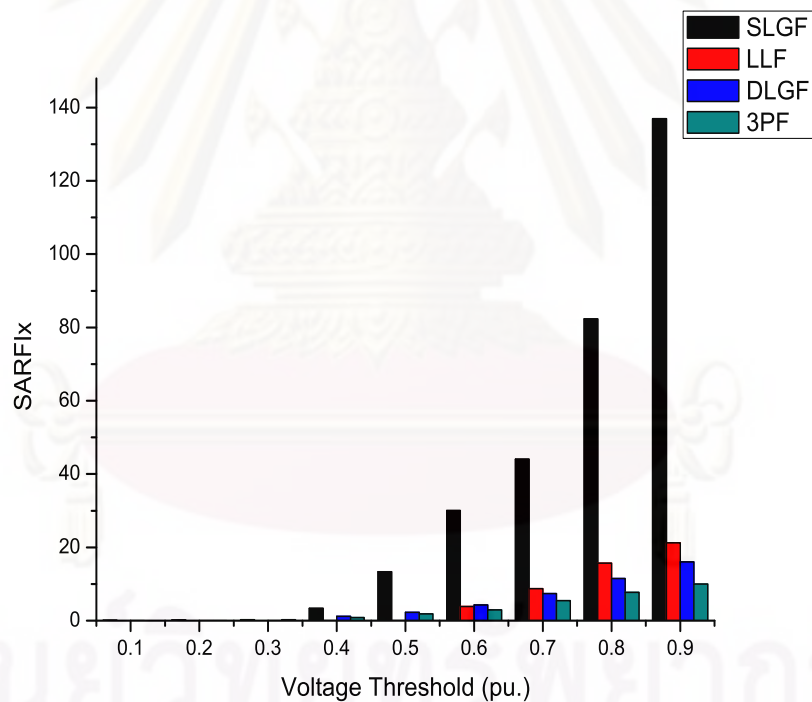


Figure 5.24:  $SARFI_X$  with the voltage threshold and the exponential fault distribution along line.

### 5.3.6.2 $SARFI_{curve}$

In this case,  $SARFI$  index is considered with the sensitive equipment characteristic curve (ITIC) and protective devices. It means that  $SARFI_{curve}$  results are analyzed not only the

magnitude of voltage sags, but also the duration of voltage sags.

The sensitive characteristic curve is used to analyze the sags of the sensitive equipment. It can determine and show when fault event is in the damage area of the sensitive equipment. When any fault occurs in the power system, the sensitive load point will experience voltage sags. The sags on customer site should be considered by analyzing magnitude and duration of any sag event. The magnitude of sag event can be determined by using the fault position method. Meanwhile, the duration of sags event is analyzed by protection system. Coordination of protective devices with the sensitive characteristic curve will show how a protective device can protect and isolate the sags event or not.

Table 5.15 shows  $SARFI_{curve}$  with consideration of the characteristic curve and different fault distribution along line for the sensitive load at bus 2. For SLGF,  $SARFI$  indices are 84.16, 83.27, and 88.31 with uniform, normal, and exponential fault distribution along line, respectively. We can see that fault distribution impacts on the load when a SLGF fault occurs. Fault distribution should be taken into account for analyzing  $SARFI$  indices. Figure 5.25 illustrates  $SARFI_{curve}$  results with fault distribution considered.

Table 5.15:  $SARFI_{curve}$  with ITIC and fault distribution considered

Fault Type	Fault Distribution		
	Uniform	Normal	Exponential
SLGF	84.16	83.27	88.31
LLF	15.19	15.49	15.62
DLGF	11.37	11.46	11.67
3PF	7.59	7.68	7.73

Figure 5.26 and table 5.16 show  $SARFI$  spectrum with the sensitive characteristic curve and MCS consideration. Table 5.16 shows that  $SARFI_{curve}$  are 186.92, 24.87, and 41.64 for phase  $a$ ,  $b$ , and  $c$  when applying MCS, respectively.

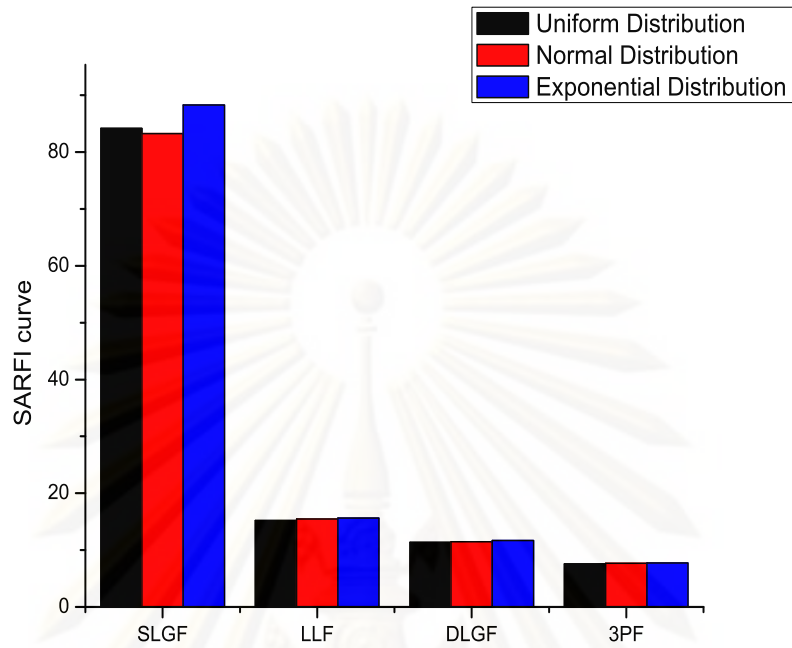


Figure 5.25:  $SARFI_{curve}$  with fault distribution and the characteristic curves considered.

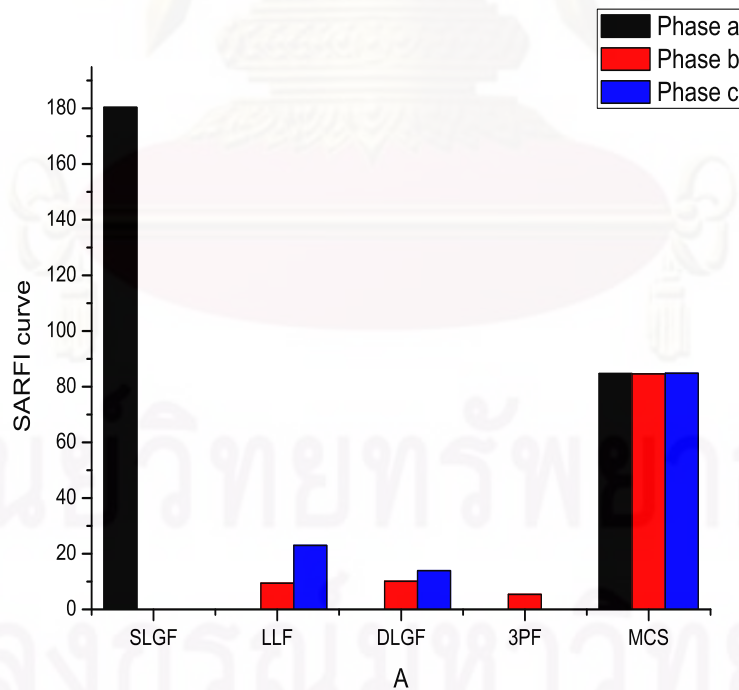


Figure 5.26:  $SARFI_{curve-MCS}$  with the sensitive characteristic curve and Monte Carlo Simulation consideration on analyzing fault problems.



Table 5.16:  $SARFI_{curve-MCS}$  with the sensitive characteristic curve and Monte Carlo Simulation consideration on analyzing fault problems.

Fault Type	Phase <i>a</i>	Phase <i>b</i>	Phase <i>c</i>
SLGF	180.35	0	0
LLF	0	9.48	22.95
DLGF	0	10.11	13.96
3PF	0	5.39	0
MCS	84.68	84.53	84.78

### 5.3.6.3 $SARFI$ Indices with Expansion Test System

In this section, we will assume expansion length of lines and loads of RBTS bus 2 test system about 5 times to analyze  $SARFI$  indices. Table 5.17 shows  $SARFI_X$  with expanding the test system about 5 times and fault distribution consideration for four types of fault. In table 5.18,  $SARFI_{curve}$  is shown with consideration characteristic curve. Moreover, table 5.19 shows  $SARFI$  with Monte Carlo simulation and expansion of length of lines.

Table 5.17:  $SARFI_X$  with expanding length of lines in the test system.

Voltage threshold	Uniform distribution				Normal distribution				Exponential distribution			
	SLGF	LLF	DLGF	3PF	SLGF	LLF	DLGF	3PF	SLGF	LLF	DLGF	3PF
0.1	0.06	0	0	0	0.05	0	0	0	0.07	0	0.01	0
0.2	0.09	0	0.01	0.01	0.1	0	0.01	0.01	0.13	0	0.02	0.01
0.3	0.13	0	0.02	0.15	0.15	0	0.02	0.12	0.19	0	0.02	0.07
0.4	2.27	0	0.87	0.68	1.69	0	0.75	0.64	1.17	0	0.94	0.87
0.5	9.99	0.03	1.29	0.84	9.89	0.06	1.52	1.10	14	0.09	2.21	1.53
0.6	13.77	1.64	1.86	1.21	17.05	1.70	2.29	1.53	23.53	2.94	3.25	2.19
0.7	21.66	3.04	2.92	1.92	25.69	3.82	3.40	2.19	34.98	5.04	4.65	3.01
0.8	33.31	5.70	4.19	2.56	37.49	6.71	4.75	2.96	45.55	7.81	5.63	3.54
0.9	47.35	8.95	5.79	3.61	52.99	10.14	6.45	3.83	54.49	12.14	7.43	4.21

Table 5.18:  $SARFI_{curve}$  with expanding length of lines in the test system.

Voltage threshold	Fault distribution		
	Uniform	Normal	Exponential
SLGF	38.72	37.49	42.07
LLF	6.71	6.71	7.25
DLGF	4.85	4.75	5.24
3PF	3.02	2.96	3.29

Table 5.19:  $SARFI$  with expanding length of lines in the test system and Monte Carlo simulation consideration.

Voltage Threshold	Phase a	Phase b	Phase c
0.1	0.49	0.49	0.49
0.2	1.11	1.14	1.13
0.3	1.96	1.97	1.97
0.4	4.78	4.74	4.74
0.5	11.97	11.99	11.99
0.6	19.36	19.28	19.28
0.7	28.35	28.33	28.33
0.8	40.04	40.15	40.14
0.9	58.23	57.68	57.68
MCS	40.35	39.97	39.97

## 5.4 Discussion

A method to analyze type of protective devices based on coordination of protection and the characteristics of sensitive equipment has been presented in this chapter. Numerical results show the effect of the proposed method in determined which type of protection device can protect and coordinate with the sensitive equipment. The fault position method is applied in the proposed method. It shows that fault position should be considered in analyzing type of protection device for preventing sags on sensitive equipment. 80K and 100K fuses are used to analyze in sections 5.3.1 and 5.3.2. The proposed method determines a operation point based on a coordination of protective devices and sensitive equipment. This operation point analyzes a protective device that can protect a sensitive equipment or not.

Sag frequency is analyzed with different voltage thresholds in section 5.3.3. Different fault distributions and fault types are applied to determine sag frequency for voltage thresh-

old ranging from 10% to 90% of the nominal voltage. Table 5.2 shows that the maximum sag event when single line-to-ground faults occur and uniform fault distribution consideration, is 101.64 sag with the nominal ranging from 60 to 70%, while, the maximum sag frequency with normal and exponential fault distributions are 92.48 and 94.93 with same voltage threshold ranging, respectively. Results mean that different fault distributions will effect to sag frequency when a fault occurs along line. Moreover, sag frequency by applying MCS is also considered in the section 5.3.3. Most of sag frequency for phase  $a$ ,  $b$ , and  $c$  with random faults occur are from 60 – 80%, 70 – 90%, and 40 – 80% of the nominal voltage, respectively.

In this chapter, the area of vulnerability for sensitive equipment based on protection coordination and characteristic of sensitive equipment is also presented. It is analyzed based on consideration of protection coordination for different fault types. Simulation results show that the sag frequency taking the protection coordination into account is lower than sag frequency without the protection coordination consideration in sections 5.3.4 and 5.3.5. It means that protection coordination should be considered to analyze voltage sag on sensitive equipment.

Two types of sag indices, i.e.  $SARFI_X$  and  $SARFI_{curve}$ , are also described in order to analyze numbers of customer that will be impacted by voltage sags. Not only the analytical technique but also stochastic simulation are used to take into account sag indices.  $SARFI_{curve}$  is calculated with different fault distributions in section 5.3.6.2. From table 5.15,  $SARFI$  is 83.27 with normal fault distribution consideration, while,  $SARFI$  with uniform and exponential fault distributions are 84.16 and 88.31, respectively. It shown that different fault distributions will impact  $SARFI_{curve}$ .  $SARFI_{curve}$  for phase  $a$  with MCS for all fault events (fault types, fault locations, and fault lines) is higher when SLGF occurs with only stochastic fault locations and fault lines (SLGF is about 85% fault event in power system). Moreover,  $SARFI_{curve}$  is higher than  $SARFI_X$  in section 5.3.6.1. It means that coordination between protective devices and sensitive equipment is effected because sensitive equipment will be protected by protection coordination.

# CHAPTER VI

## CONCLUSIONS AND FUTURE WORK

### 6.1 Conclusions

Voltage sags have gained more interest due to their consequences on the performance of sensitive equipment. Voltage sags is a short duration reduction in rms voltage between 0.1 and 0.9 pu. with duration from 0.5 cycles to 1 minute. Voltage sags that effect sensitive load are usually caused by faults somewhere in transmission and distribution systems.

Voltage magnitude and duration are essential characteristics of voltage sags. The magnitude of voltage sags is the remaining magnitude expressed in percent or per unit. The voltage sag duration is defined as the flow duration of the fault current in a network. This duration is normally determined by fault clearing time.

The characteristic of sags is defined based on the magnitude and duration of sags; and described by voltage tolerance curves, e.g. ITIC or SEMI curves.

A proposed method is presented to analyze impacts of voltage sags and protection coordination on sensitive equipment in distribution systems. In this dissertation, the fault position method is used to calculate fault currents and fault voltages. It is a powerful tool for short-circuit calculation in the meshed or large power systems. Moreover, this method is also used for fault calculation. Fault distribution is also applied to the fault position method in order to analyze impacts of voltage sags when the fault occurs along line.

Moreover, a stochastic simulation which is Monte Carlo Simulation is presented in this dissertation for simulating a random fault problem. Monte Carlo Simulation is applied to the fault position method with fault parameters such as types of fault, fault positions, fault lines.

The coordination of protection devices is presented as fault clearing process in distribution systems. The general coordination in distribution system is that the fuse should only operate for a permanent fault on the load feeder, however if a fault is a temporary fault or a fault occurs behind the recloser, the recloser should disconnect the circuit and give a fault a chance to clear. Therefore, poor coordination adversely impacts the overall power quality. To protect the sensitive equipment, the coordination of protection devices should apply with the characteristic of the equipment.

Considering the coordination of protection devices and the characteristic of equipment, the area of vulnerability for the sensitive equipment is presented. The area of vulnerability for the sensitive equipment shows the region of the network that includes a part of line or



whole line where the occurrence of the fault will lead to voltage sags at the sensitive load. Based on the area of vulnerability, the expected sags frequency can be determined to analyze impacts of sags.

Sag indices are presented and determined by using two stochastic methods, e.g. an analytical method and Monte Carlo Simulation approach. Different types of fault and fault distributions are also applied.

Contributions of this dissertation are

- Coordination between characteristic of protective devices and sensitive equipment is proposed to investigate impacts of voltage sags on sensitive equipment. The proposed method was able to analyze a operation point which is determined by characteristics of protective device and sensitive equipment. Based on the operation point, types of protective devices are analyzed to prevent voltage sag on sensitive equipment. In addition, a fault position method is a powerful tool for calculating short-circuit in a large or meshed systems. It was applied in the proposed method to the calculation of voltage sag when a fault occurs at bus or along line.
- Sag frequency with consideration of different fault distributions can be determined. This dissertation used the fault position method to apply different types of fault such as fault locations, fault lines, and fault clearing process as an extension of the method for fault calculation. Various stochastic parameters are included in the proposed method to calculate and determine voltage sags of the sensitive equipment. The details of system fault statistic are used to analyze sag events. The fault distribution for the fault along line should apply into the method for the assessment of a stochastic fault on line. Moreover, the area of vulnerability can also be determined based on the proposed method with consideration of protection coordination. It is very useful to analyze the effect of protective devices and fault distributions in sag on sensitive equipment. When the proposed method is applied in RBTS bus 2 test system which is close to an actual distribution system, it shows that fault distributions and coordination of protective devices should be used to analyze voltage sags on sensitive equipment.
- *SARFI* index shows the number of customer could not be served. Two sags indices,  $SARFI_X$  and  $SARFI_{curve}$ ; are shown based on the sag threshold and the sensitive characteristic curve. The proposed method is also applied to analyze *SARFI* with different fault distributions and characteristic of protective devices. Moreover, MCS is also applied and simulated in the proposed method taking into account more complex random factors for fault events. Generally, faults are known as random events, hence

*SARFI* should be analyzed by using stochastic fault parameters. By using MCS, results of sag index are expected close to the actual value.

## 6.2 Future Work

This dissertation presents a proposed method to analyze voltage sags with consideration of coordination between protective device and sensitive equipment. The method requires sensitive equipment data, fault distributions, and time-current characteristic curves of the protective devices. However, the method also has some limitations, and it has not been tested with actual systems. Some recommendations for future work are as follows.

- **Application to real systems**

The proposed method can be applied to a real system to analyze the validity of the method. The effect of fault events occur at bus or along line can be checked with the real record data.

- **Comparing protective devices**

This dissertation has presented how to determine and choose a suitable protective devices based on considering coordination of protection and the equipment sensitivity. It is very useful to improve the system configuration to prevent sags on the sensitive load in the practice. In this dissertation, the fuse parameters are determined based on the setting point, therefore, the proposed method need to compare with real protection system in the distribution systems. Moreover, optimal location and setting for protective devices will consider in future work.

- **Including actual fault distribution**

Fault distribution is presented as uniform, normal, and exponential distributions. In addition, MCS is also used to simulate fault events as stochastic values. However, it just only stochastic equation, therefore, the method can be improved if actual fault distribution can be obtained.

## REFERENCES

- [1] IEEE Standard 1159-1995. *IEEE Recommended Practice for Monitoring Electric Power Quality*.
- [2] M. H. J. Bollen. What is power quality. *Electric Power System Research*. 66. 1. (2003): 5–14.
- [3] M. H. J. Bollen. *Understanding Power Quality Problems: Voltage Sags and Interruption*. New York: IEEE Press. 2000.
- [4] C. Sankaran. *Power Quality*. CRC Press. 2001.
- [5] S. Santoso, J. Lamoree, W. M. Grady, E. J. Powers, and S. C. Bhatt. A scalable pq event identification system. *IEEE Transactions on Power Delivery*. 15. 2. (2000): 738 – 743.
- [6] R. C. Dugan, M. F. McGranaghan, and H. W. Beaty. *Electrical Power Systems Quality*. McGraw Hill. 2000.
- [7] R. C. Dugan, S. Santoso, M. F. McGranaghan, and H. W. Beaty. *Electrical Power Systems Quality*. McGraw-Hill. 2 ed.. 2002.
- [8] Standard BS EN 501560:2000. *Voltage characteristics of electricity supplied by public distribution systems*. 2000.
- [9] Standard IEC 61000 - 2 - 8. *Electromagnetic compatibility (EMC) - Part 2-8: Environment - Voltage dips and short interruptions on public electric power supply systems with statistical measurement results*. 2002.
- [10] Standard IEC 61000 - 4 - 30. *Electromagnetic compatibility (EMC) - Part 4-30: Testing and measurement techniques - Power quality measurement methods*. 2003.
- [11] P. Heine and M. Lehtonen. Voltage dip distributions caused by power system faults. *IEEE Transactions on Power Systems*. 18. 4. (2003): 1367 – 1373.
- [12] T. A. Short. *Distribution Reliability and Power Quality*. CRC Press. 2005.
- [13] M. F. McGranaghan, D. R. Mueller, and M. J. Samotyj. Voltage sags in industrial systems. *IEEE Transactions on Industry Applications*. 29. 2. (1993): 397 – 403.

- [14] S. Z. Djokic, J. V. Milanovic, and D. S. Krischen. Sensitivity of ac coil contactors to voltage sags, short interruptions and undervoltage transients. *IEEE Transactions on Power Delivery*. 19. 3. (2004): 1299 – 1307.
- [15] S. Z. Djokic, K. Stockman, J. V. Milanovic, J. J. M. Desmet, and R. Belmans. Sensitivity of ac adjustable speed drives to voltage sags and short interruptions. *IEEE Transactions on Power Delivery*. 20. 1. (2005): 494 – 505.
- [16] S. Z. Djokic, J. Desmet, G. Vanalme, J. V. Milanovic, and K. Stockman. Sensitivity of personal computers to voltage sags and short interruptions. *IEEE Transactions on Power Delivery*. 20. 1. (2005): 375–384.
- [17] J. A. Martinez-Velasco and J. Martin-Arnecló. Distributed generation impact on voltage sags in distribution networks. *9th International Conference on Electrical Power Quality and Utilisation (EPQU 2007)*. (2007): 1 – 6.
- [18] C. Radhakrishna, M. Eshwardas, and G. Chebiyam. Impact of voltage sags in practical power system networks. *IEEE/PES Transmission and Distribution Conference and Exposition*. 1. (2001): 567 - 572.
- [19] L. Comassetto, D. P. Bernadon, L. N. Canha, and A. R. Abaide. Automated coordination and optimization tool of protection devices for distribution system. *POWERENG2007*. (2007): 388–393.
- [20] S. Chaitusaney and A. Yokoyama. Prevention of reliability degradation from recloser-fuse miscoordination due to distribution generation. *IEEE Transactions on Power Delivery*. 23. 4. (2008): 2545–2554.
- [21] M. Johns and L. Morgan. Voltage sag mitigation through ridethrough coordination. *IEEE Annual Textile, Fiber and Film Industry Technical Conference*. (1994): 1 – 5.
- [22] L. E. Conrad and M. H. J. Bollen. Voltage sag coordination for reliable plant operation. *IEEE Transactions on Industry Applications*. 33. 6. (1997): 1459 - 1464.
- [23] M. T. Bishop, S. R. Mendis, J. F. Witte, and P. Myers. Overcurrent protection device miscoordination issues that result in plant outages and costly down time. *Petroleum and Chemical Industry Conference, 1996, Record of Conference Papers. The Institute of Electrical and Electronics Engineers Incorporated Industry Applications Society 43rd Annual* . (1996): 183 – 189.
- [24] M. H. J. Bollen. Fast assessment methods for voltage sags in distribution systems. *IEEE Transactions on Industry Applications*. 32. 6. (1996): 1414–1423.



- [25] M. H. J. Bollen. Characterisation of voltage sags experienced by three-phase adjustable-speed drives. *IEEE Transactions on Power Delivery*. 12. 4. (1997): 1666 – 1671.
- [26] M. H. J. Bollen. Method of critical distances for stochastic assessment of voltage sags. *IEE Proceedings Generation, Transmission and Distribution*. 145. 1. (1998): 70 – 76.
- [27] L. D. Bollen. Algorithms for characterizing measured three-phase unbalanced voltage dips. *IEEE Transactions on Power Delivery*. 18. 3. (2003): 937 – 944.
- [28] M. H. Qader, M. H. J. Bollen, and R. N. Allan. Stochastic prediction of voltage sags in a large transmission system. *IEEE Transactions on Industry Applications*. 35. 1. (1999): 152 – 162.
- [29] S. Omar Faried and S. Aboreshaid. Stochastic evaluation of voltage sags in series capacitor compensated radial distribution systems. *IEEE Transactions on Power Delivery*. 18. 3. (2003): 744 – 750.
- [30] G. J. Lee, M. M. Albu, and G. T. Heydt. A power quality index based on equipment sensitivity, cost, and network vulnerability. *IEEE Transactions on Power Delivery*. 19. 3.
- [31] F. Kinces. Voltage sag indices and statistics. Master's thesis. Chalmers University of Technology. 2004.
- [32] E. Styvaktakis. *Automating Power Quality Analysis*. Ph.D. Thesis. Chalmers University of Technology. 2002.
- [33] P. Heine, P. Pohjanheimo, M. Lehtonen, and E. Lakervi. A method for estimating the frequency and cost of voltage sags. *IEEE Transactions on Power Systems*. 17. 2. (2002): 290 – 296.
- [34] S. W. Middlekauff and E. R. J. Collins. System and customer impact: considerations for series custom power devices. *IEEE Transactions on Power Delivery*. 13. 1. (1998): 278 – 282.
- [35] P. Heine. *Voltage sags in power distribution networks*. Ph.D. Thesis. Helsinki University of Technology. Espoo. 2005.
- [36] The information technology industry council (ITD)[Online]. Available from: [www.itic.org](http://www.itic.org).
- [37] Standard IEC 61000 - 4 - 11. *Electromagnetic compatibility (EMC) - Part 4-11: Voltage dips, short interruptions and voltage variations immunity tests*. 1994.

- [38] M. Jong-Fil, Y. Sang-Yun, and K. Jae-Chul. Quantitative evaluation of the impact of repetitive voltage sags on low-voltage loads. *IEEE Transactions on Power Delivery*. 22. 4. (2007): 2395 - 2400.
- [39] J. A. Martinez-Velasco and J. Martin-Arnedo. Advanced load models for voltage dip studies in distribution networks. *IEEE PES General Meeting*. June 2004.
- [40] SEMI voltage sags tolerance [Online]. Available from: [www.semi.org](http://www.semi.org).
- [41] D.-J. Won, A. Seon-Ju, C. Il-Yop, K. Joong-Moon, and M. Seung-II. A new definition of voltage sag duration considering the voltage tolerance curve. *IEEE Bologna Power Tech Conference*. 3. June 2003.
- [42] J. A. Martinez and J. Martin-Arnedo. Voltage sag studies in distribution networks - part ii: voltage sag assessment. *IEEE Transactions on Power Delivery*. 21. 3. (2006): 1679-1688.
- [43] J. Lamoree, D. Mueller, P. Vinett, W. Jones, and M. Samotyj. Voltage sag analysis case studies. *IEEE Transactions on Industry Applications*. 30. 4. (1994): 1083 – 1089.
- [44] C. H. Park and G. Jang. Fast method to determine an area of vulnerability for stochastic prediction of voltage sags. *IEE Proceedings - Generation, Transmission and Distribution*. 152. 6. (2005): 819–827.
- [45] J. V. Milanovic, M. T. Aung, and C. P. Gupta. The influence of fault distribution on stochastic prediction of voltage sags. *IEEE Transactions on Power Delivery*. 20. 1. (2005): 278-285.
- [46] E. E. Juarez and A. Hernandez. An analytical approach for stochastic assessment of balanced and unbalanced voltage sags in large systems. *IEEE Transactions on Power Delivery*. 21. 3. (2006): 1493 – 1500.
- [47] T. Thasananutariya and S. Chatratana. Stochastic prediction of voltage sags in an industrial estate. *Conference Record of the 2005 Industry Applications Conference and Fourtieth IAS Annual Meeting*. 2. (2005): 1489 – 1496.
- [48] X. Yu. *Analyses of Power System Vulnerability and Total Transfer Capability*. Ph.D. Thesis. Texas A&M University. 2005.
- [49] C. H. Park and G. Jang. Stochastic estimation of voltage sags in a large mesh network. *IEEE Transactions on Power Delivery*. 22. 3. (2007): 1655–1664.

- [50] M. T. Aung, J. V. Milanovic, and C. P. Gupta. Propagation of asymmetrical sags and the influence of boundary crossing lines on voltage sag prediction. *IEEE Transactions on Power Delivery*. 19. 4. (2004): 1819–1827.
- [51] B. Q. Khanh, D.-J. Won, and S.-I. Moon. Fault distribution modeling using stochastic bivariate models for prediction of voltage sag in distribution systems. *IEEE Transactions on Power Delivery*. 23. 1. (2008): 347–354.
- [52] R. Billinton and R. N. Allan. *Reliability Evaluation of Engineering Systems*. New York: Plenum Press. 1992.
- [53] R. Billinton and R. N. Allan. *Reliability Evaluation of Power Systems*. New York: Plenum Press. 1994.
- [54] L. Y. Seng. *Probabilistic Assessment of Voltage-Sag Occurrence and the Evaluation of the Dynamic Voltage Restorer*. Ph.D. Thesis. University of Maschester Institute of Science and Technology.
- [55] J. C. Gmez and M. M. Morcos. Coordination of voltage sag and overcurrent protection in dg systems. *IEEE Transactions on Power Delivery*. 20. 1. (2005): 214–218.
- [56] B. Wang, W. Xu, and Z. Pan. Voltage sag state estimation for power distribution systems. *IEEE Power Engineering Society General Meeting*. 3.
- [57] Y. S. Lim and S. G.. Analytical approach to probabilistic prediction of voltage sags on transmission networks. *IEE Proceedings - Generation, Transmission and Distribution*. 149. 1. (2002): 7 – 14.
- [58] E. Espinosa-Juarez and A. Hernandez. A method for voltage sag state estimation in power systems. *IEEE Transactions on Power Delivery*. 22. 4. (2007): 2517 – 2526.
- [59] R. J. Gopi, V. K. Ramachandramurthy, and M. T. Au. Impedance matrix approach to stochastic assessment for balanced and unbalanced voltage sags on transmission networks. *International Conference on Power Electronics and Drive Systems (PEDS 2009)*. (2009): 115-120.
- [60] M. N. Moschakis and N. D. Hatziargyriou. Analytical calculation and stochastic assessment of voltage sags. *IEEE Transactions on Power Delivery*. 21. 3. (2006): 1727-1734.
- [61] J. M. Gers and E. J. Holmes. *Protection of Electricity Distribution Networks*. London, U.K.: Inst. Elec. Eng.. 2004.
- [62] T. Gonen. *Electric Power Distribution System Engineering*. CRC Press. 2 ed.. 2007.

- [63] J. A. Martinez and J. Martin-Arnedo. Impact of distributed generation on distribution protection and power quality. *IEEE Power and Energy Society General Meeting*. (2009): 1 – 6.
- [64] J. A. Martinez and J. Martin-Arnedo. Modeling of protective devices for voltage sag studies in distribution systems. *IEEE Power Engineering Society General Meeting*. 1. (2004): 451 – 456.
- [65] S. Santoso and T. A. Short. Identification of fuse and recloser operations in a radial distribution system. *IEEE Transactions on Power Delivery*. 22. 4. (2007): 2370–2377.
- [66] IEEE Standard C37.112-1996. *IEEE Standard Inverse-Time Characteristic Equations for Overcurrent Relays*. 1996.
- [67] J. L. Blackburn. *Protective Relaying, Principles and Applications*. New York: Marcel Dekker Inc. 1998.
- [68] I. Standard. *IEEE Recommended Practice for Protection and Coordination of Industrial and Commercial Power Systems*. 1986.
- [69] I. Standard. *IEEE Recommended Practice for Protection and Coordination of Industrial and Commercial Power Systems*. 2001.
- [70] S. Chaitusaney and A. Yokoyama. Impact of protection coordination on sizes of several distributed generation sources. *The 7th International Power Engineering Conference (IPEC 2005)*. 2. (2005): 669– 674.
- [71] C. W. So and K. K. Li. Time coordination method for power system protection by evolutionary algorithm. *Thirty-Fourth IAS Annual Meeting. Conference Record of the 1999 IEEE Industry Applications Conference*. 4. (1999): 2348 – 2354.
- [72] C. W. So and K. K. Li. Time coordination method for power system protection by evolutionary algorithm. *IEEE Transactions on Industry Applications*. 36. 5. (2000): 1235 – 1240.
- [73] K. K. Li and C. W. So. Evolutionary algorithm for protection relay setting coordination. *International Conference on Power System Technology (PowerCon 2000)*. 2. (2000): 813 – 817.
- [74] T. A. Short. *Electrical Power Distribution Handbook*. CRC. 2004.



- [75] B. Wang, W. Xu, and Z. Pan;. A method to estimate voltage sag profile for power distribution systems. *Power System Technology, 2004. PowerCon 2004. 2004 International Conference on*. 2. (2004): 1763 – 1767.
- [76] X. Xiangning, T. Shun, B. Tianshu, and X. Yonghai. Study on distribution reliability considering voltage sags and acceptable indices. *IEEE Transactions on Power Delivery*. 22. 2. (2007): 1003–1008.
- [77] J. M. C. Filho, R. C. Leborgne, P. Marcio da Silveira, and M. H. J. Bollen. Voltage sag index calculation: Comparison between time-domain simulation and short-circuit calculation. *Electric Power System Research*. 78. (2008): 676–682.
- [78] J. A. Martinez and J. Martin-Arnedo. Voltage sag studies in distribution networks part iii: Voltage sag index calculation. *IEEE Transactions on Power Delivery*. 21. 1698 2006.
- [79] R. A. Barr, V. J. Gosbell, and I. McMichael. A new saifi based voltage sag index. *13th International Conference on Harmonics and Quality of Power (ICHQP 2008)* . 1–5.
- [80] P. Heine and M. Lehtonen. Probability of voltage sags depending on the characteristics of medium voltage networks. *International Conference on Probabilistic Methods Applied to Power Systems (PMAPS 2006)*. (2006): 1–7.
- [81] M. H. J. Bollen. Reliability analysis of industrial power systems taking into account voltage sags. *Conference Record of the 1993 IEEE Industry Applications Society Annual Meeting*. 2. (1993): 1461 - 1468.
- [82] G. Olguin, D. Karlsson, and R. Leborgne. Stochastic assessment of voltage dips (sags): The method of fault positions versus a monte carlo simulation approach. *IEEE Russia Power Tech*. (2005): 1-7.
- [83] R. Bollinton and W. Li. *Reliability Assessment of Electric Power Systems Using Monte Carlo Methods*. New York: Plenum Press. 1994.
- [84] S.-Y. Yun and J.-C. Kim. An evaluation method of voltage sag using a risk assessment model in power distribution systems. *Electrical Power and Energy Systems*. 25. (2003): 829–839.
- [85] U. A. Bordalo, A. B. Rodrigues, and M. G. Da Silva. A new methodology for probabilistic short-circuit evaluation with applications in power quality analysis. *IEEE Transactions on Power Delivery*. 21. 2. (2006): 474–479.

- [86] Y. Yuan, Y. Jingyan, Z. Jianhua, and X. Xiangning;. Reliability analysis of power distribution systems based on hybrid method into account of voltage sags. *The 7th International Power Engineering Conference(IPEC 2005)*. 2. (2005): 945–949.
- [87] A. Maitra, A. M. Gaikwad, and T. Short. Assessing financial feasibility of pq improvement devices using monte carlo simulations. *International Conference on Probabilistic Methods Applied to Power Systems*. (2004): 569 – 574.
- [88] N. Kagan, N. M. Matsuo, G. Vasconcelos, U. F. Castellano, J. C. Cebrian, L. M. Camilo, S. X. Duarte, H. Arango, W. H. Bernartelli, and J. Marsulo. Evaluating the risk of equipment disruption related to voltage sags. *IEEE/PES Transmission and Distribution Conference and Exposition: Latin America*. (2004): 669 – 674.
- [89] M. T. Aung and J. Milanovic. Stochastic prediction of voltage sags by considering the probability of the failure of the protection system. *IEEE Transactions on Power Delivery*. 21. 1. (2006): 322-329.
- [90] P. Yuthagovit and B. Eua-arporn. Reliability analysis of electrical distribution systems with considerations of voltage sags and protection system operation. *12CEPSI 1998*.
- [91] L. V. Tien, A. Yokoyama, T. Tayjasant, and B. Eua-Arporn. Impacts of voltage sags and protection coordination on sensitive equipment in distribution system. *The International Conference on Electrical Engineering 2009 (ICEE2009)*. (2009): .
- [92] R. Billinton, S. Kumar, N. Chowdhury, K. Chu, K. Debnath, L. Geol, E. Khan, P. Kos, G. Nourbakhsh, and J. Oteng-Adjei. A reliability test system for educational purposes - basic data. *IEEE Transactions on Power Systems*. 4. 3. (1989): 1238–1244.
- [93] R. Billinton, S. Kumar, N. Chowdhury, K. Chu, L. Goel, E. Khan, P. Kos, G. Nourbakhsh, and J. Oteng-Adjei. A reliability test system for educational purposes - basic results. *IEEE Transactions on Power Systems*. 5. 1. (1990): 319–325.
- [94] N. Chowdhury and R. Billinton. A reliability test system for educational purposes - spinning reserve studies in isolated and interconnected systems. *IEEE Transactions on Power Systems*. 6. November 1991.
- [95] L. V. Tien and T. Tayjasant. An analytical approach for stochastic estimation of voltage sags in power systems. *ECTI-CON 2008*. 2. (2008): 1029–1032.
- [96] A. Baghini, ed.. *Handbook of Power Quality*. John Wiley and Sons. 2008.



APPENDICES

ศูนย์วิทยทรัพยากร  
จุฬาลงกรณ์มหาวิทยาลัย

## Appendix A: RBTS Bus 2 Test System

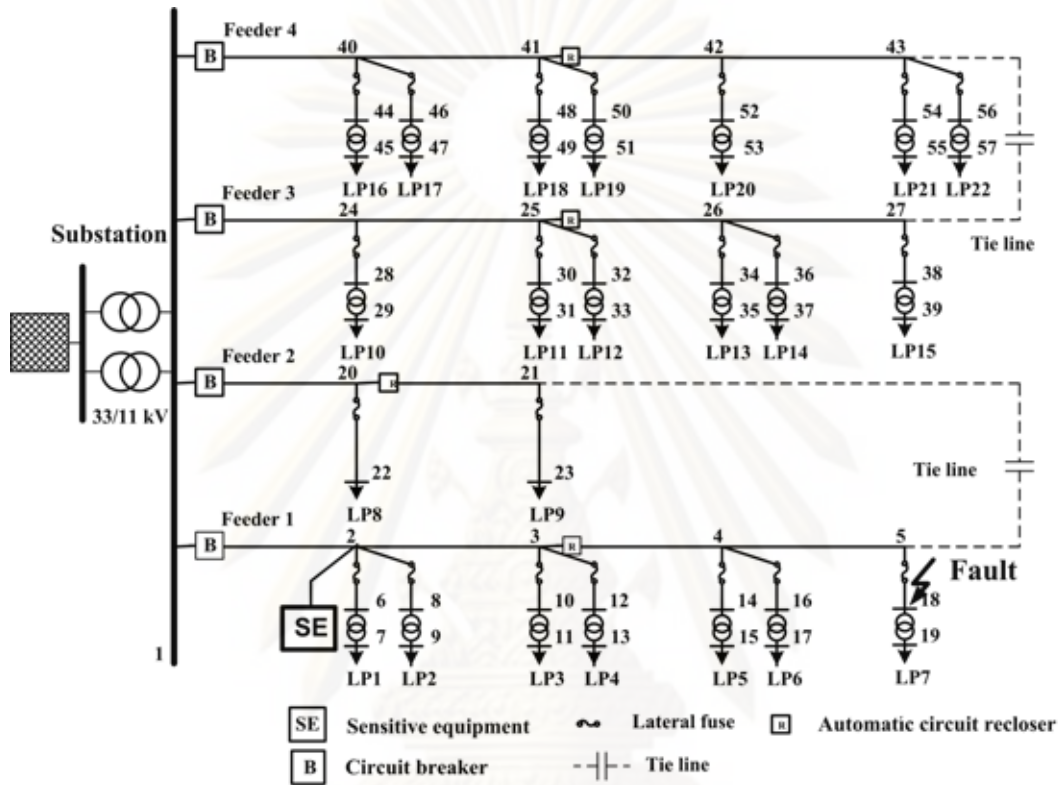


Figure A.1: RBTS bus 2 test system

ศูนย์วิทยทรัพยากร  
จุฬาลงกรณ์มหาวิทยาลัย



### Appendix B: Bus Data of RBTS Bus 2 Test System (1/2)

Bus Number	Load		Shunt		Initial Voltage		Voltage limits	
	P (MW)	Q (MVar)	G (MW)	B (MVar)	Mag. (pu.)	Ang. (pu.)	Min. (pu.)	Max (pu.)
1	0.0000	0.0000	0.00	0.00	1.00	0.00	0.95	1.05
2	0.0000	0.0000	0.00	0.00	1.00	0.00	0.95	1.05
3	0.0000	0.0000	0.00	0.00	1.00	0.00	0.95	1.05
4	0.0000	0.0000	0.00	0.00	1.00	0.00	0.95	1.05
5	0.0000	0.0000	0.00	0.00	1.00	0.00	0.95	1.05
6	0.0000	0.0000	0.00	0.00	1.00	0.00	0.95	1.05
7	0.5350	0.2960	0.00	0.00	1.00	0.00	0.95	1.05
8	0.0000	0.0000	0.00	0.00	1.00	0.00	0.95	1.05
9	0.5350	0.2960	0.00	0.00	1.00	0.00	0.95	1.05
10	0.0000	0.0000	0.00	0.00	1.00	0.00	0.95	1.05
11	0.5350	0.2960	0.00	0.00	1.00	0.00	0.95	1.05
12	0.0000	0.0000	0.00	0.00	1.00	0.00	0.95	1.05
13	0.5660	0.3132	0.00	0.00	1.00	0.00	0.95	1.05
14	0.0000	0.0000	0.00	0.00	1.00	0.00	0.95	1.05
15	0.5660	0.3132	0.00	0.00	1.00	0.00	0.95	1.05
16	0.0000	0.0000	0.00	0.00	1.00	0.00	0.95	1.05
17	0.4540	0.2512	0.00	0.00	1.00	0.00	0.95	1.05
18	0.0000	0.0000	0.00	0.00	1.00	0.00	0.95	1.05
19	0.4540	0.2512	0.00	0.00	1.00	0.00	0.95	1.05
20	0.0000	0.0000	0.00	0.00	1.00	0.00	0.95	1.05
21	0.0000	0.0000	0.00	0.00	1.00	0.00	0.95	1.05
22	1.0000	0.5533	0.00	0.00	1.00	0.00	0.95	1.05
23	1.1500	0.6363	0.00	0.00	1.00	0.00	0.95	1.05
24	0.0000	0.0000	0.00	0.00	1.00	0.00	0.95	1.05
25	0.0000	0.0000	0.00	0.00	1.00	0.00	0.95	1.05
26	0.0000	0.0000	0.00	0.00	1.00	0.00	0.95	1.05
27	0.0000	0.0000	0.00	0.00	1.00	0.00	0.95	1.05
28	0.0000	0.0000	0.00	0.00	1.00	0.00	0.95	1.05

### Appendix B: Bus Data of RBTS Bus 2 Test System (2/2)

Bus Number	Load		Shunt		Initial Voltage		Voltage limits	
	P (MW)	Q (MVar)	G (MW)	B (MVar)	Mag. (pu.)	Ang. (pu.)	Min. (pu.)	Max (pu.)
29	0.5350	0.2960	0.00	0.00	1.00	0.00	0.95	1.05
30	0.0000	0.0000	0.00	0.00	1.00	0.00	0.95	1.05
31	0.5350	0.2960	0.00	0.00	1.00	0.00	0.95	1.05
32	0.0000	0.0000	0.00	0.00	1.00	0.00	0.95	1.05
33	0.4500	0.2490	0.00	0.00	1.00	0.00	0.95	1.05
34	0.0000	0.0000	0.00	0.00	1.00	0.00	0.95	1.05
35	0.5660	0.3132	0.00	0.00	1.00	0.00	0.95	1.05
36	0.0000	0.0000	0.00	0.00	1.00	0.00	0.95	1.05
37	0.5660	0.3132	0.00	0.00	1.00	0.00	0.95	1.05
38	0.0000	0.0000	0.00	0.00	1.00	0.00	0.95	1.05
39	0.4540	0.2512	0.00	0.00	1.00	0.00	0.95	1.05
40	0.0000	0.0000	0.00	0.00	1.00	0.00	0.95	1.05
41	0.0000	0.0000	0.00	0.00	1.00	0.00	0.95	1.05
42	0.0000	0.0000	0.00	0.00	1.00	0.00	0.95	1.05
43	0.0000	0.0000	0.00	0.00	1.00	0.00	0.95	1.05
44	0.0000	0.0000	0.00	0.00	1.00	0.00	0.95	1.05
45	0.4540	0.2512	0.00	0.00	1.00	0.00	0.95	1.05
46	0.0000	0.0000	0.00	0.00	1.00	0.00	0.95	1.05
47	0.4500	0.2490	0.00	0.00	1.00	0.00	0.95	1.05
48	0.0000	0.0000	0.00	0.00	1.00	0.00	0.95	1.05
49	0.4500	0.2490	0.00	0.00	1.00	0.00	0.95	1.05
50	0.0000	0.0000	0.00	0.00	1.00	0.00	0.95	1.05
51	0.4500	0.2490	0.00	0.00	1.00	0.00	0.95	1.05
52	0.0000	0.0000	0.00	0.00	1.00	0.00	0.95	1.05
53	0.5660	0.3132	0.00	0.00	1.00	0.00	0.95	1.05
54	0.0000	0.0000	0.00	0.00	1.00	0.00	0.95	1.05
55	0.5660	0.3132	0.00	0.00	1.00	0.00	0.95	1.05
56	0.0000	0.0000	0.00	0.00	1.00	0.00	0.95	1.05
57	0.4540	0.2512	0.00	0.00	1.00	0.00	0.95	1.05

### Appendix C: Positive and Negative Sequence Impedances for Line Data of RBTS Bus 2 Test System (1/2)

Branch	From	To	R (pu.)	X (pu.)	B (pu.)	Rating (MVA)	Ratio	Angle (deg.)
1	1	2	0.0731	0.0567	0	250	0	0
2	2	3	0.0731	0.0567	0	250	0	0
3	3	4	0.0731	0.0567	0	150	0	0
4	4	5	0.0585	0.0454	0	300	0	0
5	2	6	0.0585	0.0454	0	150	0	0
6	2	8	0.0780	0.0605	0	250	0	0
7	3	10	0.0780	0.0605	0	250	0	0
8	3	12	0.0585	0.0454	0	250	0	0
9	4	14	0.0780	0.0605	0	250	0	0
10	4	16	0.0731	0.0567	0	250	0	0
11	5	18	0.0780	0.0605	0	250	0	0
12	6	7	0.0000	4.5661	0	150	1	0
13	8	9	0.0000	4.5661	0	250	1	0
14	10	11	0.0000	4.5661	0	250	1	0
15	12	13	0.0000	4.5661	0	250	1	0
16	14	15	0.0000	4.5661	0	250	1	0
17	16	17	0.0000	4.5661	0	250	1	0
18	18	19	0.0000	4.5661	0	250	1	0
19	1	20	0.0731	0.0567	0	250	0	0
20	20	21	0.0585	0.0454	0	250	0	0
21	20	22	0.0780	0.0605	0	150	0	0
22	21	23	0.0780	0.0605	0	300	0	0
23	1	24	0.0731	0.0567	0	250	0	0
24	24	25	0.0780	0.0605	0	250	0	0
25	25	26	0.0585	0.0454	0	150	0	0
26	26	27	0.0731	0.0567	0	300	0	0
27	24	28	0.0585	0.0454	0	150	0	0
28	25	30	0.0731	0.0567	0	250	0	0

### Appendix C: Positive and Negative Sequence Impedances for Line Data of RBTS Bus 2 Test System (2/2)

Branch	From	To	R (pu.)	X (pu.)	B (pu.)	Rating (MVA)	Ratio	Angle (deg.)
29	25	32	0.0780	0.0605	0	250	0	0
30	26	34	0.0731	0.0567	0	250	0	0
31	26	36	0.0780	0.0605	0	250	0	0
32	27	38	0.0585	0.0454	0	250	0	0
33	28	29	0.0000	4.5661	0	150	1	0
34	30	31	0.0000	4.5661	0	250	1	0
35	32	33	0.0000	4.5661	0	250	1	0
36	34	35	0.0000	4.5661	0	250	1	0
37	36	37	0.0000	4.5661	0	250	1	0
38	38	39	0.0000	4.5661	0	250	1	0
39	1	40	0.0780	0.0605	0	250	0	0
40	40	41	0.0731	0.0567	0	250	0	0
41	41	42	0.0731	0.0567	0	150	0	0
42	42	43	0.0585	0.0454	0	300	0	0
43	40	44	0.0731	0.0567	0	150	0	0
44	40	46	0.0585	0.0454	0	250	0	0
45	41	48	0.0585	0.0454	0	250	0	0
46	41	50	0.0780	0.0605	0	250	0	0
47	42	52	0.0780	0.0605	0	250	0	0
48	43	54	0.0731	0.0567	0	250	0	0
49	43	56	0.0780	0.0605	0	250	0	0
50	44	45	0.0000	4.5661	0	150	1	0
51	46	47	0.0000	4.5661	0	250	1	0
52	48	49	0.0000	4.5661	0	250	1	0
53	50	51	0.0000	4.5661	0	250	1	0
54	52	53	0.0000	4.5661	0	250	1	0
55	54	55	0.0000	4.5661	0	250	1	0
56	56	57	0.0000	4.5661	0	250	1	0



### Appendix D: Zero Sequence Impedances for Line Data of RBTS Bus 2 Test System (1/2)

Branch	From	To	R (pu.)	X (pu.)	B (pu.)	Rating (MVA)	Ratio	Angle (deg.)
1	1	2	0.0731	0.0567	0	250	0	0
2	2	3	0.0731	0.0567	0	250	0	0
3	3	4	0.0731	0.0567	0	150	0	0
4	4	5	0.0585	0.0454	0	300	0	0
5	2	6	0.0585	0.0454	0	150	0	0
6	2	8	0.0780	0.0605	0	250	0	0
7	3	10	0.0780	0.0605	0	250	0	0
8	3	12	0.0585	0.0454	0	250	0	0
9	4	14	0.0780	0.0605	0	250	0	0
10	4	16	0.0731	0.0567	0	250	0	0
11	5	18	0.0780	0.0605	0	250	0	0
12	6	7	0.0000	4.5661	0	150	1	0
13	8	9	0.0000	4.5661	0	250	1	0
14	10	11	0.0000	4.5661	0	250	1	0
15	12	13	0.0000	4.5661	0	250	1	0
16	14	15	0.0000	4.5661	0	250	1	0
17	16	17	0.0000	4.5661	0	250	1	0
18	18	19	0.0000	4.5661	0	250	1	0
19	1	20	0.0731	0.0567	0	250	0	0
20	20	21	0.0585	0.0454	0	250	0	0
21	20	22	0.0780	0.0605	0	150	0	0
22	21	23	0.0780	0.0605	0	300	0	0
23	1	24	0.0731	0.0567	0	250	0	0
24	24	25	0.0780	0.0605	0	250	0	0
25	25	26	0.0585	0.0454	0	150	0	0
26	26	27	0.0731	0.0567	0	300	0	0
27	24	28	0.0585	0.0454	0	150	0	0
28	25	30	0.0731	0.0567	0	250	0	0

### Appendix D: Zero Sequence Impedances for Line Data of RBTS Bus 2 Test System (2/2)

Branch	From	To	R (pu.)	X (pu.)	B (pu.)	Rating (MVA)	Ratio	Angle (deg.)
29	25	32	0.0780	0.0605	0	250	0	0
30	26	34	0.0731	0.0567	0	250	0	0
31	26	36	0.0780	0.0605	0	250	0	0
32	27	38	0.0585	0.0454	0	250	0	0
33	28	29	0.0000	4.5661	0	150	1	0
34	30	31	0.0000	4.5661	0	250	1	0
35	32	33	0.0000	4.5661	0	250	1	0
36	34	35	0.0000	4.5661	0	250	1	0
37	36	37	0.0000	4.5661	0	250	1	0
38	38	39	0.0000	4.5661	0	250	1	0
39	1	40	0.0780	0.0605	0	250	0	0
40	40	41	0.0731	0.0567	0	250	0	0
41	41	42	0.0731	0.0567	0	150	0	0
42	42	43	0.0585	0.0454	0	300	0	0
43	40	44	0.0731	0.0567	0	150	0	0
44	40	46	0.0585	0.0454	0	250	0	0
45	41	48	0.0585	0.0454	0	250	0	0
46	41	50	0.0780	0.0605	0	250	0	0
47	42	52	0.0780	0.0605	0	250	0	0
48	43	54	0.0731	0.0567	0	250	0	0
49	43	56	0.0780	0.0605	0	250	0	0
50	44	45	0.0000	4.5661	0	150	1	0
51	46	47	0.0000	4.5661	0	250	1	0
52	48	49	0.0000	4.5661	0	250	1	0
53	50	51	0.0000	4.5661	0	250	1	0
54	52	53	0.0000	4.5661	0	250	1	0
55	54	55	0.0000	4.5661	0	250	1	0
56	56	57	0.0000	4.5661	0	250	1	0

### Appendix E: Length Lines Data of RBTS Bus 2 Test System

Branch	From	To	Length (km)	Branch	From	To	Length (km)
1	1	2	0.75	29	25	32	0.80
2	2	3	0.75	30	26	34	0.75
3	3	4	0.75	31	26	36	0.80
4	4	5	0.60	32	27	38	0.60
5	2	6	0.60	33	28	29	-
6	2	8	0.80	34	30	31	-
7	3	10	0.80	35	32	33	-
8	3	12	0.60	36	34	35	-
9	4	14	0.80	37	36	37	-
10	4	16	0.75	38	38	39	-
11	5	18	0.80	39	1	40	0.80
12	6	7	-	40	40	41	0.75
13	8	9	-	41	41	42	0.75
14	10	11	-	42	42	43	0.60
15	12	13	-	43	40	44	0.75
16	14	15	-	44	40	46	0.60
17	16	17	-	45	41	48	0.60
18	18	19	-	46	41	50	0.80
19	1	20	0.75	47	42	52	0.80
20	20	21	0.60	48	43	54	0.75
21	20	22	0.80	49	43	56	0.80

ศูนย์วิทยทรัพยากร  
จุฬาลงกรณ์มหาวิทยาลัย

**Appendix F: ITI (CBEMA) Curve (Revised 2000)**

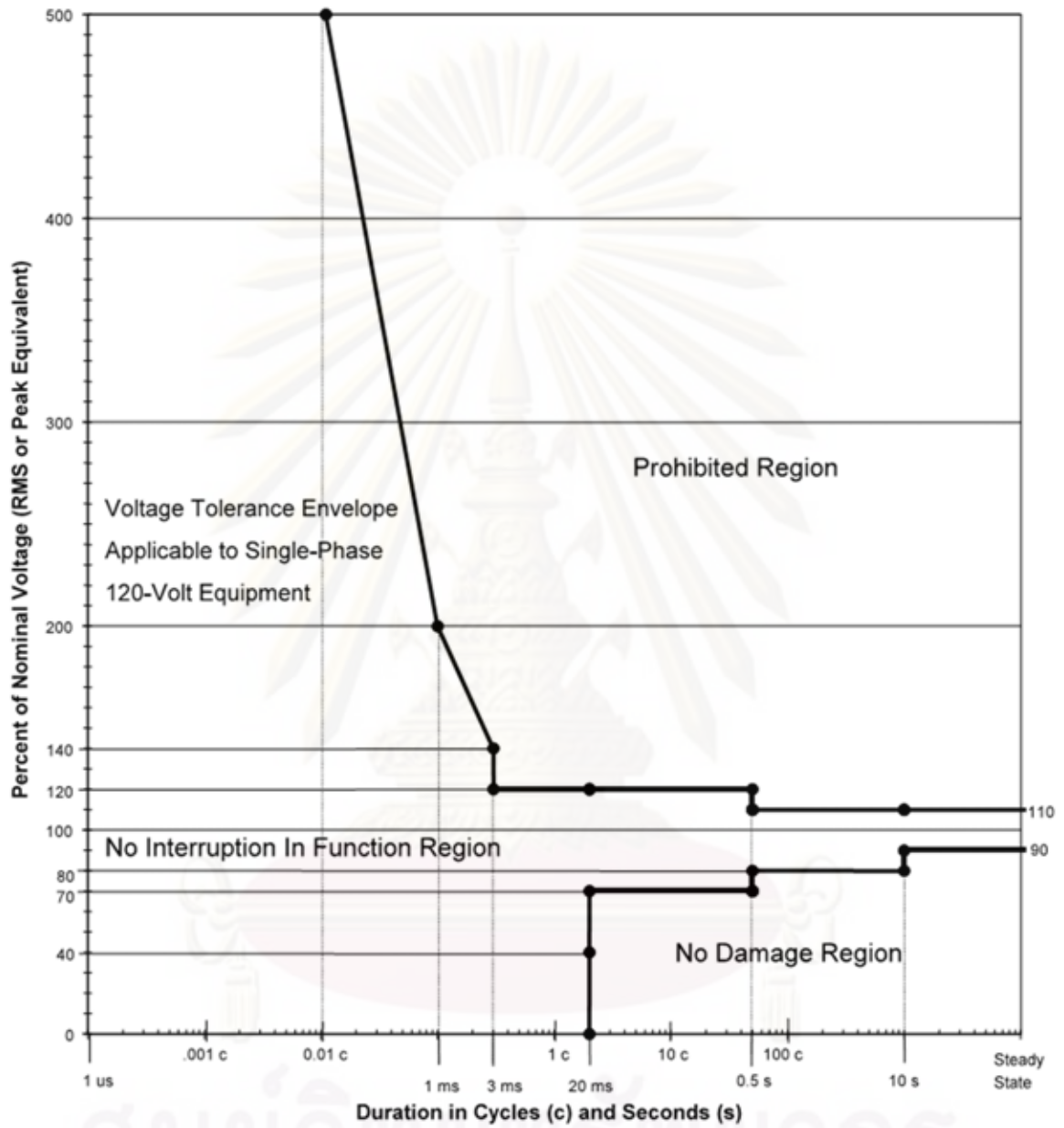


Figure F.1: ITI (CBEMA) Curve (Revised 2000).



## Appendix G: Proofs of Different During-fault Voltage Due to Resistance of Line.

This appendix shows proofs of different of during-fault voltage when LLF and DLGF occur at bus  $f$  with resistance of line consideration.

### a. Line to-line Fault (LLF)

The symmetrical components of fault current are

$$I_f^z = 0 \text{ and } I_f^p = I_f^n = \frac{V_{f,preproff}}{Z_{ff}^p + Z_{ff}^n}$$

The symmetrical components of bus voltages during fault are

$$\begin{bmatrix} V_m^z \\ V_m^p \\ V_m^n \end{bmatrix} = \begin{bmatrix} 0 \\ V_{m,preff}^p - Z_{mf}^p I_f^p \\ -Z_{mf}^n I_f^n \end{bmatrix} = \begin{bmatrix} 0 \\ 1 - Z_{mf}^p I_f^p \\ Z_{mf}^p I_f^p \end{bmatrix} = \begin{bmatrix} 0 \\ 1 - (A + jB) \\ (A + jB) \end{bmatrix}$$

Bus voltages during fault are

$$V_m^{abc} = \begin{bmatrix} 1 & 1 & 1 \\ 1 & a^2 & a \\ 1 & a & a^2 \end{bmatrix} \begin{bmatrix} 0 \\ 1 - (A + jB) \\ (A + jB) \end{bmatrix} = \begin{bmatrix} 0 \\ a^2(1 - (A + jB)) + a(A + jB) \\ a(1 - (A + jB)) + a^2(A + jB) \end{bmatrix}$$

$$V_m^{abc} = \begin{bmatrix} 0 \\ (-0.5 + j0.866)(1 - (A + jB)) + (-0.5 - j0.866)(A + jB) \\ (-0.5 - j0.866)(1 - (A + jB)) + (-0.5 + j0.866)(A + jB) \end{bmatrix}$$

$$V_m^{abc} = \begin{bmatrix} 0 \\ -0.5 + 2 \times 0.866B + j0.866(1 - 2A) \\ -0.5 - 2 \times 0.866B + j0.866(-1 + 2A) \end{bmatrix}$$

Magnitude of during-fault phase voltage at bus m are

$$\text{mag}(V_m^b) = [(-0.5 + 2 \times 0.866B)^2 + (0.866(1 - 2A))^2]^{\frac{1}{2}}$$

$$\text{mag}(V_m^c) = [(-0.5 - 2 \times 0.866B)^2 + (0.866(-1 + 2A))^2]^{\frac{1}{2}}$$

Hence,

$$\text{mag}(V_m^b) = [(0.5^2 + (2 \times 0.866B)^2 + (0.866(1 - 2A))^2 - 4 \times 0.5 \times 0.866B]^{\frac{1}{2}}$$

$$\text{mag}(V_m^c) = [(0.5^2 + (2 \times 0.866B)^2 + (0.866(1 - 2A))^2 + 4 \times 0.5 \times 0.866B]^{\frac{1}{2}}$$

From above equations, we can see that magnitudes of during-fault voltage of phases  $b$  and  $c$  are equal when  $B$  is zero. It means that when resistance of line is considered, magnitudes of phases  $b$  and  $c$  voltage during fault are not same.

### b. Double line-to-ground Fault (DLGF)

The symmetrical components of fault currents is given by

$$I_f^p = \frac{(Z_{ff}^n + Z_{ff}^z)V_{f,pref}}{Z_{ff}^p Z_{ff}^n + Z_{ff}^p Z_{ff}^z + Z_{ff}^n Z_{ff}^z} = \frac{a_2 + jb_2 + a_0 + jb_0}{a_3 + jb_3} = A_1 + jB_1$$

$$I_f^n = \frac{-Z_{ff}^z V_{f,pref}}{Z_{ff}^p Z_{ff}^n + Z_{ff}^p Z_{ff}^z + Z_{ff}^n Z_{ff}^z} = \frac{a_0 + jb_0}{a_3 + jb_3} = A_2 + jB_2$$

$$I_f^z = \frac{-Z_{ff}^n V_{f,pref}}{Z_{ff}^p Z_{ff}^n + Z_{ff}^p Z_{ff}^z + Z_{ff}^n Z_{ff}^z} = \frac{a_2 + jb_2}{a_3 + jb_3} = A_0 + jB_0$$

Hence,

$$A_1 + jB_1 = \frac{(a_3(a_0 + a_2) + b_3(b_0 + b_2)) + j(-b_3(a_0 + a_2) + a_3(b_0 + b_2))}{a_3^2 - b_3^2}$$

$$A_2 + jB_2 = \frac{a_0 a_3 + b_0 b_3 + j(a_3 b_0 - a_0 b_3)}{a_3^2 - b_3^2}$$

The phase currents at the faulted bus are

$$I_f^{abc} = \begin{bmatrix} 1 & 1 & 1 \\ 1 & a^2 & a \\ 1 & a & a^2 \end{bmatrix} \begin{bmatrix} I_f^z \\ I_f^p \\ I_f^n \end{bmatrix} = \begin{bmatrix} 1 & 1 & 1 \\ 1 & a^2 & a \\ 1 & a & a^2 \end{bmatrix} \begin{bmatrix} A_0 + jB_0 \\ A_1 + jB_1 \\ A_2 + jB_2 \end{bmatrix}$$

$$I_f^{abc} = \begin{bmatrix} 0 \\ A_0 + jB_0 + a^2(A_1 + jB_1) + a(A_2 + jB_2) \\ A_0 + jB_0 + a(A_1 + jB_1) + a^2(A_2 + jB_2) \end{bmatrix}$$

$$I_f^{abc} = \begin{bmatrix} 0 \\ A_0 - 0.5(A_1 + A_2) - 0.866(B_1 - B_2) + j(B_0 - 0.5B_1 + 0.866A_1 - 0.5B_2 - 0.866A_2) \\ A_0 - 0.5(A_1 + A_2) + 0.866(B_1 - B_2) + j(B_0 - 0.5B_1 - 0.866A_1 - 0.5B_2 + 0.866A_2) \end{bmatrix}$$

Magnitudes of fault current for phases  $b$  and  $c$  are

$$\text{mag}(I_f^b) = [(A_0 - 0.5(A_1 + A_2) - 0.866(B_1 - B_2))^2 + (B_0 - 0.5(B_1 - B_2) + 0.866(A_1 - A_2))^2]^{\frac{1}{2}}$$

$$= [(A_0 - 0.5(A_1 + A_2))^2 + (0.866(B_1 - B_2))^2 - 2(A_0 - 0.5(A_1 + A_2))0.866(B_1 - B_2) + (B_0 - 0.5(B_1 + B_2))^2 + (0.866(A_1 - A_2))^2 + 2(B_0 - 0.5(B_1 + B_2))0.866(A_1 - A_2)]^{\frac{1}{2}}$$

$$\text{mag}(I_f^c) = [(A_0 - 0.5(A_1 + A_2) + 0.866(B_1 - B_2))^2 + (B_0 - 0.5(B_1 - B_2) - 0.866(A_1 - A_2))^2]^{\frac{1}{2}}$$

$$= [(A_0 - 0.5(A_1 + A_2))^2 + (0.866(B_1 - B_2))^2 + 2(A_0 - 0.5(A_1 + A_2))0.866(B_1 - B_2) + (B_0 - 0.5(B_1 + B_2))^2 + (0.866(A_1 - A_2))^2 - 2(B_0 - 0.5(B_1 + B_2))0.866(A_1 - A_2)]^{\frac{1}{2}}$$

If magnitudes of  $I_f^b$  and  $I_f^c$  are equal, therefore, the different of above magnitudes is zero, and shown in following

$$2(A_0 - 0.5(A_1 + A_2))0.866(B_1 - B_2) - 2(B_0 - 0.5(B_1 + B_2))0.866(A_1 - A_2) = 0$$

$$\Leftrightarrow A_1 B_2 - A_2 B_1 = 0 \text{ or } A_1 B_2 = A_2 B_1$$

$$I_f^p = A_1 + jB_1 \Leftrightarrow I_f^p \times B_2 = A_1 B_2 + jB_1 B_2$$

$$I_f^n = A_2 + jB_2 \Leftrightarrow I_f^n \times B_1 = A_2 B_1 + jB_2 B_1$$

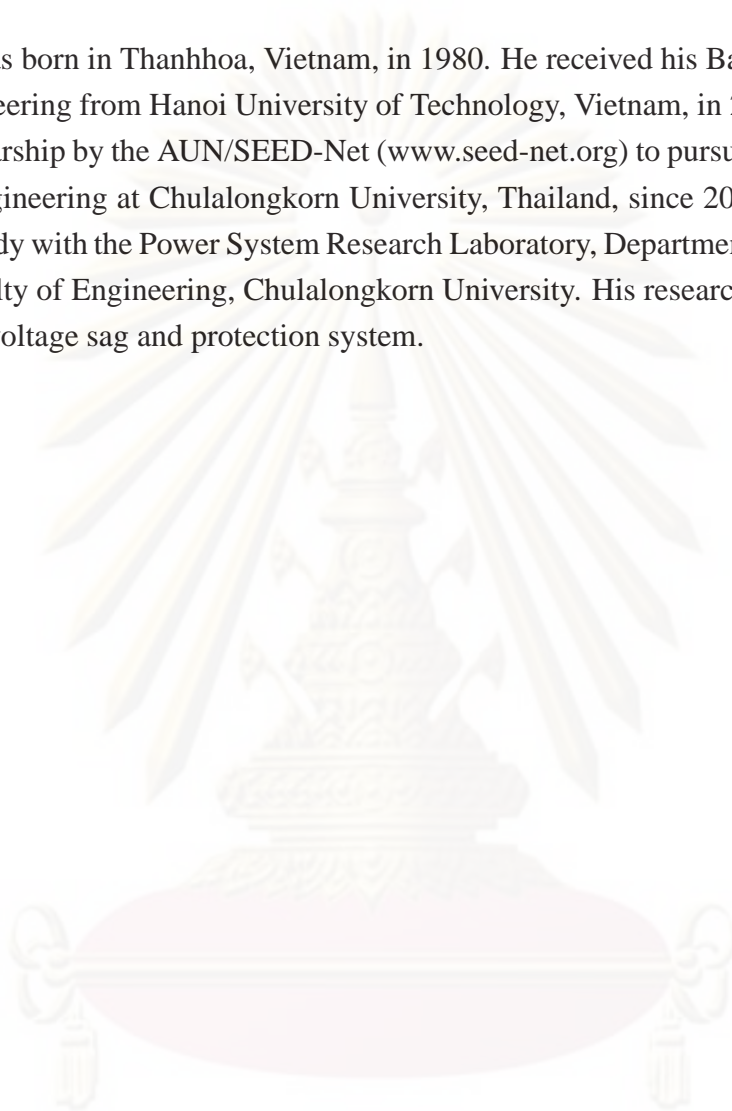
$$\text{Hence, } I_f^p \times B_2 = I_f^n \times B_1$$

Therefore, if above equation is correct, we can show that angles of  $I_f^p$  and  $I_f^n$  are same.

However, angles of  $I_f^p$  and  $I_f^n$  are not the same because of resistance of line, transformer, or generator. It means that during-fault currents and voltages for DLGF occur between phase  $b$  and  $c$  are not the same when we consider resistance of line, transformer or generator.

## BIOGRAPHY

Le Viet Tien was born in Thanhhoa, Vietnam, in 1980. He received his Bachelor's degree in electrical engineering from Hanoi University of Technology, Vietnam, in 2003. He has been granted a scholarship by the AUN/SEED-Net ([www.seed-net.org](http://www.seed-net.org)) to pursue his Ph.D. degree in electrical engineering at Chulalongkorn University, Thailand, since 2006. He conducted his graduate study with the Power System Research Laboratory, Department of Electrical Engineering, Faculty of Engineering, Chulalongkorn University. His research interest includes power quality, voltage sag and protection system.



ศูนย์วิทยทรัพยากร  
จุฬาลงกรณ์มหาวิทยาลัย